

UNIVERSITY OF LONDON

DISSERTATION FOR M.Sc. IN PHYSICS

JANUARY 1957.

TITLE: ULTRASONIC PROPAGATION IN SOLIDS

SUPERVISOR: DR. W. H. GEORGE.

NAME: ASOKKUMAR SOM

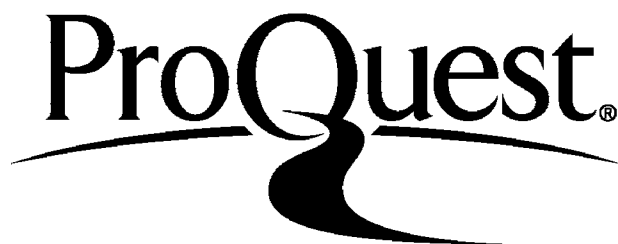
ProQuest Number: 10107225

All rights reserved

INFORMATION TO ALL USERS

The quality of this reproduction is dependent upon the quality of the copy submitted.

In the unlikely event that the author did not send a complete manuscript and there are missing pages, these will be noted. Also, if material had to be removed a note will indicate the deletion.



ProQuest 10107225

Published by ProQuest LLC(2016). Copyright of the Dissertation is held by the Author.

All rights reserved.

This work is protected against unauthorized copying under Title 17, United States Code  
Microform Edition © ProQuest LLC.

ProQuest LLC  
789 East Eisenhower Parkway  
P.O. Box 1346  
Ann Arbor, MI 48106-1346

## CONTENTS.

		<b>Page.</b>
	ABSTRACT.	1
Chapter I	INTRODUCTION.	3
Chapter II	ELASTIC WAVES IN SOLIDS.	
	Relation between stress and strain and the generalized form of Hooke's law.	11
	Elastic moduli for isotropic media.	15
	Elastic waves in solids (cubic crystals).	16
Chapter III	ABSORPTION.	
	Loss from thermal relaxation.	18
	Definition of internal friction.	20
	Plastic flow and elastic hysteresis.	24
	Attenuation due to scattering.	26
	Anharmonic coupling.	29
	Visco-elastic solids.	32
	Loss due to thermal conductivity.	34
Chapter IV	HEAT AND ULTRASONIC TRANSMISSION.	
	Introduction.	35
	Debye's theory of heat transmission in solids.	37
Chapter V	ULTRASONIC SOURCES.	
	Magnetostriction oscillators.	40
	Crystal oscillators.	44
	Piezoelectric effect.	44
	Quartz crystal source.	45
	Oscillator circuit.	47
	Special properties of quartz.	50
	Other crystal sources.	51
	Barium titanate and its special properties.	52
	Methods of crystal mounting.	55
	Coupling medium.	58

## CONTENTS.

		Page
Chapter VI	OPTICAL METHODS.	
	Introduction.	60
	Method of Schaffer and Bergmann.	62
	Advantages and disadvantages.	68
	Method of Hiedemann and Hoesch.	70
	Method of Bar and Walti.	71
	'Wedge' method.	74
	Advantages and disadvantages.	76
	Rotating plate technique.	80
	Methods of Willard.	86
	Determination of elasto-optical constants.	92
Chapter VII	RESONANCE METHODS.	
	Introduction.	97
	Measurement of internal friction in single and polycrystals.	98
	Relaxation due to dislocation at low temperature.	116
	Measurement in rubbers and rubber-like polymers.	123
Chapter VIII	PULSE TECHNIQUE.	
	Introduction.	131
	Advantages and Disadvantages.	134
	Experimental arrangement of Mason and Mc.Skimin.	138
	Balancing circuit.	142
	Buffer amplifier.	144
	Method for more precise measurement.	144
	Use of the comparator oscillator.	147
	Advantages of water buffer.	147
	Analysis of experimental results on polymers.	154
	Measurements at low temperature and the relation to dislocation theory.	165

CONTENTS.

	<b>Page</b>
<b>Chapter IX. SOLID DELAY LINES.</b>	
<b>Introduction.</b>	171
<b>Early History.</b>	171
<b>Design considerations.</b>	173
<b>Factors influencing delay time.</b>	173
<b>Equivalent circuit.</b>	174
<b>Variable solid delay lines.</b>	179
<b>ACKNOWLEDGMENT.</b>	181
<b>LIST OF SYMBOLS USED.</b>	182
<b>LIST OF TABLES.</b>	184
<b>LIST OF DIAGRAMS.</b>	185
<b>REFERENCES.</b>	188

1

ABSTRACT.

This dissertation gives a critical survey of the present state of knowledge in the field of ultrasonic propagation in solids.

Acoustic waves of high frequency suffer absorption during propagation and the analysis of this absorption has both theoretical and technical interest. The observed loss mechanisms in solids <sup>include</sup> ~~are~~ : thermal conductivity, thermoelastic relaxation, scattering, plastic flow, structural relaxation, anharmonic coupling and magnetic effects.

Theoretical explanations of these various types of losses in single and polycrystalline solids and also in high polymers, such as in rubbers and plastics are given. For reliable measurements, suitable transducers and precision experimental techniques are essential. Ultrasonic generators such as magnetostrictive, piezo electric, and the recently developed multicrystalline ceramic transducers are described. The experimental procedures for the measurement of sound velocity and attenuation during propagation are broadly grouped into three classes, (a) Resonant methods, (b) Optical methods, and (c) Pulse techniques.

Optical diffraction methods are extensively used for velocity measurement and for the

determination of elastic and elasto-optic constants of solids, whereas the Resonant and Pulse methods are used for both velocity and absorption measurement.

At megacycle frequencies, at present, the pulse technique is the only method for precision absorption measurement. The recent measurement of attenuation at low temperatures and the relation with 'dislocation' theory are discussed. Attenuation measurements lead to another practical application in the use of certain solids, as delay lines in radar systems and in devices for storing informations. A chapter on solid delay lines has been included. The equivalence of the theory of heat and high frequency sound transmission and the earlier theory of heat transmission by Debye, have been discussed.

CHAPTER IINTRODUCTION.

The systematic study of ultrasonic propagation in solids began in about 1925. Most of the early work was directed to measuring the velocity of ultrasonic waves in solids, in the form of plates, rods, bars etc., and thereby the early workers studied the velocity dispersion, reflection from plates at various angles of incidence and the scattering of the sound waves.

Amongst the earlier workers, Boyle and Sproule (1929, 1931) measured the longitudinal velocity in metallic and non-metallic rods excited piezo-electrically by attaching a small plate of quartz. Their object was to test Raleigh's formula for the velocity of longitudinal waves in rods. Taking into account the increases and decreases of cross section caused by longitudinal compression and expansion, the velocity of longitudinal waves in rods was given by Raleigh as:-

$$C_L = \sqrt{E/\rho} / \sqrt{1 + \frac{k^2 \pi^2 \sigma^2 \gamma^2}{4l^2}}$$

where  $k$  is an integer characterising the mode of vibration,  $\sigma$ , Poissons ratio,  $\gamma$ , the radius and

$l$  the length of the rod. Boyle and Sproule verified Raleigh's correction factor. Giebe and Schiebe<sup>4</sup> (1931),



Rohrich<sup>5</sup> (1932), Schoeneck<sup>6</sup> (1935) and Ruedy<sup>7</sup> (1935) made similar experiments covering a wider range of frequencies. They all proved further departures from simple relations of elastic wave propagation in solids, and found disagreement with Raleigh's formula. At high frequencies coupling occurs between the elastic longitudinal oscillations and simultaneous radial modes of oscillations. Giebe and Blechschmidt<sup>8</sup> (1933) gave a theory of these processes. Ruedy also observed coupling between longitudinal and radial modes with consequent lowering of velocity of transmission along the rod as the frequency increases. He envisaged also the scattering of radiation at the grains boundaries in the crystalline structure, a fact later proved experimentally by Mason and McSkimin<sup>9</sup> (1947) and by Roth<sup>10</sup> (1948).

The Late Lord Raleigh treated mathematically the problem of the reflection of plane sound waves at a plane interface common to two media. He also treated the problem of the reflection of the waves from and transmission through a parallel faced partition of finite thickness, which obstructed the waves in their passage through a medium.

Boyle and Lehman<sup>11</sup> (1926) and Boyle and Rawlinson<sup>12</sup> (1928) made measurements on the transmission

of ultrasonics in metal plates and established a relation between the ratio of incident and reflected energy of a plate suspended in a liquid. The same relation had been derived earlier by Raleigh who gave the expression as

$$R = \frac{\left( \frac{c_p}{c_1 \rho_1} - \frac{c_1 \rho_1}{c_p} \right)^2}{4 \cot^2 2\pi d/\lambda_1 + \left( \frac{c_p}{c_1 \rho_1} + \frac{c_1 \rho_1}{c_p} \right)^2}$$

where  $c_1$  and  $\lambda_1$  represent the velocity and the wavelength of sound in the reflecting medium, and  $d$  the thickness of the plate. At normal incidence the transmission is a minimum for a quarter wave plate. Richards<sup>13</sup> (1932) suggested that from such measurements of reflected and transmitted energy, the velocity of propagation in solids could be calculated.

In 1921,<sup>14</sup> arising out of a theoretical investigation by L. Brillouin, a number of ingenious and very beautiful optical methods have been devised which reveal unmistakably, the presence of stationary and progressive waves of very high frequency passing through transparent liquids and solids.

Brillouin visualized the diffraction of light waves in a transparent medium stratified by sound waves as analogous to diffraction of X-rays by parallel equidistant atomic layers in crystals as explained

by Bragg. The regular succession of compressed and expanded layers equally spaced, form a diffraction grating.

Experimental observation of the above phenomena was first made independently by P. Debye and F.W. Sears<sup>15</sup> of America and R. Lucas and P. Biquard<sup>16</sup> of France in 1932. The elementary theory of the diffraction of light by ultrasonic waves was put forward by C.V. Raman and N.S. Nath (1936.)<sup>17</sup> They started from the simple basic idea that the incident plane waves of light, after transmission through the medium traversed by the sound waves, assume a corrugated form owing to the fluctuations in the density and consequently also in the refractive index of the medium.

The Fourier analysis of the emerging corrugated wave front, can be used to give the observed diffraction effects, when the emergent waves are brought to a focus by the lens of the observing telescope. The results derived from the theory, give a satisfactory explanation of the observations of Bar (see chapter VI) regarding the changes in the diffraction pattern, when ultrasonic intensity and the wavelength of the incident light are varied.

Schaffer and Bergmann (1934) have shown that ultrasonic waves in transparent solids act as diffraction gratings for light. (see chapter VI ). The intensity and polarization of light diffracted by ultrasonic

waves in solids were calculated by Hans Mueller<sup>18</sup> (1937). Mueller pointed out the essential idea that the optical diffraction in solids may be interpreted on the basis of the theory of Raman and Nath, if due account is taken of the photoelastic effects arising from the periodic strains caused by the sound waves. The calculated intensity distributions for natural and polarized incident light agree with the observations of Schaffer and Bergmann on glasses, quartz and calcite. The observations made by Hiedeman and Hoesch in glass blocks were also explained by Nath and Mueller<sup>19</sup> (1938).

Since 1932, a number of optical diffraction methods have been developed for measuring the velocity of propagation and the elastic properties of transparent and opaque solids.

Recently there has been more interest in measuring the velocity of ultrasonic propagation in solids and absorption during propagation.

The energy losses of a sound wave which is propagated through a solid, may be attributed to several different mechanisms. The chief of them are thermal conductivity, thermo-elastic relaxation, thermal or mechanical relaxation, plastic flow, elastic hysteresis, and scattering. (see chapter III). Different mechanisms appear to act in different regions of the frequency scale.

For each type of loss, different laws hold for different frequency ranges. Again, the observed attenuation depends greatly on the type and crystalline structure of the material, and may change with the kind of pre-treatment to which a material has been subjected.

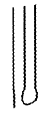
In polycrystalline specimens, the effect of crystal anisotropy increases the absorption and in single crystals and amorphous solids, the absorption is much less. Again, the elastic anisotropy of the individual crystallites which are randomly oriented, makes the material appear more inhomogenous to applied stresses and these inhomogenities lead to scattering of sound waves.

The high polymers such as plastics and rubbers, are classed as visco-elastic because of their relatively large energy absorption or viscosity coefficient. In examining the dynamic behaviour of these high polymers, study of the viscous behaviour is of the same importance as the study of their ordinary elastic moduli. The response of rubber-like materials to forces varying with time, has both theoretical and technical interest. A knowledge of the dynamic behaviour of rubber must be added to a knowledge of its static behaviour to establish a complete theory of rubber-like elasticity. The results of the study of

the dynamic elastic modulus as a function of frequency and temperature, give the magnitudes of the molecular energy barriers which must be overcome as the material undergoes a deformation in response to an external force.

The attenuation of sound waves in high polymers <sup>is</sup> are mainly viscous. Here, one encounters the phenomenon of visco-elastic relaxation. Within a relaxation region which may extend over a wide frequency range, the loss per cycle is constant and below and above, the relaxation region attenuation increases. Recent interest in the mechanical properties of plastics has led to a search for suitable methods for determining such important quantities as attenuation and phase shift from which dynamic elastic moduli and dynamic viscosities can be calculated. A study of their behaviour with frequency often throws considerable light on the molecular structures involved.

Radar research has contributed greatly to the development of electronic measurement techniques, and particularly to those which were related to pulse production and measurement. The recent development of short pulse technique has made available pulsed ultrasonics as a very convenient tool for investigating such mechanical properties of matter as (a) the various dissipative properties of solids, (b) the velocity of



longitudinal and shear waves, in solid specimens,  
(c) the dynamic elastic constants and the connection  
between the grain size of the metal crystallites and  
Rayleigh's fourth power scattering law.

CHAPTER 11Elastic Waves in solids.Relation between stress and strain and the generalized form of Hooke's law.

From the theory of elasticity (Love <sup>20</sup>1925), it is seen that the deformation in any elementary region is completely specified by the six strain components, viz.

$$\begin{aligned} e_{xx} &= \frac{\partial u}{\partial x} & e_{xy} &= \frac{\partial v}{\partial x} + \frac{\partial u}{\partial y} \\ e_{yy} &= \frac{\partial v}{\partial y} & e_{yz} &= \frac{\partial w}{\partial y} + \frac{\partial v}{\partial z} \\ e_{zz} &= \frac{\partial w}{\partial z} & e_{zx} &= \frac{\partial u}{\partial z} + \frac{\partial w}{\partial x} \end{aligned}$$

and that the traction across the arbitrary plane passing through the elementary region is specified completely by the six stress components.

$$X_x, Y_y, Z_z, Y_z, Z_x \text{ and } X_y$$

The generalized form of Hooke's law states that for small deformations the strain is proportional to the stress, so that the strain components are linear functions of stress components.



$$e_{xx} = S_{11} X_x + S_{12} Y_y + S_{13} Z_z + S_{14} Y_z + S_{15} Z_x + S_{16} X_y$$

$$e_{yy} = S_{21} X_x + S_{22} Y_y + S_{23} Z_z + S_{24} Y_z + S_{25} Z_x + S_{26} X_y$$

$$e_{zz} = S_{31} X_x + S_{32} Y_y + S_{33} Z_z + S_{34} Y_z + S_{35} Z_x + S_{36} X_y$$

$$e_{yz} = S_{41} X_x + S_{42} Y_y + S_{43} Z_z + S_{44} Y_z + S_{45} Z_x + S_{46} X_y$$

$$e_{zx} = S_{51} X_x + S_{52} Y_y + S_{53} Z_z + S_{54} Y_z + S_{55} Z_x + S_{56} X_y$$

$$e_{xy} = S_{61} X_x + S_{62} Y_y + S_{63} Z_z + S_{64} Y_z + S_{65} Z_x + S_{66} X_y$$

**Conversely, the stress components are linear function of strain components.**

Hence

$$X_x = C_{11} e_{xx} + C_{12} e_{yy} + C_{13} e_{zz} + C_{14} e_{yz} + C_{15} e_{zx} + C_{16} e_{xy}$$

$$Y_y = C_{21} e_{xx} + C_{22} e_{yy} + C_{23} e_{zz} + C_{24} e_{yz} + C_{25} e_{zx} + C_{26} e_{xy}$$

$$Z_z = C_{31} e_{xx} + C_{32} e_{yy} + C_{33} e_{zz} + C_{34} e_{yz} + C_{35} e_{zx} + C_{36} e_{xy}$$

$$Y_z = C_{41} e_{xx} + C_{42} e_{yy} + C_{43} e_{zz} + C_{44} e_{yz} + C_{45} e_{zx} + C_{46} e_{xy}$$

$$Z_x = C_{51} e_{xx} + C_{52} e_{yy} + C_{53} e_{zz} + C_{54} e_{yz} + C_{55} e_{zx} + C_{56} e_{xy}$$

$$X_y = C_{61} e_{xx} + C_{62} e_{yy} + C_{63} e_{zz} + C_{64} e_{yz} + C_{65} e_{zx} + C_{66} e_{xy}$$

The quantities  $S_{11}, S_{12}, \dots$  are the elastic constants and the quantities  $C_{11}, C_{12}, \dots$  are the elastic coefficients. It may be shown that the matrix of the elastic constants  $\|S\|$ , and the matrix of elastic coefficients  $\|C\|$ , may be regarded as the reciprocal of each other and it can be shown in general

$$\text{that } C_{jk} = C_{kj}$$

$$\text{and } S_{jk} = S_{kj}$$

These symmetry relations of the matrices reduce the number of independent constants from 36 to 21.

For a cubic crystal  $C_{14} = C_{15} = C_{16} = C_{24} = C_{25} = C_{26} = C_{34} = C_{35} = C_{36}$

supposing that the co-ordinate axes are parallel to the cube edges

$$\text{also } C_{11} = C_{22} = C_{33}$$

$$\text{and } C_{12} = C_{13} = C_{21} = C_{23} = C_{31} = C_{32} \text{ as the axes are equivalent.}$$

Now the array of values of the elastic stiffness constant is therefore reduced for a cubic crystal to the matrix

$$\|C_{ij}\| = \begin{vmatrix} C_{11} & C_{12} & C_{12} & 0 & 0 & 0 \\ C_{12} & C_{11} & C_{12} & 0 & 0 & 0 \\ C_{12} & C_{12} & C_{11} & 0 & 0 & 0 \\ 0 & 0 & 0 & C_{44} & 0 & 0 \\ 0 & 0 & 0 & 0 & C_{44} & 0 \\ 0 & 0 & 0 & 0 & 0 & C_{44} \end{vmatrix}$$

Because of the dominant role of the cubic system in metals, it is desirable to have the relations between the elastic constants and coefficients in this system.

The equation for the  $C$ 's in terms of  $S$ 's are

$$C_{11} = \frac{S_{11} + S_{12}}{(S_{11} - S_{12})(S_{11} + 2S_{12})}$$

$$C_{12} = \frac{-S_{12}}{(S_{11} - S_{12})(S_{11} + 2S_{12})}$$

$$C_{44} = \frac{1}{S_{44}}$$

From these equations  $S$ 's may be found in terms of the  $C$ 's.

$$S_{11} = \frac{C_{11} + C_{12}}{(C_{11} - C_{12})(C_{11} + 2C_{12})}$$

$$S_{12} = \frac{-C_{12}}{(C_{11} - C_{12})(C_{11} + 2C_{12})}$$

$$S_{44} = \frac{1}{C_{44}}$$

These relations may be expressed in terms of two shear constants  $S_{44}$ ,  $2(S_{11} - S_{12})$  and the compressibility  $3(S_{11} + 2S_{12})$  as follows :-

$$S_{44} = 1/c_{44}$$

$$S_{11} - S_{12} = 1/c_{11} - c_{12}$$

$$S_{11} + 2S_{12} = 1/c_{11} + 2c_{12}$$

#### Elastic moduli for isotropic media.

For isotropic bodies the elastic properties are independent of orientation of the axes of co-ordinates and stress-strain relations can be shown (Sokolnikoff<sup>21</sup> 1956) that they are simply expressed by the constants  $\lambda$  and  $\mu$  introduced by G. Lamé.

$$c_{44} = \frac{1}{2} (c_{11} - c_{12})$$

$$= \mu.$$

$$c_{12} = \lambda.$$

Again it is easy to express the constants  $\lambda$  and  $\mu$  in terms of Young's modulus and Poisson's ratio as :-

$$\lambda = \frac{E \sigma}{(1 + \sigma)(1 - 2\sigma)}$$

$$\mu = \frac{E}{2(1 + \sigma)}$$

$$\sigma = \frac{\lambda}{2(\lambda + \mu)}$$

and

$$E = \frac{\mu(3\lambda + 2\mu)}{\lambda + \mu}$$

Elastic waves in solids (cubic crystal).

Considering the forces acting on an element of volume in a crystal we find for the equation of motion in  $x$  direction

$$\rho \ddot{u} = \frac{\partial X_x}{\partial x} + \frac{\partial X_y}{\partial y} + \frac{\partial X_z}{\partial z}$$

With similar equations for  $y$  and  $z$  directions,  $\rho$  is the density. Using the relations  $X_x, X_y, \dots$

$$\rho \ddot{u} = c_{11} \frac{\partial e_{xx}}{\partial x} + c_{12} \left( \frac{\partial e_{yy}}{\partial x} + \frac{\partial e_{zz}}{\partial x} \right) + c_{44} \left( \frac{\partial e_{xy}}{\partial y} + \frac{\partial e_{xz}}{\partial z} \right)$$

using the relation  $e_{xx} = \frac{\partial u}{\partial x}$ ,  $e_{yy} = \frac{\partial v}{\partial y}$ , .....

$$\rho \ddot{u} = c_{11} \frac{\partial^2 u}{\partial x^2} + c_{44} \left( \frac{\partial^2 u}{\partial y^2} + \frac{\partial^2 u}{\partial z^2} \right) + (c_{12} + c_{44}) \left( \frac{\partial^2 v}{\partial x \partial y} + \frac{\partial^2 w}{\partial x \partial z} \right)$$

One solution is given by a longitudinal wave

$$u = u_0 e^{i(\omega t - kx)}$$

moving along the X-cube edge

$$\text{then, } -\omega^2 \rho = -k^2 c_{11}$$

So that, the velocity is

$$c = \omega/k = (c_{11}/\rho)^{\frac{1}{2}}$$

Another solution is given by a transverse or shear wave moving along the Y-cube edge with the particle motion in the X-direction

$$u = u_0 e^{i(\omega t - ky)}$$

which gives

$$-\omega^2 \rho = -k^2 c_{44}$$

so that

$$c = (c_{44}/\rho)^{\frac{1}{2}}$$

There is also another shear wave which propagates along 110 directions with velocity

$$\left[ (c_{11} - c_{12}) / 2\rho \right]^{\frac{1}{2}}$$

ABSORPTION.

The analysis of attenuation of high frequency sound waves in solids is based on the classical theory of sound absorption in gases and liquids which was first developed by Stokes (1851) and Kirchoff (1868).

For liquids and gases the dissipative forces are due to viscosity and thermal conduction and these effects can be treated analytically.

In solids the behaviour is found to be much more complex and to vary considerably with the nature of the solid.

The loss mechanisms that have been observed to cause loss in solids are thermal conductivity, thermoelastic relaxation, scattering, plastic flow, structural relaxation, an harmonic coupling and magnetic effects. (Kittel<sup>2</sup> 1947). It appears from the literature that in general no complete explanations are at present available and more experimental data are required for the establishment of a correct theory.

Loss from Thermal Relaxation.

This type of loss arises from the incomplete establishment of thermal equilibrium in a system. Energy dissipation

results whenever all parts of a system are not at the same temperature. The dissipation becomes particularly pronounced when the period of heating and cooling cycle is comparable with the time required for heat exchange between different parts of the system.

The mechanism of this type of absorption has been simply explained by Zener<sup>23</sup> (1937) who considers the thermal conditions operating during the transverse vibration of a reed. In a vibrating reed the thermo-elastic part of the internal friction arises from the flow of heat back and forth across the reed. When a reed is bent, the outer side becomes cooled and the inner is heated, the state of affairs which is reversed in the other half of the cycle.

When the motion takes place very slowly, the transfer of mechanical energy into heat takes place reversibly and under such isothermal conditions there is an absence of internal friction. The same result will occur at very high frequencies where the mechanical vibrations are too rapid for heat transfer to take place and the conditions are adiabatic.

At intermediate frequencies there is, however, a resultant heat flow which results in loss of energy.



Definition of Internal friction  $Q$ .

In a vibrating solid, the displacement vector  $U(\gamma, t)$  is determined by a differential equation of the form

$$\partial^2 U / \partial t^2 + L U = F + f \quad (1)$$

and by a set of boundary conditions.

$F$  = applied body force per unit mass

$-LU$  = force acting upon unit mass due to the elasticity of the solid.

The elastic coefficients in the operator  $L$  are taken to be the isothermal coefficients. The forces per unit mass which arise from temperature changes, from viscosity etc. are denoted by  $f$ .

When  $F$  is a periodic function of time, the solutions of the equation<sup>(1)</sup> are

$$F(\gamma, t) = \mathcal{F}(\gamma) e^{i\omega t}$$

$$f(\gamma, t) = f(\gamma) e^{i\omega t}$$

$$U(\gamma, t) = U(\gamma) e^{i\omega t}$$

The equation<sup>(1)</sup> becomes

$$(L - \omega^2)U = \mathcal{F} + f \quad (2)$$

In general  $U$  and  $f$  are not in phase with each other and it is just this difference in phase between  $U$  and  $f$  which gives rise in damping.

If  $U$  is real,  $f$  will be complex.

$$f = f_1 + i f_2 \quad \dots \quad (2)$$

where  $f_1$  and  $f_2$  are real and imaginary parts. Further if  $U_0$  be the solution of equation ( 2 ) when  $f$  is neglected. Since the force  $f$  has only a small effect upon the solution of the equation ( 2 ), it may be calculated assuming the displacement of the solid to be given by  $U_0$ .

Then the ratio

$$Q^{-1} = \frac{|\int U_0 \cdot f_2 \, dv|}{|\int U_0 \cdot L U_0 \, dv|}$$

is a measure of the internal friction of a solid, the integration being over the entire solid. This definition is analogous to the definition of  $Q$  of an electrical circuit. Here as in the electrical analogy,  $Q$  is in general a function of frequency.

Zener has derived an expression for the thermo elastic

$Q$  of a reed vibrating transversely to be

$$Q^{-1} = \frac{E_s - E_T}{E_s} \cdot \frac{f_0 f}{f_0^2 + f^2}$$

where  $f$  is the frequency of vibration

$E_s$  = adiabatic Young's modulus

$E_T$  = isothermal Young's modulus

$f_0$  = relaxation frequency.

the relaxation frequency  $f_0$  is given by

$$f_0 = \left(\frac{\pi}{2}\right) \left(\frac{D}{d^2}\right)$$

where  $D = \frac{k}{c_p \rho}$

= thermal diffusion constant

$d$  = reed thickness in the plane of vibration.

'Q' is expressed in terms of  $\alpha$  (pressure attenuation coefficient)

$$Q = 2\pi \left( \frac{\text{energy stored}}{\text{energy dissipated/cycle}} \right)$$

Energy density of a plane sound wave is given by  $\frac{p^2}{2\rho c^2}$

Intensity =  $\frac{p^2}{2\rho c}$

and  $P = P_0 e^{-\alpha x}$

Now considering the rate of energy dissipation in a slab of unit area and thickness  $\Delta x$  in the direction of sound wave, the rate of dissipation is the difference between the intensities into and out of the slab.

since  $\frac{\partial I}{\partial x} \Delta x = \frac{p^2 \alpha \Delta x}{\rho c}$

The dissipation in the slab per cycle is

$$\frac{p^2 \alpha \Delta x}{\rho c f}$$

Since,  $Q = 2\pi \left[ \frac{p^2 \Delta x / 2\rho c^2}{p^2 \alpha \Delta x / \rho c f} \right]$

$$= \frac{\pi f}{\alpha c^2}$$

$$\text{which gives } \alpha = \left( \frac{\pi f}{c} \right) Q^{-1}$$

$$= \left( \frac{\pi}{\lambda} \right) Q^{-1}$$

Zener<sup>24</sup> (1938) pointed out that the stress in a vibrating polycrystalline solid varies from crystal to crystal because of the elastic anisotropy of single crystals. In addition, the single crystals are randomly oriented in the polycrystalline solid. Hence strains which are macroscopically homogeneous are not microscopically homogeneous. This stress fluctuation gives rise to heat currents between adjacent crystals and ~~which~~ results in absorption.

The damping is of the form

$$Q^{-1} = \frac{C_p - C_v}{C_v} \cdot Q \frac{f_0 f}{f_0^2 + f^2}$$

where  $Q$  is the factor introduced by Zener (1938) to denote that fraction of total strain energy which is associated with fluctuations in dilation.

$f_0$ , the relaxation frequency may be calculated from the expression

$$f_0 = \frac{\pi D}{2d^2}$$

$D$  = Coefficient of thermal diffusivity

$d$  = thickness of the reed in the plane of vibration.

Plastic flow and elastic hysteresis.

It has long been observed that plastic deformation introduces hysteresis loops in stress-strain curves. The stress-strain curve is straight and reversible provided the yield stress is not exceeded. Once the yield stress is exceeded with accompanying plastic deformation, the stress-strain curve is no longer reversible. It was soon found that this hysteresis disappears with aging slowly at room temperature within a few minutes at 100°c.

The concept of viscous slip at grain boundaries was introduced. (Zener<sup>25</sup> 1948) The current view is that the hysteresis introduced by plastic deformation arises through the partial mobility of dislocations introduced by deformations. It looks as though all the deformation is confined to localized slip bands. The dislocations must then be within the slip bands themselves and a high concentrations of dislocations would impart to the slip bands a viscous like behaviour.

Ke<sup>26</sup> (1947) investigated the probable causes of loss of energy in solids and he ascribed the loss in polycrystals as due to viscous slip at crystal boundaries. He carried out experiments on the damping of torsional oscillations in pure aluminium and has shown that the loss

could be adequately accounted for by assuming that the metals at the boundaries of crystals behave in a viscous manner.

Wegel and Walther<sup>27</sup> (1935) determined  $Q$  of commercial materials and found in general that  $Q$ 's are roughly independent of frequency.

The expression for  $Q$  neglecting viscosity and thermal losses was given by Mason (1950) as:-

$$Q = \frac{B}{2A} = \frac{2\pi f / v}{2\pi f (H_{11} / c_{11}^{\sigma})} = \frac{c_{11}^{\sigma}}{H_{11}}$$

which shows that this type of dissipation produces a loss directly proportional to the frequency and does not affect the velocity to a first approximation.

Read<sup>28</sup> (1940) found that the logarithmic decrement of annealed single metal crystals varies inversely with frequency and is of the order  $10^{-4}$  to  $10^{-5}$  for frequencies of the order 50 Kcs/sec. and absorption coefficient  $\alpha$  was independent of frequency.

Mason and McSkimin<sup>9</sup> (1947) found for the value of  $\alpha$  a term linear in  $f$  which implies that the mechanical hysteresis loop is independent of frequency so that the energy lost per cycle is constant. The absorption coefficient must be approximately proportional to the first power of the frequency.

Ordinary viscosity gives terms quadratic in  $f$  and relaxation mechanisms gives term quadratic in  $f$  at low frequencies and independent of  $f$  at high frequencies.

#### Attenuation due to Scattering.

In polycrystals, sound scattering occurs because of a difference of density between adjacent elements of the medium or because of difference in elasticity. These polycrystals are made of a number of small sized crystals that are randomly oriented. It is probable that the difference in density of successive grains is negligible but a difference in elasticity with direction occurs since the grains are not all lined up and the elasticity depends on grain direction.

Mason and McSkimin<sup>9</sup> (1947) first calculated this type of loss due to scattering. Raleigh's formula (1929)<sup>2</sup> for the scattering of a single particle is given by

$$\frac{S.A}{I.A} = \frac{\pi T}{R\lambda^2} \left[ \frac{\Delta K}{K} + \cos \theta \frac{\Delta \rho}{\rho} \right]$$

where  $T$  = vol. of the particle  
 $R$  = distance of the particle from the point of observation.  
 $K$  = elasticity of the medium

- $\Delta K$  = difference in elasticity  
 $\theta$  = angle between the direction of observation  
 S.A. = scattered amplitude  
 I.A. = incident amplitude

Neglecting  $\Delta \rho / \rho$ ,

The energy scattered from a single particle  
 is proportional to the square of scattered amplitude  
 integrated over a sphere of radius  $R$ .

$$\begin{aligned}
 \text{S.E.} &= (I.A.)^2 \frac{\pi^2 T^2}{\lambda^4 R^2} \cdot 2\pi R^2 \left(\frac{\Delta K}{K}\right)^2 \int_0^{2\pi} \sin \theta d\theta. \\
 &= (I.A.)^2 \frac{4\pi^3 T^2}{\lambda^4} \cdot \left(\frac{\Delta K}{K}\right)^2.
 \end{aligned}$$

Now if a large number of grains are concentrated in a  
 volume of area  $A$  and length  $\delta x$ , assuming random  
 scattering from all particles, the total scattered  
 energy (S.E.) will be the sum of the S.E. from each of  
 the particles.

$$\text{Total S.E.} = (I.A.)^2 \frac{4\pi^3}{\lambda^4} \sum_{k=1}^N \left( T_k^2 \left(\frac{\Delta K}{K}\right)_k^2 \right)$$

$$\text{or, } \frac{\text{Total S.E.}}{(I.A.)^2} = \frac{4\pi^3}{\lambda^4} \sum_{k=1}^N T_k^2 \sum_{k=1}^N \frac{\left(\frac{\Delta K}{K}\right)^2}{N}$$

assuming no relation between  $T$  and inhomogeneity of  
 elasticity.



$$\text{or } \frac{\text{Total S.E.}}{(\text{l.A.})^2} = \frac{4\pi^3}{\lambda^4} \sum_{k=1}^N T_k^2 \left( \frac{\Delta \bar{k}}{k} \right)^2$$

$\left( \frac{\Delta \bar{k}}{k} \right)^2$  is the space average of the quantity  $\left( \frac{\Delta k}{k} \right)^2$ .

For a distribution of particle sizes, that does not differ much from the average, the first summation is

$$NT^2 = VT = A dx T$$

where  $V = A dx$  - volume under consideration

Now total incident energy =  $A \cdot (\text{l.A.})^2$

$$\therefore \frac{\text{Total S.E.}}{\text{Total I.E.}} = \frac{4\pi^3 dx T}{\lambda^4} \left( \frac{\Delta \bar{k}}{k} \right)^2$$

This determines the energy attenuation factor.

$$\begin{aligned} E_0 &= E_i - E_s \\ &= E_i e^{-\alpha dx} = E_i (1 - \alpha dx) \end{aligned}$$

where

$E_i$  - incident energy

$E_s$  - scattered energy

$E_0$  - energy of the wave out of the section

Hence,

$$\alpha = \frac{4\pi^3 T}{\lambda^4} \left( \frac{\Delta \bar{k}}{k} \right)^2$$

Mason and McSkimin expressed the attenuation according to the eqn.

$$A = B_1 f + B_2 f^4$$

which indicates that a component of attenuation is proportional to the frequency and another component is proportional to fourth power of the frequency.

The component proportional to frequency is the same as observed for most metals and solid materials at low frequencies (Wegel and Walther<sup>21</sup> 1935) and indicates the presence of an elastic hysteresis. The term proportional to the fourth power is indicative of a scattering of energy similar to the scattering of sound by small particles which as Raleigh has shown, produces a scattered energy compared to the incident energy that increases as the fourth power of frequency.

#### Anharmonic Coupling

The absorption of sound in solids depends substantially upon the relation between the wave length of sound and the length of the free path of Debye's heat phonons. If the wavelength of the sound is small in comparison with the length of the free path of Debye's heat phonons,

then the absorption of sound may be regarded as an absorption of the sound quantum produced in collision with Debye's heat phonons.

Such type of losses was theoretically calculated by Landau and Rumer<sup>29</sup> (1937) and Akhieser<sup>30</sup> (1939)

Landau and Rumer have shown that sound waves of high frequency (exceeding the inverse collision interval of the thermal phonons) differs from that at the mechanism of absorption in insulators at low frequency. The absorption coefficient is here proportional to frequency, where-as in the low frequency region it is proportional to its square.

Gurevich<sup>31</sup> (1945) showed that in metals, the absorption coefficient is also proportional to the frequency and is so large that sound<sup>at</sup> of such frequencies ~~that~~ propagation in metals ceases.

Gurevich formulated the Kinetic equation for the variation of the number of phonons due to their interaction with electrons, as:-

$$\frac{dN_g}{dt} = \sum \alpha f_g \left\{ (N_g + 1) n_{f+g} (1 - n_f) - N_g n_f (1 - n_{f+g}) \right\}$$

where

$N_g$  = the number of sound quanta (phonons) with a quasi momentum  $g$ .

$n_f$  = number of electrons with a quasi momentum  $f$ .

$\alpha f_g$  = probability of their interaction.

This equation is finally reduced to

$$\begin{aligned} \frac{dN_g}{dt} &\approx \frac{U_0^2 g}{2Mc\epsilon_0} (N_g^0 - N_g) \\ &= \frac{N_g^0 - N_g}{\tau} \end{aligned}$$

where  $M$  = mass of an atom

$C$  = velocity of sound

$N_g^0$  = being the equilibrium distribution  
function of the phonons.

$U_0$  = an energy of the order of atomic energies  
(the periodic part of the energy of an  
electron in the field of the lattice)

$\epsilon_0$  = boundary energy of Fermi distribution.

The time of damping  $\tau$  is given by the expression

$$\tau_g \approx \frac{Mc}{g} \frac{\epsilon_0}{U_0^2} = \frac{Mc^2}{U_0^2} \epsilon_0 \frac{1}{\omega}$$

which shows that the absorption is proportional to the  
sound frequency. If  $\tau_\omega$  is the period of sound  
vibrations, then

$$\frac{\tau_g}{\tau_\omega} \approx \frac{Mc^2 \epsilon_0}{U_0^2}$$

since  $U_0 \sim \epsilon_0$

$$\tau_g / \tau_\omega \sim Mc^2 / \epsilon_0$$

This expression is usually less than unity, which means  
that all the sound waves for which the above calculations  
hold are absorbed so strongly that propagation ceases.  
As these theoretical calculations apply to very high

frequencies of the order of  $10^{11}$  cycles/second (at room temperature) it is not experimentally possible so far to see whether such type of losses actually occur or not.

### Visco-Elastic Solids.

Maxwell<sup>32</sup> (Kolsky 1953) expressed the rate of strain of a substance in two terms, one proportional to and in phase with the stress and one in phase with the rate of stress.

$$\dot{s} = \frac{\dot{\sigma}}{K} + \frac{\sigma}{\eta} \quad (1)$$

K being elastic and  $\eta$  a viscous coefficient. Such materials are known as visco elastic, when there is merely a restoring force proportional to displacement

$s = \frac{\sigma}{K} +$  a constant, and the material is purely elastic.

when  $\sigma = \eta \dot{s}$ , it is purely viscous.

Now if a sinusoidal stress  $\sigma = \sigma_0 e^{i\omega t}$  is applied to a visco elastic substance, then substituting in (1) we have:-

$$\dot{s} = \sigma \left( \frac{1}{\eta} + \frac{i\omega}{K} \right)$$

If we denote the impedance of the system as  $\sigma/\dot{\epsilon}$  then

$$Z = \left( \frac{1}{\eta} + \frac{i\omega}{K} \right)^{-1} = \eta \frac{1 - i\omega\eta/K}{1 + \omega^2\eta^2/K^2}$$

The quantity  $\eta/K$  has the dimension of time, and is called the relaxation time  $\tau$ , because of its relevance to the simple relaxation phenomena.

The real part of the viscosity can be written as

$$\eta (1 + \omega^2\tau^2)^{-1}$$

The effective elastic modulus rises in the region of frequency for which  $\omega \approx \tau^{-1}$  from its low frequency to its high frequency value.

At any pulsation

$$K_{\omega} = K_0 + K_{\infty} (1 + \omega^2\tau^2)^{-1}$$

where  $K_0$  = modulus for slowly applied stress

$K_{\infty}$  = modulus for rapid vibration

Simultaneously there is an absorption of the oscillatory energy put into the body.

The phase difference between stress and strain can be expressed as an angle  $\delta$ , whose tangent is the ratio of the imaginary and real parts of the impedance

$$\tan \delta = \frac{K_0}{K_{\infty}} \cdot \frac{\omega\tau}{1 + \omega^2\tau^2}$$

At low frequencies stress and strain are in phase. The tangent of the phase difference rises where  $\omega = \tau^{-1}$  to  $\frac{1}{2} K_0/K_{\infty}$  thereafter to  $\pi/2$

This difference in phase represents a loss in power.

$\tan \delta$  which is used as a measure of internal friction is analogous to the power factor in alternating current theory.

### Losses due to Thermal conductivity

The absorption of sound caused by thermal conductivity is given by <sup>33</sup> (Mason 1950) as

$$\alpha = \frac{2\pi^2 f^2}{\rho v^3} \left[ \frac{k}{c_v} \cdot \frac{c_{11}^\sigma - c_{11}^\theta}{c_{11}^\sigma} \right]$$

It appears from the above equation that the thermal losses increase as the square of the frequency and hence it is a very significant factor in single metal crystals at frequencies above 1000 Mc/sec.

CHAPTER IVHeat and Ultrasonic Transmission.Introduction:

Most of the heat energy is concentrated in the frequency range from  $10^6$  to  $10^7$  megacycles and ~~until~~ at present no procedures ~~are~~ available with which vibrations could be applied to a solid body at frequencies anywhere approaching those of heat.

So neither confirmation nor refutation of equivalence of the theory of heat and high frequency sound transmission has been experimentally achieved.

Recently, however, for the studies of ultrasonic delay line, procedures were employed that could handle frequencies of the order of megacycles and Mason<sup>34</sup> (1949) has shown that at these very high frequencies sound transmission began to show characteristics similar to those of heat transmission.

On examining the curves in figure (53) it is seen that the solid curve in the figure is for heat transmission and this includes no absorption, and it is higher and the peak occurs later, than the dotted curve which includes absorption.

Both curves are obviously the members of the same family, but the upper curve is for frequencies of the order of millions of megacycles and includes no absorption, while the dotted curve is at a frequency



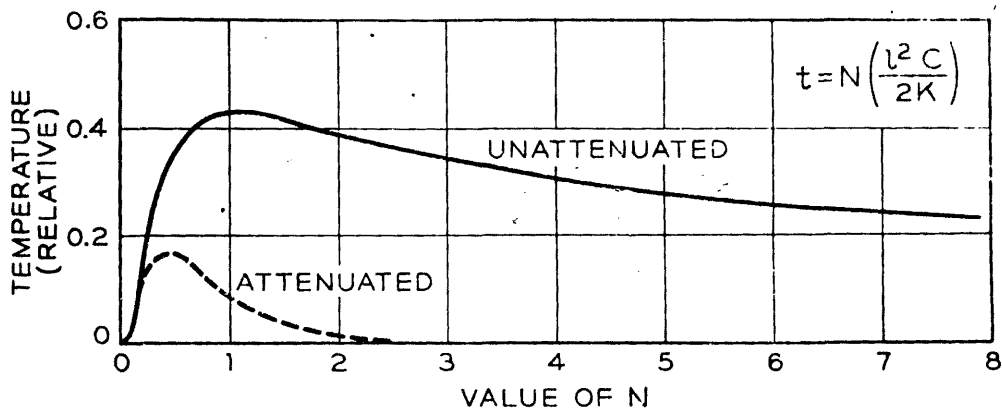


Fig. 58—Curves showing relationship between temperature and time. Solid line for heat transmission; dashed line for sound transmission at ultrasonic frequencies.

of about 12 megacycles and includes absorption. The solid curve represents heat transmission and the dotted one is acoustic, but the acoustic transmission with proper parameters will give both curves and thus it is evident that heat transmissions may be accounted for by considering it as acoustic transmission occurring at much higher frequencies.

With these studies as a basis, it was found that heat transmission, after making corrections for the differences in frequency, is basically the same as that of sound and thus it was possible to verify experimentally the earlier theory of Debye.

#### Debye's theory of heat transmission in solids.

The theory of heat transmission was first given by Debye. Since heat is a mechanical vibration of crystal lattice, Debye suggested that it was probably transmitted by the relative motion of the adjacent molecules as is an acoustic wave. Einstein treated the solid as an assembly of atoms oscillating at a constant frequency  $\nu$  and assuming that each oscillator could have only certain discrete energy levels given by  $n h \nu$  where  $h$  is the Planck's constant and  $n$  is any integer.

A few years later Debye produced a more satisfactory treatment without the obviously simplifying assumption that each oscillating atom had the same frequency. Debye treated the solid as a continuum

neglecting its atomic structure and regarded the heat content as residing in the energy of stationary elastic waves, the wave length of which is large in comparison with the distances between the atoms.

The single characteristic frequency  $\nu$  postulated by Einstein is now replaced by a spectrum of frequencies, which Debye assumed to end sharply at a maximum frequency  $\nu_m$ . In elastic solids there are both longitudinal and transverse vibrations with ~~with~~ different velocities of wave propagation. The number of transverse vibrations is twice the number of longitudinal vibrations and it can be shown that the number of modes of vibration lying between the frequencies

$\nu$  and  $\nu + d\nu$  is

$$4\pi V \left( \frac{1}{c_l^3} + \frac{2}{c_t^3} \right) \nu^2 d\nu$$

where,  $V$  is the volume of the solid.

The number of modes of vibration in a crystal lattice is not, however, infinite but is limited to  $3N$  where  $N$  is the number of lattice points in volume  $V$ .

Thus there must be an upper limit to vibration frequency such that,

$$\begin{aligned} & 4\pi V \left( \frac{1}{c_l^3} + \frac{2}{c_t^3} \right) \int_0^{\nu_m} \nu^2 d\nu \\ &= \frac{4\pi V}{3} \left( \frac{1}{c_l^3} + \frac{2}{c_t^3} \right) \nu_m^3 = 3N. \end{aligned}$$

Debye also used the quantum approach used by Einstein and assumed that the energy of vibrations of the atom is limited to integral multiples of  $h\nu$ .

The equation for the specific heat of a solid is given by the expression

$$C_v = F(T/\theta) \\ = 9NKT^3/\theta^3 \int_0^{\theta/T} \frac{\varphi^4 \exp(\varphi)}{\{\exp(\varphi)-1\}^2} d\varphi$$

where  $\varphi = h\nu/KT$

$N$  is the number of atoms in a gram atom and  $\theta$  is the Debye characteristic temperature.

$$\theta = \frac{h\nu_m}{k} \\ = \frac{h}{k} \left[ \frac{9N}{4\pi V} \left( \frac{1}{C_l^3} + \frac{2}{C_t^3} \right) \right]^{\frac{1}{3}}$$

Zucker<sup>35</sup> (1955) calculated Debye temperature for polycrystalline aluminium using the above relationship and checked the values obtained against those found by specific heat measurements.

CHAPTER VUltrasonic Sources.

In general, as generators of ultrasonic waves, two types of sources are used for work on solids. Magnetostriction generators are used for lower frequencies but for frequencies greater than 120 Kc/sec crystal sources are invariably employed. Recent developments of multicrystalline ceramic compounds ~~find~~<sup>provide</sup> also a convenient source of ultrasonic generation, but not very much use of these ceramic compounds ~~have~~<sup>has</sup> been found in the literature so far for work on solids.

Elementary theory of these sources, the method of generation, the mounting of the crystals are described and more details of the applied techniques are described in chapters VII and VIII .

Magnetostriction Oscillators.

A ferromagnetic rod such as iron, cobalt or nickel, when placed in an alternating magnetic field, suffers a change in length owing to its molecular rearrangement. This ~~shortening~~<sup>change</sup> of length is very small, but if the frequency of the exciting field is in resonance with the natural frequency of the rod, the magnitude of this change in length may be of the order of one thousandth of its length.

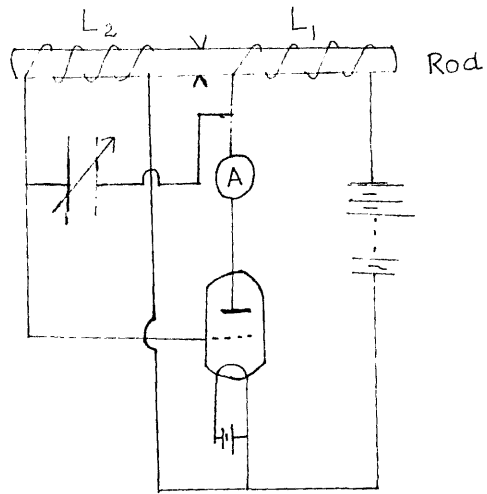


FIG. 1 PIERCE'S MAGNETOSTRICTION OSCILLATOR.

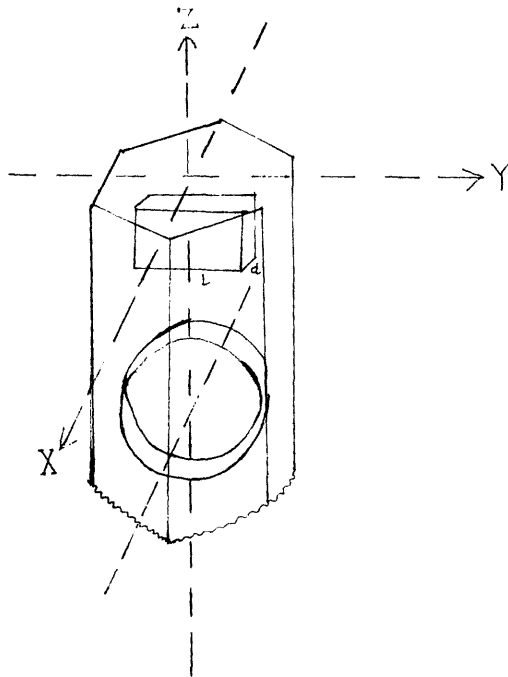


FIG 6 CUTTING OF QUARTZ PLATES FROM A CRYSTAL.

and causes it to be deformed. This deformation is propagated along the rod towards its other end and temporarily it exists as deformation within the grid coil. The state of magnetisation is changed by this deformation, and consequently a small e.m.f. is induced into the grid and produces an amplified current in the plate circuit and in <sup>the</sup> plate coil. The oscillatory current in the system is thus built up to a large amplitude with a frequency determined by the longitudinal mechanical vibration of the rod.

The materials used in the magnetostriction oscillators comprise of ferromagnetic materials - iron, nickel, cobalt and their alloys. Of these, nickel itself, glow ray and nichrome give a moderate amplitude of oscillation and have a low temperature coefficient of frequency. Combinations of materials may also be used for vibrating bars. Materials of different temperature coefficients may be combined to get a desired characteristic. One material with negative temperature coefficient may form one part of the bar while a piece with positive temperature coefficient may form the other part. In this way temperature coefficient is balanced out and the bar is more stable to temperature changes. These bars may be either longitudinally composite or concentrically composite depending on how they are joined.

In simple materials, the magnetostriction effect decreases as the temperature rises and vanishes at the Curie point. Again in solid parts, there is usually some loss due to eddy currents which flow in the material and there are losses also due to hysteresis. The use of laminations cuts down these losses but even then the loss effect is not negligible.

Vincent<sup>38,39</sup> (1929, 1931) and Pierce and Noyes<sup>40</sup> (1938) have devised suitable circuits to maintain the oscillations and it was found that for better results the rods should be initially polarised, i.e. have some permanent magnetisation before the alternating field is applied.

#### Crystal Oscillators.

For generation of high ultrasonic frequencies, crystal oscillators are used, and since most of the work of any importance in ultrasonic propagation in solids has been carried out at frequencies of the megacycle region, crystal oscillators are found most suitable. Crystals can be made to vibrate by employing either the piezoelectric or electrostrictive effect.

#### Piezoelectric Effect.

In 1880, the brothers Pierre and Jacques Curie discovered the piezoelectric effect which occurs in certain crystals



having one or more polar axes. If such a crystal is rotated by  $180^\circ$  about one of these axes, it can not be made to coincide with its original position, i.e. the crystal lacks a centre of symmetry. On applying a mechanical stress along a given direction an electric field is produced, the magnitude of which is directly proportional to the applied pressure. Thus if the crystal is suitably cut in the form of a parallel faced slab or disc, equal positive or negative electric charges appear on the opposite faces. Shortly after the discovery of this effect, its converse effect, i.e. if an electric field is applied along one of the axes, the crystal is mechanically strained, was predicted by Lippmann in 1881. The Curie brothers verified this prediction and showed that this converse effect was equal and opposite to the direct effect. The effect was found in the following crystals: quartz, ammonium dihydrogen-phosphate, potassium dihydrogen phosphate, lithium sulphate, rochelle salt, dipotassium tartrate and tourmaline.

#### Quartz Crystal Source.

The quartz is the most commonly used crystal for work on solids and hence it is more elaborately discussed.

Fig. 6 illustrates a quartz crystal suitably prepared for cutting with its three mutually

perpendicular axes, X, Y and Z. The piezoelectric effect will occur if an electric field is produced along either the X- or Y- axis, but not along <sup>the</sup> Z-axis, the optic axis, about which the crystal is symmetrical. Plates may be cut with their surfaces perpendicular to the X-axis as shown in fig. 6 or to the Y-axis and they are designated as X-cut and Y - cut plate respectively. The plates can be set in vibration by the aid of an alternating electric field supplied by a suitable thermionic valve oscillator. In X-cut crystals, longitudinal mechanical vibrations occur in both X and Y directions. These are known as 'thickness' and 'length' vibrations respectively.

If the frequency of the alternating field is in resonance with one of the natural frequencies of the crystal, a high degree of electromechanical coupling is obtained.

The fundamental frequencies of vibration are given by

$$f_d = \frac{1}{2d} \sqrt{\frac{C_{11}}{\rho}}$$

for 'thickness' vibrations and

$$f_l = \frac{1}{2L} \sqrt{\frac{E}{\rho}}$$

for 'length' vibrations, where  $C_{11}$  is the characteristic modulus of elasticity for oscillations of this type and direction,  $d$  the thickness of the plate,  $\rho$  its density,  $E$  its Young's modulus and  $l$  the length.

Substituting the values for quartz, these equations become <sup>4)</sup>(Bergmann 1949) :-

$$f = 285,500/d \quad \text{Kc/sec.}$$

and

$$f = 272,500/l \quad \text{Kc/sec.}$$

'length' vibrations are thus useful for the production of lower frequencies and the 'thickness' vibrations for higher frequencies. With 'thickness' vibrations it is seen that the plate must be very thin if very high frequencies are to be obtained.

Thus there is an upper limiting value for frequency beyond which the plate is too thin. This has two disadvantages, the first being that the plate may be easily broken, and secondly, for a given potential difference across the electrodes, the exciting field becomes so high that the dielectric property of the crystal vanishes. Ny Tse Ze (1927) has reported an upper frequency limit of 50 Mc/sec. for which the plate was only 0.054 mm. thick. He showed, however, that this difficulty may be overcome by using thicker crystals and exciting them at one of their odd upper partials.

#### Oscillator Circuit.

The connection between the quartz and the electric oscillator may be made in several ways. The earliest simplest form consists of putting the crystals in

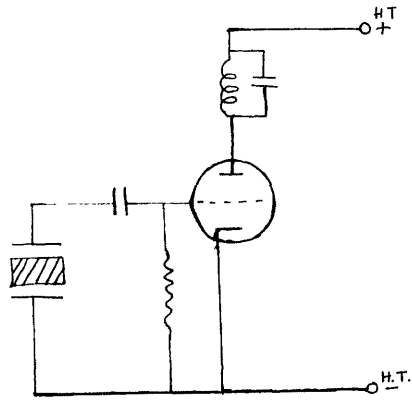


FIG. 2. PIERCE'S OSCILLATOR

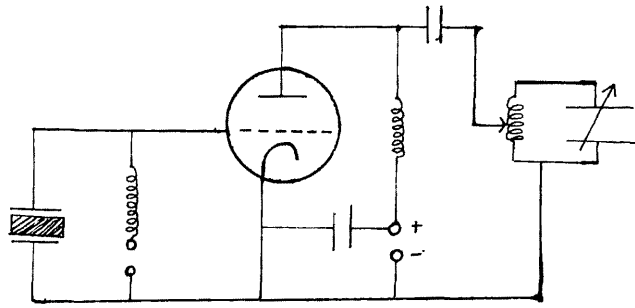


FIG. 3. MODIFIED PIERCE CIRCUIT.

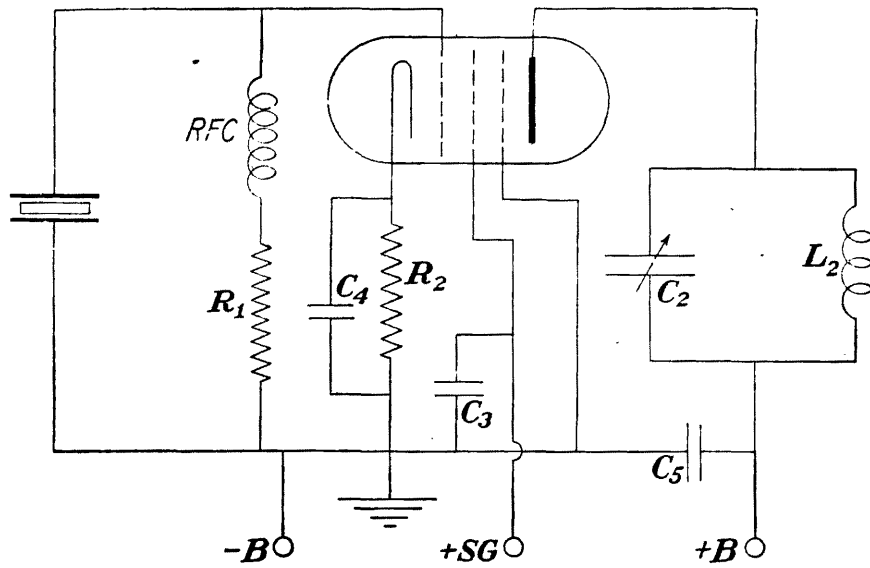


Fig. 4.—Pentode piezo-oscillator.

FIG. 4. PIERCE-MUELLER CIRCUIT.

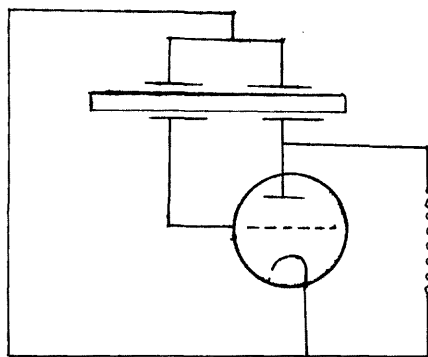


FIG. 5. CADY'S OSCILLATOR.

parallel with the capacity of the oscillating circuit. The oscillator circuit is here, <sup>the</sup> well known one of Hartley. The oscillating circuit, made up of a self induction and a variable condenser, is tuned to the natural frequency of the quartz by varying the capacity. This type of circuit, fig. 2 , is used when powerful vibrations, particularly in liquids or solids, are to be generated.

The vacuum tube may be either a triode or a pentode. The advantages offered by these tubes are higher amplification, greater power without fracturing the crystal and higher frequency stability from the action of the screen grid. When a pentode valve is used, the suppressor grid may be earthed or for more power a small positive potential may be given.

Pierce developed such oscillators, which were further improved by him and later modified by Muller and Crossley.

Another of the earliest type of piezo oscillator was devised by Cady in 1921 and was modified by Van Dyke in 1922.

In the Pierce Muller circuit, as illustrated in fig. 4 , both grid leak and cathode bias are used. A very small auxiliary condenser may be connected between grid and plate if the grid - plate capacitance provides

insufficient feed-back. To safe-guard the crystal the capacitance of this condenser should be as small as possible. Cady's oscillator works on the principle of piezo electric feed back and it is essentially an amplifier with input and output coupled through a crystal with the two parts of the electrode. Neither condenser or coil is used and the anode circuit contains only resistance of a few thousand ohms. For greater output crystals can be cemented together with the faces of the same polarity in the same direction. Although stacked crystals do not add their power output arithematically, nevertheless very great increments of power can be achieved. Mosaics of crystals add to their directional qualities as well as to the power output. For concentrated ultrasonic beams, Gruetmacher<sup>42</sup> (1935) suggested the use of concave plates and Lablaw<sup>43</sup> (1945) investigated with curved quartz crystals and observed that a curved crystal seems to give somewhat greater amplitude of ultrasonic output than a perfectly flat one for a specific voltage impressed.

#### Special properties of Quartz.

Quartz is by far the most suitable of all the piezo-electric crystals for ultrasonic generations, especially to work in solids at higher ultrasonic frequencies. It is physically robust and non-hygroscopic and it can withstand a reasonably high temperature. Quartz is

easy to cut and very thin specimens may be obtained. Its piezoelectric properties do not disappear until the temperature is raised above  $575^{\circ}\text{C}$ ., so that it can operate over a wide temperature range. Its elastic qualities are good, it gives a very sharp resonance curve and its electrical resistivity is high ( $3 \times 10^{16}$  ohm-cm, perpendicular to the optic axis). Above all, Quartz is extremely durable and chemically stable, and is scarcely affected by acids except hydrofluoric acid with which 'etching' is generally done. Only at high temperature and pressure quartz is partially soluble in water.

Other crystal sources:

Quartz crystals are expensive and now-a-days quartz is becoming increasingly difficult to obtain. There are a number of substitutes but none of them is anything like as suitable. For example, Rochelle salt crystals, which display both piezoelectric and electrostrictive properties, are easy to grow, but they are susceptible to moisture. If the relative humidity of the surrounding atmosphere is less than 35%, the substance dehydrates, owing to its low vapour pressure and if greater than 85% moisture is absorbed, then the crystal slowly dissolves. At  $55^{\circ}\text{C}$ ., Rochelle salt breaks up into

sodium tartrate and potassium tartrate.

Ammonium dihydrogen phosphate (A.D.P.) and potassium dihydrogen phosphate (K.D.P.) crystals are strongly piezoelectric and they do not contain water of crystallisation. So they do not dehydrate but they deliquesce at 93% relative humidity. Both crystals have a volume leakage due to transmission of ions through them.

Ethylene diamine tartrate (E.D.T.) and dipotassium tartrate (D.K.T.) crystals have high 'Q' factors but these also deliquesce when the humidity is high. The properties of these crystals have been discussed in detail by Mason<sup>33</sup> (1950). Use of these crystals are not very frequent for work on solids and they are mentioned in the experimental techniques, chapter VII.

#### Barium Titanate and its special properties.

Owing to high cost of large quartz slabs and limited supply, much work has been done since the last war for the development of barium titanate transducers. These are multicrystalline ceramic compounds of titanium. The small crystals of barium titanate with their axes distributed in all directions are fused together, with a small amount of binding substance. Barium titanate is commonly called ferro-electric, since it exhibits



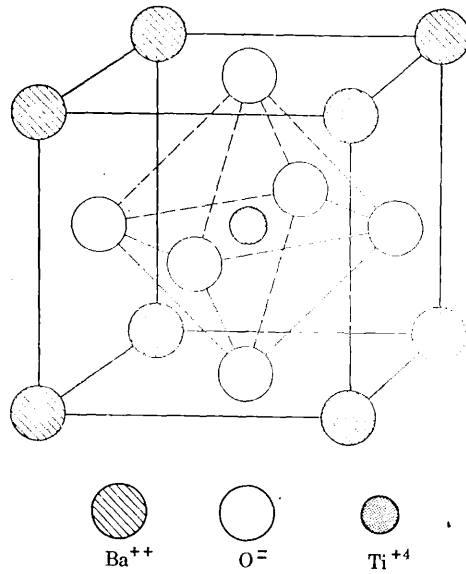


Fig. 7.0. Crystal structure of barium titanate.

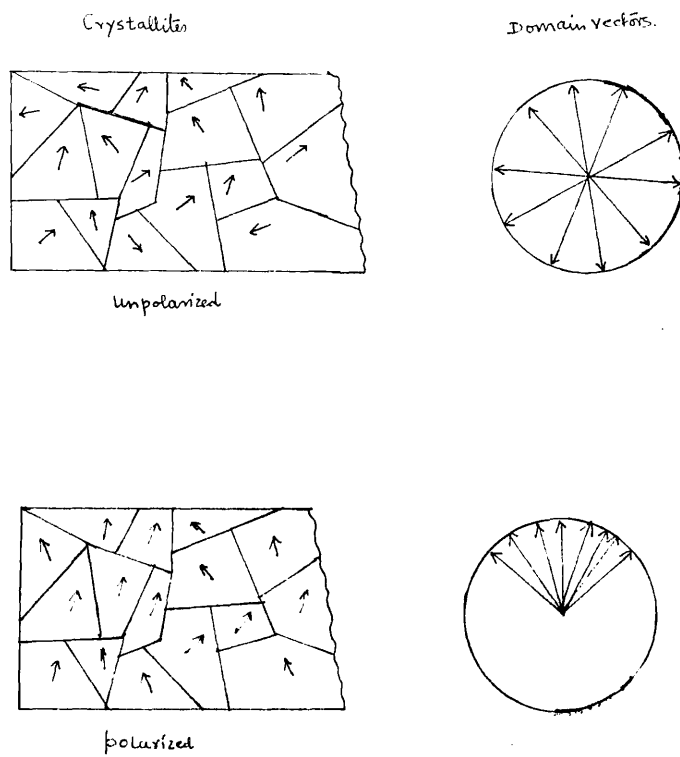


FIG. 8. Domain alignment by polarization in barium titanate

certain dielectric properties that are analogous to the special magnetic properties of ferromagnetic materials. They possess electro mechanical couplings of the order of fifty times that of quartz and have proved most useful in the generation of high ultrasonic frequencies. The dielectric constant of barium titanate has a value of 1200 to 1500 at room temperature and at 120<sup>o</sup>c, the dielectric constant may be as high as 9000. If the temperature is raised above this temperature, its crystal structure is changed from tetragonal to cubical. The crystal structure of barium titanate is shown in the fig. 7 in which the titanium atom is taken as the centre of symmetry. Because of its small size relative to the surrounding ions, the titanium atom is easily displaced by an electric field. In the tetragonal phase of barium titanate, the titanium atom tends to move towards one of the face centred oxygen atoms, owing to the potential distribution between two opposite oxygen atoms. Each crystal cell, therefore, has a dipole moment which may be oriented toward any of the six oxygen atoms. Since the orientation of the dipole moment within one cell is influenced by the orientations in the neighbouring cells, there are regions of parallel alignments called "domains". If a strong electric field is applied, the electric axes of the domains oriented at right angles to the field are turned

into the direction of the field and a uniaxial crystal is created.

In a barium titanate ceramic, many small crystallites are baked together and it can be moulded in any shape. Each small crystallite is subdivided into electric domains. A large biasing field will switch the domains into some degree of alignment with the field vector. This process is called prepolarization. A schematic picture of the polarization process in barium titanate ceramic is shown in fig. 6. .

#### Methods of crystal mounting.

To derive the maximum efficiency from the crystal proper considerations must be given for its mounting in a holder. The crystal before its mounting, is cleaned and plated to make electrical contact with the apparatus and also to distribute the charge more evenly over its surface. Cleaning of such crystals is done by initially boiling the crystal in 40:1 solution of sulphuric acid and potassium dichromate for about five minutes. It is then cooled and rinsed in distilled water. Again the crystal is boiled in potassium hydroxide for about three minutes and rinsed in distilled water. Finally it is boiled in distilled water and in ethyl alcohol. Drying

is then done on <sup>a</sup>wire screen.

For better results, <sup>the</sup> following points should be considered for mounting:-

- (a) The mechanical damping of the crystal must be a minimum.
- (b) The frequency and amplitude of vibration should be constant.
- (c) Materials used for the holder <sup>of</sup> the crystal electrodes should be physically and chemically stable.

If mechanical pressure is applied to any part of the crystal, except at the nodal points, vibrations will be damped. If the pressure exerted is sufficiently high, the crystal stops oscillating altogether. The weight of the electrodes should be very small. They may consist of sheets of metal foil cemented to the crystal surfaces but it is better to coat the surfaces of the plate with very thin metallic layers either by electrolysis, evaporation or by cathode sputtering. Metals such as silver, gold, aluminium or chromium are generally used for coating. Care should be taken that the deposit is uniform. Vigoureux <sup>44</sup> (1950) advised that the metal should be removed carefully from the edge of the plate leaving a narrow region clear of metal at the rim. In this way surface leakage between the electrodes is reduced.

For work on solids, the simplest way to mount a crystal

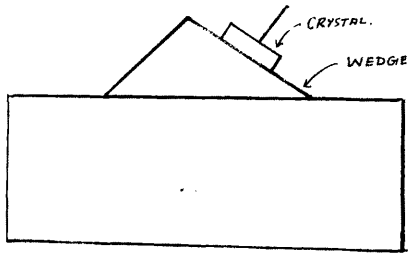


FIG. 11.  
Simple crystal holder for work in  
solids. (Angular propagation)

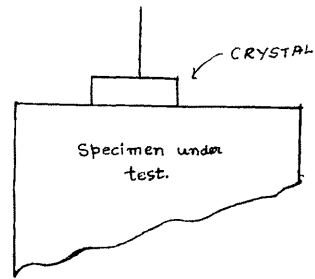


FIG. 9.  
Simple crystal holder.

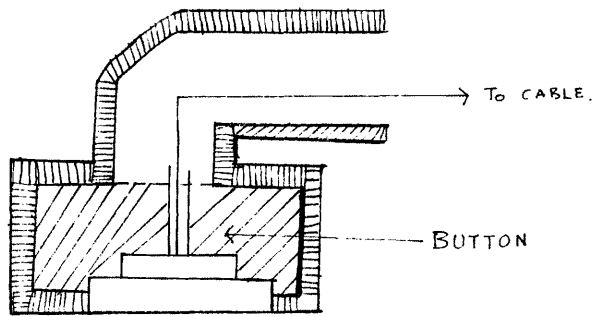


FIG. 10. Button holder.

is merely to lay it on the medium into which ultrasonics will have to be transmitted. The high voltage end of the radio frequency generator is connected to its back face. A suitable return circuit is provided by earthing the crystal's front face on the medium itself. (fig. 9 ) Bachmann<sup>45</sup> (1934) suggested to support the crystal around its side by pins or knife edges, which barely constrains it. This means of mounting is not very convenient as it is difficult to handle the unit. For test work, another type of mounting is to fix the back face of the crystal (fig. 10 ) to a solid support usually called a 'button'. The crystal is supported about the edges of the button and so mounted that it is constrained a minimum amount. The crystal is cemented into the button with a thin film of cement.

Holders for the purpose of angular propagation are shown in fig. 11

Arrangements for nodal mountings are described in chapter VII.

#### Coupling medium.

For ultrasonic propagation in solids, proper consideration should be <sup>be given to</sup> ~~made~~ for coupling the vibrating crystal to the investigating solid sample. If the crystal is placed

simply on the surface of the solid, very little energy will be transmitted through the interface into the material because of the great difference in specific acoustic impedance at the interface. Hence it is necessary to use some kind of coupling medium.

The coupling medium may be considered as a transformer which matches the impedance of the crystal to that of the solid example. Experiments on various liquids were made, particularly various types of transformer oil, glycerine, water, benzene, chlor<sup>?</sup>ine, sugar solutions, soap suds, mercury and various amalgams.

When Y - cut crystals are used, a mixture of rosin and oil is used, as the shear waves will not be efficiently transmitted through the liquid. The Y-cut crystals may be cemented permanently to the <sup>test-piece</sup> ~~medium~~ by a wax or cement.

For measurements at low temperature Rinehart<sup>46</sup> (1941) and Durand<sup>47</sup> (1936) tried several kinds of coupling materials. At room temperature, they found cellulose acetate is most useful and for low temperature measurements para-rubber dissolved in vaseline gave better results.

CHAPTER VIOptical Methods.Introduction.

In 1922, Leon Brillouin treated theoretically the problem of light scattering in a liquid through which ultrasonic waves were travelling. He predicted that the regular pattern of density variations in the liquid could act towards the light as a diffraction grating or as a crystal acts towards X-rays. Brillouin mentioned the possibility of experimental verification of his calculations making use of elastic waves set up in a liquid by a quartz crystal-driven by a high frequency oscillator.

The experiment was done independently in 1932 by Lucas and Biquard and Debye and Sears. A simple arrangement of such an experiment has a quartz of 300 Kc/s driven by a Hartley oscillator and radiating into a liquid contained in a glass-sided trough. A parallel beam of light from a sodium lamp, after passing through a slit, traverses the ultrasonic beam at right angles. In a telescope the light will be seen separated into the direct beam bordered on each side by diffraction maxima and minima.

Debye and Sears in order to see whether ultrasonic waves are markedly transmitted by a solid, put a glass block of cross section equal to the trough



and immersed it in the liquid. They concluded that the diffraction effect may be seen also in solids, if ultrasonic waves of high intensity are used.

Bachem, Hiedemann and Asbach<sup>48</sup> (1934)

described an optical arrangement for rendering visible ultrasonic waves by the method of secondary interferences. Considerable use of these phenomena has been made in measuring the velocity of sound in solids and liquids.

In transparent solids, the application of the Debye-Sears diffraction method or Bachem-Hiedemann stationary wave interference method, is usually more difficult due to the following reasons.

- (1) Flat, polished optical surfaces are essential and the material must be homogenous. Sufficient homogeneity is not found in many materials.
- (2) To make the optical effects visible, considerable higher acoustic intensities are required. This may result in undue local heating of the test materials, especially with plastics where the attenuation is large. Special arrangements should be made to keep the temperature uniform.

Despite all these limitations, optical techniques are extensively used for measuring the sound velocity in both

transparent and opaque solids.

The optical methods depend mainly on an analysis of standing waves. They are limited to higher ultrasonic frequencies ( $f > 1 \text{ Mc/s}$ ) and seldom yield information on losses. These optical methods, however, have some advantages over other methods, in that they require only small quantities of test materials and are ideally suited for the analysis of elastic properties of single crystals.

For the determination of sound velocity in solids, Schaffer and Bergmann<sup>49</sup> (1934) first used the optical diffraction technique. Their method was used also by a number of workers for the determination of elastic constants of solids. The newer methods of Bar and Walti<sup>50</sup> (1934), Bez-Bardili<sup>51</sup> (1935), Bhagabantam<sup>52</sup> (1944), Schneider and Burton<sup>53</sup> (1948) and Willard<sup>54</sup> (1951) are more precise. In the following pages, the various methods are discussed in detail, together with a summary of the results obtained.

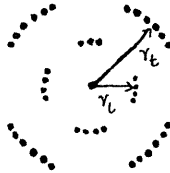
#### (A) Method of Schaffer and Bergmann.

Schaffer and Bergmann<sup>49</sup> (1934) used the phenomenon of diffraction of light by sound waves and determined the elastic constants of transparent solids. In this dynamical method, the crystal is usually taken in the

form of a cube. The cube may be excited with high frequency vibrations by a thin quartz crystal coupled through an oil film to one of its faces. Multiple reflections and mode coupling at the boundaries produce within the sample, a three-dimensional system of standing waves of both compressional bulk type and the transverse shear type. The experimental arrangement for producing diffraction images is shown in fig. 53. The light diffracted by the elastic strain lattice produces on the screen, regular systems (circles, ellipses, or higher order contours), which closely correspond to the Laue diagrams obtained by X-ray diffraction in crystals.

For isotropic solids, the characteristic diffraction pattern depends on the elastic constants, but for anisotropic solids, it depends also on the direction of light propagation. The diffraction images are completely independent of the external shape of the vibrating body.

For isotropic materials, like glass, the diffraction pattern consists of two concentric rings as shown in fig. page 64.



According to the theory given by Fues and Ludloff<sup>55</sup> (1935) the inner circle is formed by the diffraction of light by an elastic space grating generated by the longitudinal waves. The larger ring is produced by the shear waves whose smaller wavelength produces a larger angle of diffraction, according to the equation:-

$$\begin{aligned} \sin \theta_n &= \frac{n \lambda_0}{\lambda} \\ &= n \lambda_0 \frac{f}{c} \end{aligned}$$

where

- $\theta_n$  = angle of diffraction of the  $n$ th order
- $\lambda_0$  = wavelength of light
- $\lambda$  = wavelength of sound
- $c$  = velocity of sound
- $f$  = frequency.

The shear modulus is then given by

$$\begin{aligned} \mu &= \left( A f \lambda_0 / r_t \right)^2 \rho \\ &= c_t^2 \rho \end{aligned}$$

where  $A$  = distance between the centre of the specimen and the screen

$\rho$  = density of the specimen

$c_t$  = velocity of shear waves

It can be shown that

$$r_l / r_t = c_l / c_t$$

The value of Poissons ratio becomes

$$\begin{aligned} \sigma &= \frac{2 - (r_l / r_t)^2}{2 - 2(r_l / r_t)^2} \\ &= \frac{2 - (c_l / c_t)^2}{2 - 2(c_l / c_t)^2} \end{aligned}$$

Hence, from the measured radii of these circles, the elastic constants can be easily deduced.

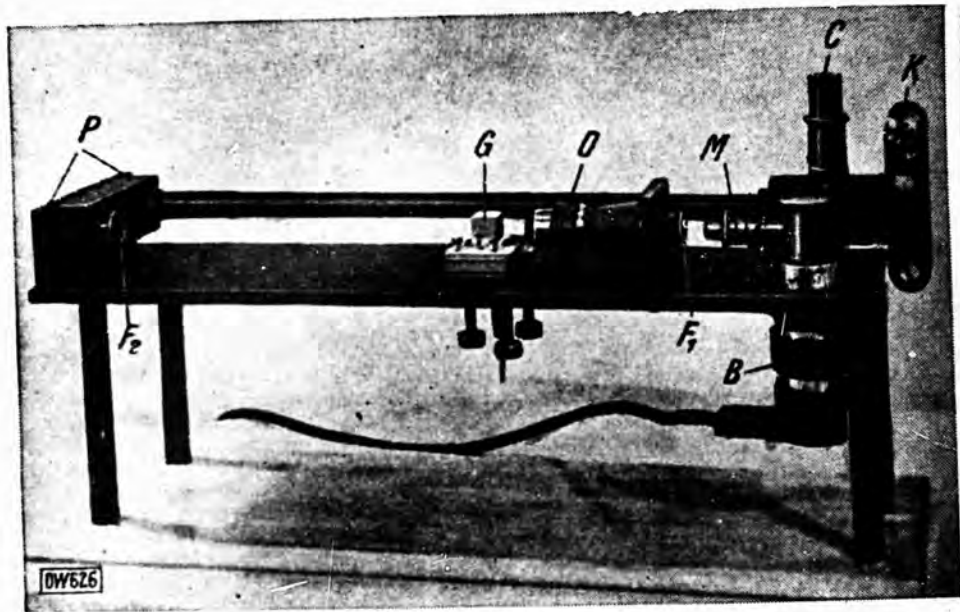


FIG. 53. EXPERIMENTAL APPARATUS OF  
SCHAFFER AND BERGMANN.

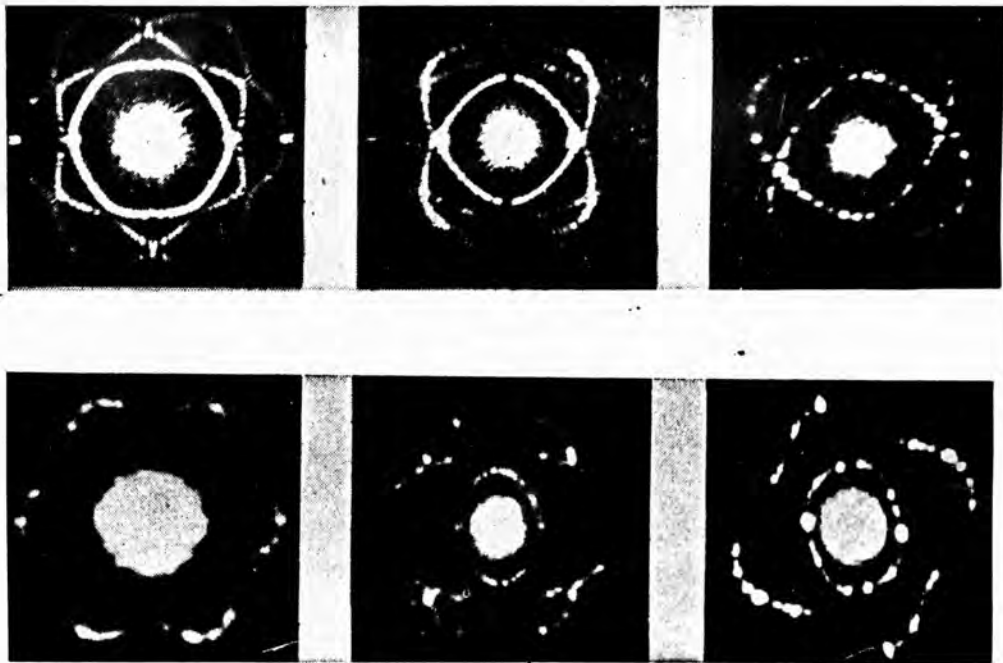


FIG. 54. TYPICAL DIFFRACTION PHOTOGRAPHS.

In anisotropic solids, the analysis is complicated in that the observed pattern depends on the orientation of the light beam with respect to the crystal axis on the planes of polarization of the light (Schaffer and Bergmann<sup>56</sup> 1935).

In a later experiment, Schaffer, Bergmann and Goehlich<sup>51</sup> (1937) made a systematic determination of seventy varieties of Schott's optical glass. The photographs were made with a cube of glass excited elastically from below and both polarized and unpolarized light were used. Typical photographs are reproduced in fig. 54 .

For unpolarized light, the inner circle produced by longitudinal waves comes out brighter and for light polarized at  $45^{\circ}$  and viewed through a crossed analysing Nicol, it is seen that the inner circle has almost disappeared. In the outer ring, the diffraction image<sup>is</sup> extinguished in both axial points.

With elliptically polarized light, the intensities of the two circles are equal.

A portable apparatus for optical determination of elastic constants of glasses and crystals, designed by Schaffer and Bergmann is shown in fig. 53.

Advantages and disadvantages.

The method of Schaffer and Bergmann has the great advantage that all the elastic constants may be determined from one and the same sample and the values so obtained for anisotropic bodies represent a system of constants complete in itself.

But apart from its serious limitation to only transparent solids, the method is difficult because of the necessity of using a very small circular aperture which produces a comparatively weak diffraction pattern. The intensity is too small for visual observation. The finding of resonance points of such a pattern takes a long time and to evaluate, the diffraction pattern must be photographed.

Some of the difficulties mentioned above were eliminated by Szymanowski<sup>58</sup> (1944) who determined the elastic constants of glass by using the modification of the method.

The transparent sample was cemented to a quartz which was excited by an oscillator of variable frequency. A strong source of polarized light, after passing through an adjustable slit, was made slightly convergent by a lens and then passed through the transparent sample to be investigated. The light after passing through the sample and the crossed Nicol, forms a magnified image of the slit which is viewed by a



microscope with micrometer eyepiece. The quartz is excited to one of its modes and the sample is set into strong resonant longitudinal oscillations which diffract the light. The sample is also set at the same time into transverse vibration, giving another diffraction pattern superimposed on the longitudinal pattern.

For the diffraction pattern due to longitudinal waves, one line is formed on each side of the central slit image, whereas two lines are formed on each side equidistant from the central image for the transverse waves. The distance between the two lines can be easily measured by the travelling wires of the micrometer eye-piece. The values of  $\sigma$ ,  $\mu$ , and  $E$  are given by the relations -

$$\sigma = \frac{1 - 2(d_l/d_t)^2}{2 - 2(d_l/d_t)^2}$$

$$\mu = \frac{\nu^2 k^2}{(d_t/2)^2}$$

$$E = 2\mu(1+\sigma)$$

where  $d_l$  = distance between two parallel lines for the longitudinal diffraction pattern,

$d_t$  = distance between two parallel lines for transverse diffraction pattern,

$\nu$  = resonance frequency

$\rho$  = density of the sample

$k$  = apparatus constant obtained by calibration with a grating having a known grating constant.

The resonance frequency was measured either by beats or with an accurate wave meter.

Szymanowski's values for the elastic constants of a sample of soft glass viz.,

$$\mu = 3203 \text{ Kg/mm}^2$$

$$E = 7889 \text{ Kg/mm}^2$$

$$\sigma = 0.2315$$

agree well with the accepted values for such kind of glass.

#### Method of Hiedemann and Hoesch.

Hiedemann and his colleagues (1935) at Cologne developed a method for measuring the elastic constants of glass.

A quartz was cemented to a glass block and excited elastically. Ordinary and polarized light were used and the sound wave grating was made directly visible by the method of secondary interferences. The longitudinal sound wave was measured by using ordinary light and Hiedemann and Hoesch<sup>59</sup> (1935) regarded the sound wave grating when examined between crossed Nicols as due to transverse waves, the wavelength of which can be measured directly.

This method has the advantage over that of Schaffer and Bergmann in that the accuracy of the direct measurement of the grating spacing is somewhat higher

but the method is more troublesome as it requires two sets of photographs of the two sound wave gratings. Furthermore the method cannot be used with either anisotropic or opaque bodies. No systematic measurements were carried out in the above way.

#### Method of Bar and Walti.

Bar and Walti<sup>50</sup> (1935) described a method which is entirely different from that of Schaffer and Bergmann, for determining<sup>in</sup> elastic constants of isotropic solids. The method was further modified by Bez-Bardili<sup>51</sup> (1935) and later by Bhagabantam<sup>52</sup> (1944) whose improved form is known as the 'wedge' method. The material, which need not be optically transparent, is in the form of a narrow wedge. The quartz generator is applied to one side at a height above the tip which determines the thickness of the wedge to be traversed.

During the experiment, the wedge is immersed in a liquid. The principle behind this method is that if an ultrasonic wave travelling in a liquid meets a plane parallel plate of an isotropic solid of thickness, 'd' part of the wave is reflected and part transmitted. Maximum transmission takes place with vertical incidence if the relation  $n\lambda/2 = d$  holds where n is a whole number and  $\lambda$  sound wave length in the plate. If the ray of

sound meets the plate obliquely at an angle  $\theta$  to the normal and is refracted at an angle  $(H)$  to the normal for the longitudinal wave, the relation for maximum transmission is given by

$$n \lambda' / 2 = d \cos (H)$$

Again

$$R^2 = \frac{\lambda}{\lambda'} = \frac{\sin \theta}{\sin (H)} \text{ where } \lambda \text{ is the wavelength of the sound in the liquid.}$$

$R$ , the index of refraction for sound passing from liquid to plate.

From those relations,

$$\sin^2 \theta = R^2 - \left( \frac{n\lambda}{2} \right)^2 \frac{1}{d^2}$$

For oblique incidence, transverse waves are produced in it having a shorter wavelength  $\bar{\lambda}'$  and for which the index of refraction is  $\bar{R} = \lambda / \bar{\lambda}'$

and

$$\sin^2 \theta = \bar{R}^2 - \left( \frac{n\lambda}{2} \right)^2 \frac{1}{d^2}$$

The Poisson's ratio may be deduced from the relation

$$\sigma = \frac{k^2 - 2}{2(k^2 - 1)} \quad \text{where } k \text{ is the ratio of } \frac{\bar{R}}{R} = \frac{\lambda'}{\bar{\lambda}'}$$

The evaluation of  $R$  and  $\bar{R}$  were carried out

graphically.

This method has two disadvantages.

- (1) It is not easy to separate in the observations the longitudinal and transverse wave system by choosing a suitable angle of incidence.
- (2) At certain angles of incidence 'exchange waves' are produced by the transverse wave generated by reflection at the farther wall.

Bez-Bardili<sup>51</sup> (1935) measured the elastic constants of aluminium, iron, copper, brass and glass. For this purpose ultrasonic waves of known velocity were passed through a liquid and the path was made visible on a screen by means of the circular diaphragm method of Bar and Meyer<sup>60</sup> (1933). A plane parallel plate of the substance to be investigated was put in the liquid and arranged so as to be set at a measured angle to the sound wave. The critical angle of total reflection was observed both for longitudinal and transverse waves and the velocity of sound was then calculated for two sorts of waves. Bez-Bardili further determined the velocity of sound from the maxima of the plate's transmission of the two waves in relation to the angle of incidence using the similar method of Bar and Walti. The accuracy of the value of the constants measured was about 1%.

A. Schock

Abkürzung  
1952

"Wedge" Method.

The determination of the elastic constants of solids including some Indian rocks by the ultrasonic wedge method has engaged the attention of Bhagabantam (1944) and his co-workers for several years. Bhagabantam and Bhimsenachar<sup>52</sup> (1944) first described the wedge method, and employed it for determining the elastic constants of two cubic crystals, viz., pyrites and galena. Later Bhagabantam and Rao<sup>61</sup> (1946) measured the elastic constants of glass, steel, brass and platinum in the frequency range 3-16 Mc/s using the same method. It was further used by the same workers to determine the elastic constants of diamond<sup>62</sup> (1946) and zircon<sup>63</sup> (1955)

Rao<sup>61, 65, 66</sup> (1947, 1948, 1949) used the 'wedge' method and determined the elastic constants of potassium alum, chromium alums and some mixed alums and later published the values of the elastic constants of ammonium, potassium and chromium alums belonging to the cubic system and sections parallel to (100), (110) and (111) faces and using the frequency range of 8 Mc/s. The elastic constants of sodium chlorate and sodium bromate were also measured.

The 'wedge' method developed by Bhagabantam and Bhimsenachar is described as follows.

A suitably cut and silvered quartz or tourmaline 'wedge' is used as a piezo electric vibrator.

A series-fed Hartley oscillator using a Mullard D.O.24. valve serves as the source of excitation. As the frequency of the electrical circuit is varied, different points on the 'wedge' are thrown into resonance and it thus gives a continuous ultrasonic spectrum. The range of the spectrum depends upon the angle of the wedge. The crystal plate is placed on an annular brass electrode. The wedge is laid on the crystal using some liquid for securing good acoustical contact. The top of the wedge is touched lightly by a spring which keeps the wedge and the crystal pressed on to the brass electrode. The mount is provided with levelling screws to facilitate accurate alignment. The arrangement is then dipped into a trough containing carbon tetrachloride. The ultrasonic beam from the wedge passes through the crystal and then enters the liquid. A beam of light with the usual optical arrangement is made to pass through the ultrasonic grating in the liquid and Debye-Sears diffraction effects are observed. When the frequency of the wedge corresponds to the fundamental or a harmonic of the longitudinal vibration of the plate, the sound beam is best transmitted and the Debye-Sears pattern will have the maximum intensity. The transmission frequency is measured with a wavemeter. Using the relation  $C_L = 2df$

where  $C_L$  = velocity of the longitudinal sound wave in a direction parallel to the thickness of the plate

$d$  = measured thickness

$f$  = frequency of the fundamental

and substituting the value of  $C$  in Christoffel's equation, the effective elastic constant is calculated from the relation

$$C'_{33} = C_l^2 \rho \quad \text{where } \rho \text{ is the density}$$

of the material.

#### Advantages and Disadvantages of the 'Wedge' method.

As this method does not permit the transmission of thickness transverse waves, it is not suitable for obtaining the full set of elastic constants.

Bhagabantam and Rao<sup>61</sup> (1946) used a sufficiently small and thin specimen and could excite the shear mode only very feebly.

Balkrishna<sup>67</sup> (1955) who studied the elastic properties of some Indian rocks employing the 'wedge' method reported that on account of the special feature of the rocks, namely, their heterogeneous nature in composition, grain size etc., the 'wedge' method is unsuitable to excite the shear modes in rocks like granite, dolerite etc. The novelty of the method consists in the use of a continuous ultrasonic spectrum and the employment of the



Debye-Sears effect as a delicate test for maximum transmission.

The method is also suitable when specimens are available in small bits.

Ramchandra Rao and Venugopal Rao<sup>68</sup> (1955) reported a modified wedge method<sup>of</sup> determining the shear wave velocities in isotropic solids. In this method the specimen is placed at an angle to the sound beam instead of in contact with the piezo electric wedge as in the case of<sup>the</sup> normal wedge method. The velocity of sound waves in the material is calculated, employing the following Raleigh's expression for maximum transmission of sound waves through a plane parallel plate at oblique incidence:

$$\left(\frac{c}{c_1}\right)^2 = \sin^2\phi + \left(\frac{c}{2d} \cdot \frac{\eta}{f}\right)^2$$

- Where
- $c$  = velocity in the surrounding medium
  - $c_1$  = velocity of sound in the solid
  - $d$  = thickness of the specimen
  - $\eta$  = order of the transmission maximum
  - $\phi$  = angle of incidence.

This modified 'wedge' method is particularly very useful for measuring the velocity in rocks where it is very difficult to excite the shear modes at normal incidence.

TABLE NO. 1

Elastic constants of Alkali halides (in units of  $10^{11}$  dynes/cm<sup>2</sup>)

	Huntington	Bergmann	Durand	Bridgeman	Hunter & Siegal
<b>LiF.</b>					
C <sub>11</sub>	9.74 - 0.01	11.77			
C <sub>12</sub>	4.04 - 0.02	4.33			
C <sub>44</sub>	5.54 - 0.03	6.28			
<b>NaCl</b>					
C <sub>11</sub>	4.85 - 0.01	4.67	4.99	4.70	4.86
C <sub>12</sub>	1.23 - 0.02	1.23	1.31	1.23	1.19
C <sub>44</sub>	1.265 - 0.025	1.19	1.270	1.281	1.28
<b>KBr</b>					
C <sub>11</sub>	3.45 - 0.07			3.33	
C <sub>12</sub>	0.54 - 0.03			0.58	
C <sub>44</sub>	0.508 - 0.005			.621	
<b>KI</b>					
C <sub>11</sub>	2.690 - 0.005			2.67	
C <sub>44</sub>	0.362 - 0.001			0.421	



"Rotating Plate Technique"

Another suitable technique based on the principle of Bez-Bardili for the measurement of velocities and elastic constants of solids was described by Schneider and Burton<sup>53</sup> (1948).

Krishna Murty and Balkrishna<sup>69</sup> (1953) used the similar technique for the measurement of ultrasonic velocities in some Indian rocks. The method depends upon the variation in intensity of transmitted energy with an angle between the incident beam and the sample plate. A plane parallel sheet of material is used for the sample and is rotated about the vertical axis which is perpendicular to the horizontal sound beam. The sound beam strikes the sample plate at an angle  $\theta$ . Since the velocity in the solid is usually greater than the velocity in the liquid, the wave trains in the solid are refracted away from the normal and the following relations hold.

$$\begin{aligned} n_l &= \sin \theta / \sin \phi_d = c_{liq} / c_l \\ n_t &= \sin \theta / \sin \phi_t = c_{liq} / c_t \end{aligned} \quad (1)$$

Where

- $n_l$  = index of refraction for dilatation waves,
- $n_t$  = index of refraction for shear waves,
- $c_{liq}$  = velocity of sound in the liquid.

$C_t$  = velocity of shear waves in the solid  
 $C_l$  = velocity of dilatation waves in the solid.

$\phi_d$  increases as  $\theta$  increases, until at a value when  $\theta = \theta_1$ ,  $\phi_t = 90^\circ$  which means that the dilatational waves are totally reflected and then the transmitted energy is the minimum.

If  $\theta$  is decreased further to  $\theta_2$ ,  $\phi_t$  become  $90^\circ$ , shear waves are totally reflected.

At  $\theta_1$ , and  $\theta_2$  the above relation becomes

$$C_l = C_{\text{liq}} / \sin \theta_1 \quad \text{and} \quad C_t = C_{\text{liq}} / \sin \theta_2$$

Determining experimentally the values of  $\theta_1$  and  $\theta_2$  and substituting ~~in~~  $C_l$  and  $C_t$  may be calculated.

This "rotating plate" method has the following advantages.

- (i) Simple sample shape may be employed thereby extensive sample preparation may be avoided.
- (ii) The method does not involve the sample thickness.
- (iii) The sample is not damaged by the testing procedure.
- (iv) No tedious calculations are required for evaluating the result and the method is simple and rapid.

But it has been observed by Schneider and Burton that

ultrasonic velocities as measured by this method show a marked dependence on the thickness of the plate used. Although there is no simple expression relating the sample thickness and the accuracy of the equation (1) an empirical relation was proposed by both Bez-Bardili and Sanders<sup>70</sup> (1939) that if the product of the sample thickness (in centimeters) and measuring frequency (in Mc/s) is greater than 4 cm Mc/s, the Eq. (1) will be valid.

Both Vedam<sup>71</sup> (1950) and Ramchandra Rao<sup>72</sup> (1950) independently reported the measurement of elastic constants of various samples of glass and potash alum respectively, by a method which consists in the use of a quartz plate attached to the substance under investigation, and the variation of ultrasonic energy transmitted through the substance inside the liquid, with the frequency, is studied over the entire resonance breadth of the quartz. Since the resonance breadth of the quartz crystal covers a fairly wide region, the ultrasonic energy transmitted through the sample will exhibit a series of sharp maxima which are close to one another, when the frequency of the oscillator is continuously varied, and it can be easily detected by using the Debye-Sears and Lucas-Bizuard arrangement. Each of these transmission maxima corresponds to the excitation of one of the harmonics of the longitudinal vibrations of the crystal, and the

differences between the successive maxima are found to be identical corresponding very nearly to the longitudinal fundamental of the crystal plate. Using the value of the longitudinal fundamental frequency of the crystal thus determined and the thickness of the crystal, the longitudinal velocity and hence the effective elastic constant at a particular direction is calculated.

With this type of set up, Ramchandra Rao, found that the shear modes do not come up prominently and overcame this difficulty by employing a Y-cut quartz plate for determining the velocities of shear modes; a main advantage of this method.

Further, higher accuracy in determination of elastic constants is attained by this method because of the large thickness of the crystal used and the increased number of transmission maxima obtained with moderate powers of the oscillator.

On the other hand, this method has the drawback that it requires a crystal block of thickness of the order of 1 to 1.5 cm and is not suitable for crystals available in very small sizes.

TABLE NO. 3

Elastic constants of cubic crystals in  $10^{11}$  dynes/cm.<sup>2</sup>

Crystal	C <sub>11</sub>	C <sub>12</sub>	C <sub>44</sub>	Measured by
Galena	12.70	2.98	2.48	Bhagabantam & Sehasgiri- Rao
Chromite	32.25	14.37	11.67	Doriaswami, M.S.
Diamond	95.00	39.0	43.0	Bhagabantam & Bhimasenachar.
Pyrite	36.02	-4.64	10.52	Doriaswami, M.S.
Fluorspar	16.44	5.02	3.47	Bhagabantam, S.
Magnetite	27.25	10.6	3.71	Doriaswami, M.S.
Sodium Chlorate	5.09	1.55	1.18	Bhagabantam & Suryanarayana
Rock Salt	4.97	1.27	1.27	Bhagabantam, S.
Zinc Blende	10.73	7.22	4.12	Bhagabantam & Suryanarayana
Ammonium alum	2.50	1.06	0.88	Rao Sundra R.V.G.
Potassium alum	2.56	1.07	0.86	: : :
Chromium alum	2.37	0.93	0.77	: : :



TABLE NO. 3

Elastic constants of cubic crystals in  $10^{11}$  dynes/cm.<sup>2</sup>

Crystal	C <sub>11</sub>	C <sub>12</sub>	C <sub>44</sub>	Measured by
Barium Nitrate	5.93	1.89	1.21	Rhimsenachar & Behasgiri Rao
Lead Nitrate	4.56	3.09	1.37	: : :
Strontium Nitrate	4.73	2.18	1.46	: : :
Lithium fluoride	11.9	4.58	5.42	Rao Sundra R.V.G.
Sodium Bromate	5.31	1.91	1.49	: : :

Methods of Willard

<sup>5A</sup> Willard (1951) described three sound wave interference methods for measuring the longitudinal and transverse ultrasonic velocity in opaque as well as transparent solids.

The first one <sup>is</sup> the immersed block method. Here one beam travels entirely in a reference liquid, while the other beam travels a parallel path in an immersed transparent test specimen. The test material must be transparent and have two optical faces and one acoustic face.

The second one is the immersed prism method where one beam travels entirely in a reference liquid while the other beam travels an adjacent course through an immersed, transparent or opaque test prism, and on into the liquid at an angle to the first beam.

The third one is the isosceles prism method where the test material may be opaque and must have three acoustic faces with known angular inclination, and the attachment of at least one sound generator to the prism.

The three methods described by Willard are simple and direct. Longitudinal and transverse velocities may be measured independently in opaque as well as transparent solids. Materials with a wide range of impedance and attenuation may be measured. The accuracy of measurements <sup>is</sup> ~~are~~ comparable with that obtainable by past

methods. Table 4 gives the results of the velocity and attenuation measurements by the above methods.

TABLE NO. 4

Material	Velocity $C_L \times 10^5$	Velocity $C_T \times 10^5$	Attenuation A	Density $\rho$
Dural 17st.	6.5	3.12		2.7
Brass half-hard	4.7	2.11		8.5
Polystyrene	2.35	1.12	2	1.06
Tenite, cellulose acetate butyrate, 13% plasticizer	2.02		10	1.21
Polyvinyl formal	2.68		10	1.24
Polyvinylidene Chloride	2.4		18	1.71
Plexiglass, polymethyl methacrylate	2.68		5	1.18
Poly n-butyl methacrylate	1.96		5	1.05
Poly i-butyl methacrylate	2.08		6.	1.05
Neoprene	1.51		20	0.99
Polyethylene (A at 3-30 Mc)	2.0		4.7 $\frac{1}{11}$	0.90
Nylon 6-6 (A at 3-30 Mc)	2.68		10 $\frac{1}{15}$	1.14

TABLE NO. 4

Material	Velocity $C_L \times 10^{-5}$	Velocity $C_T \times 10^{-5}$	Attenuation A	Density $\rho$
Nylon 6-6 (A at 3-30 Mc)	2.56		1.0 $f^{1.5}$	1.11
Water for reference	1.50		0.015	1.00

Measured velocities of longitudinal  $C_L$  and transverse  $C_T$  waves in cm/sec at 25° c and 2.5 Mc. Longitudinal attenuation in db/cm at 25° c and 2.5 Mc except as noted. Density in gram/cm<sup>3</sup>,  $f$  in Mc.

Following the explanations of Raman and Nath<sup>17</sup> (1936) on the Debye-Sears effect, Sreekandath<sup>13</sup> (1956) has recently reported a new method for measuring ultrasonic wave velocity in solids.

The method is capable of<sup>a</sup> high degree of accuracy but is applicable only to homogenous solids which have<sup>a</sup> small absorption coefficient.

TABLE NO. 5Velocity of ultrasonic waves in some rocks.

Rock	Density in gm/cm <sup>3</sup>	Grain size	C <sub>L</sub> M/sec	C <sub>T</sub> M/sec
quartzite	2.51	0.1 mm.	6621	3400
quartzite	2.56	0.3 mm.	5610	3030
quartzite	2.54	0.6 mm.	5060	2700
Limestone	2.80	fine	7069	3403
Limestone	2.82	medium	6400	3200
Limestone	2.81	coarse	6260	3065

In coarse grained rocks, the velocities are low and the absorption is high. In fine grained rocks, the velocities are high and the absorption is low.

Determination of Elasto-Optical Constants.

Isotropic substances like glasses, possess two elastic constants  $C_{11}$  and  $C_{12}$  which are related to Young's modulus, Modulus of rigidity and Poisson's ratio by the following relations:-

$$E = \frac{C_{11} - C_{12}}{C_{11} + C_{12}} (C_{11} + 2C_{12})$$

$$\eta = \frac{C_{11} - C_{12}}{2}$$

$$\sigma = \frac{C_{12}}{C_{11} + C_{12}}$$

Again these substances have two Pockel's elasto-optic constants  $p_{11}$  and  $p_{12}$  which are related to the corresponding piezo-optic constants  $q_{11}$  and  $q_{12}$  by the relations

$$p_{11} = C_{11} q_{11} + 2C_{12} q_{12}$$

$$p_{12} = C_{11} q_{12} + C_{12} (q_{11} + q_{12})$$

Instead of the parameters  $p_{11}$  and  $p_{12}$  it is now usual to use

$p$  and  $q$  where

$$p = \frac{1}{2} \mu p_{12}$$

$$q = \frac{1}{2} \mu p_{11}$$

$\mu$  being the refractive index.

The calculation of these index variations is a problem of photoelasticity. An elastic wave creates periodically varying strains which in turn produce local periodic alterations of the optical index ellipsoid. These



pulsations of the index ellipsoid determine the fluctuations of the index of refraction for light polarized in any direction.

For determining the absolute values of the strain optical constants, a measure of the absolute change in the refractive index for light polarized parallel and perpendicular to the direction of pressure is needed. The value of  $(p - q)$  can be determined by stressing the glass and measuring the difference between the two refractive indices for light propagation parallel and perpendicular to the direction of pressure. With light polarized at  $45^\circ$  to the direction of pressure, the light emerging from the glass cube under stress will be elliptically polarized, which can be analysed with the help of a Babinet's Compensator.

Then it can be shown that the measured fringe shift  $x$  for a stress  $P$  is given by the relation

$$(p - q) = \frac{C_{11} - C_{12}}{\mu^2 P d} \cdot \frac{\lambda}{b} x.$$

where

$d$  = length of the path of light within the glass.

$b$  = distance between the two successive fringes in the Babinet's Compensator for wavelength

$\mu$  = refractive index of the glass in the undeformed state.

Thus by measuring the fringe shift for a known stress  $P$ , the value of  $(p - q)$  can be determined if  $(C_{11} - C_{12})$  is known.

The method applied for the determination of elasto-optical constants is similar to that of Schaffer and Bergmann (1934) as described before. The theory of the characteristic diffraction pattern formed, is given by Fues and Ludloff<sup>55</sup> (1935) according to which the inner ring is produced by the longitudinal waves and the outer ring is produced by the transverse waves.

$$r_l = \frac{D\lambda}{2\pi} \sqrt{\frac{\rho\omega^2}{c_{11}}}$$

$$r_t = \frac{D\lambda}{2\pi} \sqrt{\frac{2\rho\omega^2}{c_{11}-c_{12}}}$$

D = distance between the glass cube and the photograph plate.

$\rho$  = density.

$\lambda$  = wavelength of light

$\omega = 2\pi f$  ,  $f$  = frequency

$r_l$  = radius of the ring formed by longitudinal waves.

$r_t$  = radius of the ring formed by transverse waves.

Thus by measuring  $r_l$  and  $r_t$  ,  $c_{11}$  and  $c_{12}$  can be calculated.

Bergmann and Fues<sup>74</sup> (1936) measured the elasto-optical constants of five different optical glasses and their results agree well with that of Pockel's.

Mueller<sup>75</sup> (1938) has shown that the above method with slight modification can be used to determine the value of glass and cubic crystals.

Using a horizontal slit and incident light polarized at  $45^\circ$  to it, the direction of polarization of the first order longitudinal pattern will be oriented at an angle  $\theta$  when

$$(\tan \theta + 45) = \frac{J_1(R\nu)}{J_1(\nu)}$$

$J_1$  = first order Bessel function

$$R = p/q$$

$$\nu = \frac{2\pi aL}{\lambda}, \quad \begin{array}{l} a \text{ is a function of the sound amplitude,} \\ L \text{ the width of the ultrasonic field,} \\ \lambda = \text{wavelength of light.} \end{array}$$

If now, the variation of  $\theta$  with sound amplitude is plotted

$$\theta \text{ approaches a limiting value } \theta_1 \\ \text{when } (\tan(\theta_1 + 45)) = R = p/q$$

Vedam<sup>71</sup> (1950) measured the elasto-optical constants of glass by a slightly modified method of Mueller (1938).

Expanding the equation for more accurate results,

$$\begin{aligned} \tan(\theta + 45) &= \frac{J_1(R\nu)}{J_1(\nu)} \\ &= R \left[ 1 - \frac{\nu^2}{8}(R^2 - 1) + \frac{\nu^4}{192}(R^4 - 3R^2 - 1) + \dots \right] \end{aligned}$$

for the first order longitudinal pattern.

Neglecting the terms involving  $\nu^4$  and higher orders,  $(\tan(\theta + 45))$  when plotted against the square of the sound amplitude, a straight line is obtained from which the value of  $R$  can be calculated when  $\nu = 0$ .

Iyengar<sup>76</sup> (1955) experimentally studied the Lucas-Biquard

effect of optical refraction in a sound field and has shown that the effect enables the determination of the absolute changes of refractive index and the ratio of elasto-optical constants.

The ratio of strain optical constants in glasses for three wavelengths of light is given below:

	$P_{12} / P_{11}$		
Glass	3893 Å	5461 Å	4338 Å
I	1.37	1.38	1.40
II	1.54	1.52	1.57

Iyengar concluded that his arrangements are valid also for crystalline media.

CHAPTER VIIResonance Method.Introduction:

The principle of this method of measuring elastic and dissipative properties of materials is that if an oscillating force of constant amplitude and of frequency which can be varied, is applied to a mechanical system, the amplitude of the resulting vibration passes through a maximum at a frequency which is known as the resonant frequency of the system. The value of this resonant frequency depends on the elastic properties of the system whilst the breadth of the resonance peak gives a measure of the dissipative forces which are present.

Most of the early work for measuring internal dissipation in solids at high frequency was done by this method.

If suitable precautions are taken to eliminate extraneous damping due to air resonance, loss at the supports, etc., both the internal friction and the elastic constants of a specimen may be determined by this method and measurements have been made by using longitudinal, flexural and torsional oscillations at high frequencies. The method may be used when damping is so large that free oscillations decay too rapidly for accurate measurements to be made, but the method is

not very suitable for specimens with very low internal friction since the resonance peak becomes too sharp for accurate work. The main disadvantage of the resonance method is that the coupling between the driving system and the specimen may result in a change in resonant frequency and in the shape of the resonance peak. It is sometimes necessary to carry out a series of measurements, with varying degrees of coupling, to allow for this effect.

Quimby<sup>77</sup> (1925) was among the first to employ the resonance technique for measuring internal friction in solids. Later, Quimby<sup>78</sup> (1932) in co-operation with Lewish Balamuth, W.T. Cooke, Fred Rose, Sidney Siegel, Clarke Williams and Jerrold Zacharias, developed a number of composite piezoelectric oscillators. These composite oscillators, with their succeeding developments are described in the following pages. The typical values of the elastic constants and internal dissipation measured by different workers are tabulated and compared.

Measurement of internal friction in single and poly-crystals.

The method described by Zacharias<sup>79</sup> (1933) for the measurement of Young's modulus over a wide range of temperature was applied to single crystals of pure nickel

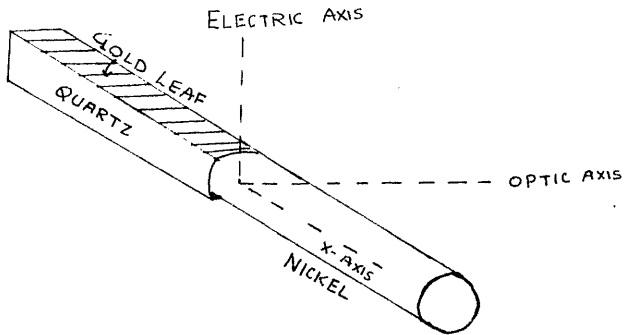


FIG. 12 COMPOSITE OSCILLATOR [ZACHARIAS]

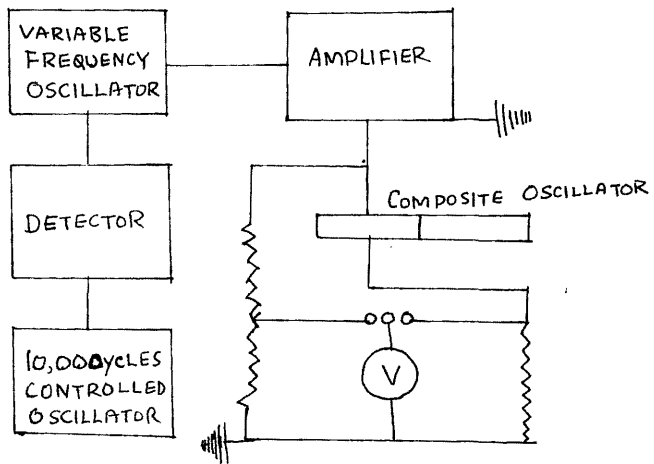


FIG. 13. THE ELECTRICAL CIRCUIT ARRANGEMENT.

and to hard-drawn polycrystalline commercial nickel between 30°c to 400°c and in the frequency range of 17 Kc/s to 105 Kc/s. The values of the Young's modulus were calculated from the relationship given by Raleigh as:-

$$E_1 = \rho_1 f_n^2 (4L_1^2 + 2\pi^2 \sigma^2 r_1^2)$$

where

$E_1$  = Young's modulus for the direction of cylinder axis.

$f_n$  = fundamental frequency of free longitudinal vibration.

$\rho_1$  = density of the material

$L_1$  = length of the rod

$\sigma$  = Poisson's ratio

$r_1$  = radius of the rod.

The specimen forms one part of a composite piezoelectric oscillator of the sort described by Quimby. A quartz rod of square cross section equal in area to that of the specimen is so cut from a crystal that the optic axis is perpendicular to one pair of opposite sides and an electric axis to the other. The latter pair is coated with gold leaf. One end of the nickel rod (as shown in the fig. 12) is thinly copper-plated and covered with a molten mixture of copper oxide and boric oxide. The rods are then cemented together in a vacuum under pressure at a temperature of 600°c. The oscillator is



supported by fine wires and a sinusoidal potential difference is established between the coatings of gold leaf. The electric field in the quartz is accompanied by a piezoelectric stress proportional thereto. In consequence of this harmonically varying stress, a stationary state of forced longitudinal vibration is established in the composite rod.

The schematic diagram of the electrical circuit is given in fig. 13. .

The composite oscillator lies in a fused silica boat on two fine wires located at the nodes of vibration. The boat is situated at the centre of a horizontal electric furnace about which is wound a Solenoid. An astatic magnetometer is mounted above the Solenoid and over the specimen. The specimen was demagnetized with a diminishing alternating current in the Solenoid before each observation. The temperature of the specimen is measured with a chromel-alumel thermocouple. Zacharias concluded that the variation of Young's modulus with temperature in these nickel samples depends on the previous thermal history of the samples. Between  $30^{\circ}$  and  $200^{\circ}\text{c}$ , Young's moduli for annealed specimens were found to decrease about 13%. This is again followed by an increase to the Curie point of about 6% and above the Curie point by a linear decrease. For hard-drawn specimens and specimens quenched at  $1100^{\circ}\text{c}$ ,

the minimum is wholly absent. Young's modulus was found to decrease continuously to the Curie point where the temperature coefficient changes abruptly.

Cooke<sup>8c</sup> (1936) measured the variation of internal friction and elastic constant with magnetization in iron by an experimental method which utilizes the properties of a separately excited composite piezoelectric oscillator as described before. In this method the composite oscillator forms one arm of an a.c. bridge which is excited by an alternating voltage of constant amplitude and variable frequency. The a.c. bridge has been described by Stratton (1926). Values of the decrements and moduli are deduced from the observed variation of the electrical impedance of the oscillator with frequency. The precision of decrement measurement fails when this quantity is as great as the order of  $10^{-3}$ .

Brown<sup>9a</sup> (1936) employed the method of Cooke and measured the variation of the rigidity modulus and torsional decrement, also magnetization in the unannealed and annealed Armco iron. Formulae were derived to evaluate the contributions to the moduli and decrements arising from eddy currents in the vibrating specimen by the change in magnetization produced by the varying stress. Magnetostriction and Wiedemann effect coefficients were also measured and evaluated by Brown.

Further investigations of the internal friction in single and polycrystalline metals of copper, lead, and tin were made by Read<sup>82</sup> (1938)

The experimental technique was the same as devised by Cooke<sup>80</sup> and Brown<sup>81</sup> (1936). The frequency of measurements was 38.9 kilocycles and the temperature was about 25°C. The observed longitudinal decrements for single crystals and the corresponding values obtained for polycrystals are tabled below for comparison:

	<u>Copper</u>	<u>lead</u>	<u>tin</u>	<u>measured by</u>
Single crystal	$3.6 \times 10^{-5}$	$2.8 \times 10^{-4}$	$6.9 \times 10^{-5}$	Read (1938)
Polycrystal	$3.5 \times 10^{-3}$	$4.6 \times 10^{-3}$	$5.4 \times 10^{-3}$	Forster and <sup>83</sup> Korster (1937)

It thus appears that the internal friction of a single metal crystal is substantially less than that of the polycrystalline material. The effect of internal strain on the internal friction of crystalline copper is noteworthy. Read concluded that annealing in vacuum decreases the value of internal friction for copper crystals, but the decrement values for lead and tin crystals remain unaffected by annealing.

L. Balamuth<sup>84</sup> (1934) described the composite piezoelectric oscillator and used it to measure the principal Young's modulus of rock salt between 78°K and 273°K. The electrical circuit is slightly different from that used

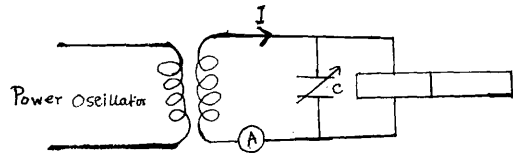


Fig. 14. The Cady Circuit.

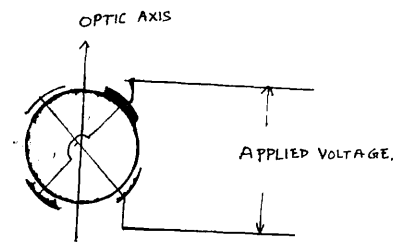


Fig. 15. Electrical connection to the quartz.

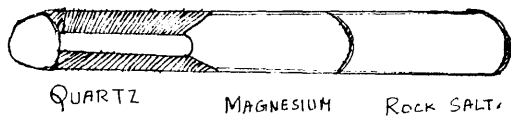


Fig. 16. Triple Oscillator.

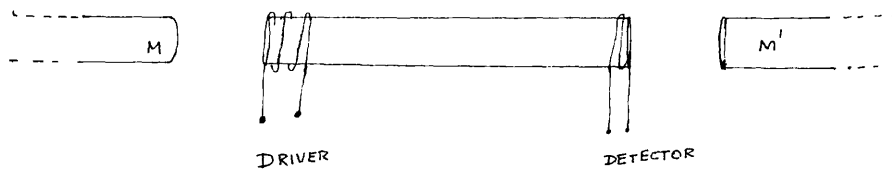


Fig. 17. Air core solenoid driver and detector.

by Zacharias.

The electrodes on the quartz are connected to the terminals of a variable condenser in a simple resonant circuit given by Cady (1922). The circuit is given in fig. 14 . This circuit is coupled so loosely to the output of a vacuum tube oscillator that the voltage induced therein is independent of the impedance. The amplitude of the current which flows in the resonant circuit is measured with a vacuum thermocouple. For temperature control, the oscillator was enclosed in the evacuated glass cylinder together with a platinum resistance thermometer, and these were placed in a liquid bath held in a Dewar flask with stirring arrangement. The liquid used at temperatures above  $213^{\circ}\text{K}$  was methanol. Between  $140^{\circ}\text{K}$  and  $213^{\circ}\text{K}$  the liquid was composed of 18.1% Chloroform, 8% ethyl chloride, 41.3% ethyl bromide, 12.7% trans-dichloroethylene and 19.9% trichlorethylene. Below  $140^{\circ}\text{K}$ , the observations were taken separately with the oscillator and thermometer immersed in liquid oxygen, liquid air and liquid nitrogen.

The frequencies of the quartz rods used were 86,691 cycles and 111,517 cycles respectively. The results obtained by Balumuth agree well with the theory.

The method of Balamuth is accurate and it can be applied to small specimens.

Rose<sup>115</sup> (1935) expended the method of Balamuth

to measure all the elastic moduli of any solid crystals at temperatures below 0°c. In 1928, Giebe and Scheibe showed that a suitably cut cylinder of quartz can be excited to torsional vibration. Rose first made use of such a crystal as a driver of a composite oscillator.

For fragile substances, like rock salt, the differential thermal expansion at the cemented interface, which accompanies any change in temperature, produces longitudinal cracks in the specimen. These are without effect upon the frequency of the longitudinal mode of vibration.

Rose overcame this difficulty by placing between the quartz and specimen cylinders, a cylinder of stout material whose coefficient of thermal expansion is very nearly the same as that of the specimen and made the use of a 'triple' oscillator.

The triple oscillator of quartz-magnesium and rock salt and the electrical connections to the quartz cylinder are shown in figs. 16 and 15 respectively.

The fundamental working formula of the piezoelectric method of all the elastic constants of any solids substance is given by the solutions for of the equation

$$m_1 \tan \gamma_1 / \gamma_2 + m_2 \tan \gamma_2 / \gamma_2 + m_3 \tan \gamma_3 / \gamma_3 - (m_1 m_2 m_3 / \gamma_1 \gamma_2 \gamma_3) \tan \gamma_1 \gamma_2 \gamma_3 = 0$$

where  $m_i$  = mass of the cylinder

$y_i$  =  $\pi f / f_i$ ,  $f$  = frequency of the applied voltage.

and  $f_i$  =  $(n/2L_i)(\mu_i/\rho_i)^{1/2}$

where  $n$  is an integer,

$L_i$  = length of the cylinder

$\mu_i$  = modulus of rigidity for the direction of cylinder axis

$\rho_i$  = density. The subscripts refer respectively to the specimen material, the quartz and the intermediate material.

The electrical circuit arrangements for measuring resonance frequencies are identical with those of Balamuth. In the first place, the fundamental frequency of the quartz cylinder alone is measured, next the intermediate cylinder is attached and the fundamental frequency of the two part oscillator is measured. Lastly the specimen cylinder is attached and the fundamental resonance frequency of the triple oscillator is measured.

Every time, the equations are solved for  $f_2$ ,  $f_3$ , and  $f_1$  respectively. The length of the three cylinders should be adjusted so that the fundamental resonance frequencies of the triple oscillator are the same within ten per cent.

Both Balamuth and Rose calculated the values of Young's modulus and rigidity modulus following the formulae given by Voigt<sup>85</sup> (1910). The results for rock salt with

Balamuth's two part oscillator and Rose's triple oscillator are tabled below. The results show excellent agreement.

TABLE NO. 6 (ROCK SALT)

T (°K)	BALAMUTH	ROSE
80	26.51	26.53
90	26.58	26.60
140	26.94	27.01
150	27.02	27.10
160	27.11	27.19
170	27.21	27.29
180	27.30	27.39
190	27.40	27.49
200	27.51	27.59
210	27.62	27.69
220	27.74	27.80
230	27.86	27.91
240	27.99	28.02
250	28.10	28.13
260	28.22	28.25
270	28.33	28.36



Durand<sup>47</sup> (1936) measured the principal adiabatic and isothermal elastic moduli and elastic constants of NaCl, KCl, and MgO over the temperature ranges 80°K to 270°K, 270°K to 480°K for NaCl, 80°K to 280°K for KCl and 80°K to 560°K for MgO. Durand used the same experimental method as that of Rose, except that the cryostatic bath liquid was petroleum ether cooled by liquid nitrogen.

Hunter and Siegel<sup>36</sup> (1942) made a series of measurements of the elastic moduli of NaCl over the range of 300°K to 1077°K, the melting temperature. The measurements were carried out by means of a tripartite piezoelectric oscillator consisting of a quartz crystal driver, an intermediate fused silica bar and the NaCl specimen. The cement used at the quartz silica interface was red shellac applied while molten. At the silica-NaCl interface, a cement consisting of a paste of sodium silicate and finely divided calcium carbonate was used.

The oscillator was suspended vertically on the axis of a tube furnace with NaCl specimen at the centre of the furnace, maintained at the desired elevated temperature. The temperature was measured with a Platinum - Platinum 10% Rhodium thermocouple, of which the hot junction was closely adjacent to the NaCl specimen.

The results of Hunter and Siegel practically

overlap with those of Durand in the temperature interval  $20^{\circ}\text{c}$  to  $230^{\circ}\text{c}$ .

Randall, Rose and Zener<sup>87</sup> (1939) used a method similar to that of Wegel and Walther (1935) to detect the contribution of intercrystalline thermal currents to the internal friction of polycrystalline metals.

In accordance with a theory developed by Zener, the internal friction is a maximum when the vibration is partly isothermal and partly adiabatic with respect to adjacent grains. By passing in small steps, from the nearly isothermal case of very small grain size through maximum internal friction to the nearly adiabatic case of large grain size, one can detect the relative importance of the polycrystalline thermal currents.

Randall, Rose and Zener performed an experiment on single phase brass of <sup>the</sup> following composition and grain diameter.

Copper	68.74%
Zinc	31.23%
Lead	0.02%
Iron	0.008%

The Alpha-brass sample had been cold rolled to 0.315 inch and then annealed at about  $600^{\circ}\text{c}$  to produce a grain size

of 0.06 mm and then cold rolled to 0.125 inch thickness. The cold rolled strips were cut to 12 inch lengths, numbered and annealed at temperatures between 50 to 900°c in 50 steps and the following table shows the annealing temperature and the average grain diameters obtained.

<u>Annealing Temperature</u> <u>in °c.</u>	<u>Diameter of average grain size</u> <u>by comparison with A.S.T.M.</u> <u>standard.</u>
350	0.006 mm.
400	0.009 mm.
450	0.015 mm.
500	0.025 mm.
550	0.037 mm.
600	0.055 mm.
650	0.080 mm.
700	0.11 mm.
750	0.15 mm.
800	0.25 mm.
850	0.5 mm.
900	1.0 mm.

All samples were etched with amonium and hydrogen peroxide.

Fig. 17 shows the general arrangement.

An electromagnetic drive was used without attaching any polepieces. The driver and the detector were air core

solenoids whose impedances were matched to the oscillator and amplifier. An alternating current of variable frequency was supplied to the driving coil from a vacuum tube oscillator. The eddy currents induced in the reed reacted with the non-axial components of a steady external magnetic field (furnished by permanent magnets) to produce longitudinal vibrations. At the pickup end a small alternating potential was induced in a reciprocal manner which was fed into the input circuit of a linear amplifier. The amplifier consisted of four pentode stages giving a maximum voltage gain of over 10, the last two plate circuits containing tuned coupling elements.

The  $Q$  of the reed was at least 100 times that of the amplifier characteristic, making the response linear to frequency over the resonance curve of the reed. Tuning the amplifier, very greatly increased the useful amplification by cutting down background noise. Final voltage amplification was read on a D.C. microammeter in a diode rectifier circuit. For more accurate results the authors minimised the loss at support with suspension of silk threads at a pair of displacement nodes. The radiation and viscous losses due to the surrounding air were minimised by reducing the surrounding air pressure to several millimeters of Hg. Varying the strength of the steady fields by moving the permanent magnet back and forth

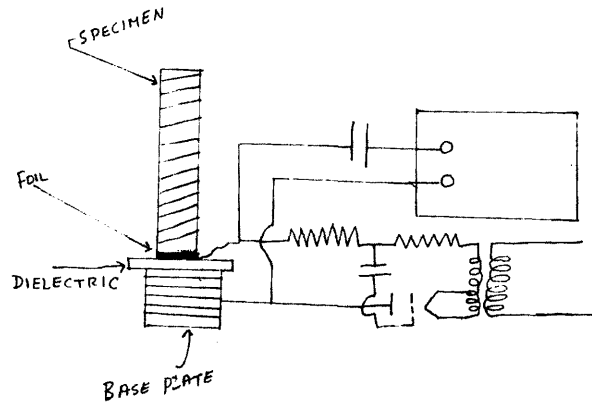


FIG. - 18 ARRANGEMENT FOR PRODUCING LONGITUDINAL OSCILLATIONS OF RODS BY ELECTROSTATIC TRACTION.

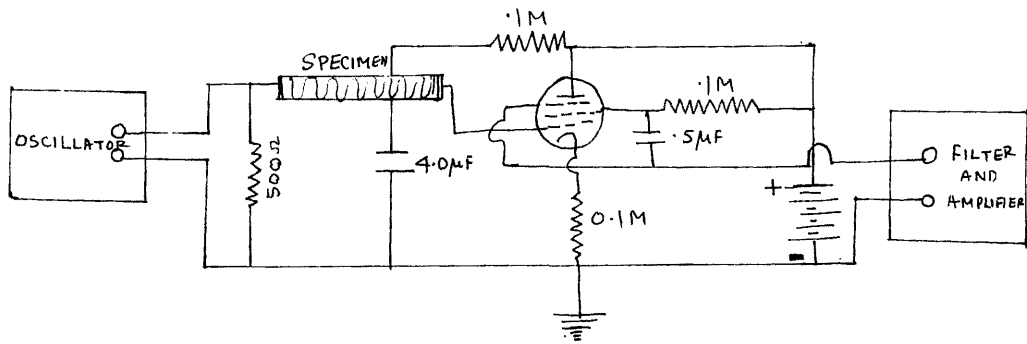


FIG. 19. ELECTRICAL CIRCUIT FOR THE ABOVE ARRANGEMENT.

produced no noticeable change in the measured internal friction, showing the eddy current losses were a negligible factor.

For measuring the elastic constants of metals, Bancroft and Jacobs<sup>88</sup> (1938) used an electrostatic method of generating longitudinal oscillations. This method has a distinct advantage that it is not subjected to thermal limitations, but the disadvantage in the use of this electrostatic method has been due to the fact that the electrostatic effects are considerably smaller than the corresponding magnetic or piezoelectric effects.

Ide<sup>89</sup> (1935) partially overcame this difficulty in the measurements of Young's modulus of aluminium, lead, nickel, steel and glass, by using very large specimens which were driven through a thin mica disc. The mica disc supported the specimens, as shown in fig. 12. Resonance was determined by a small crystal of Rochelle salt cemented to the specimen and the voltage set up amplified and read on a meter. This method lacked in accuracy because the support at the antinode does not give sharp resonance.

Bancroft and Jacobs eliminated the above difficulty and the external damping was reduced to a minimum by placing the support at three points on a nodal section. This is especially advantageous for the

measurement of internal damping. The apparatus designed by Bancroft and Jacobs is briefly described below and is shown in fig. 19 .

The specimen is mounted in an insulated spring clip which is rigidly clamped in the centre of a long brass tube and is arranged so that the air gaps between these and vibrating surfaces of the specimen are of the order of one thousandth of an inch. Very thin pieces of mica are attached to the fixed electrodes to eliminate the possibility of accidental short circuits between the specimen and the driving or pickup electrodes. The first electrode is connected to the output of a low frequency oscillator while the pickup electrode is connected to the grid of the 1603 vacuum tube. The specimen (accurately annealed carbon steel in the form of a cylindrical rod) was biased at 250 volts, and this served the double purpose of accentuating the driving force at the lower electrode and sensitizing the condenser microphone at the top.

The specimen with driving and pickup units was sealed within a gas-tight container which may be immersed in various temperature baths. ~~This is illustrated in the fig.~~ .

The power output of the pickup was small, and it was necessary to keep the input impedance of the amplifier sufficiently high. The output impedance of the

circuit shown in fig. 19 is 50,000 ohms. A high pass filter with cut off at 1000 cycles was inserted at this point to eliminate most of the stray noise which the microphone may pick up. The accuracy claimed by the authors was 0.1%.

Relaxation due to dislocations at low temperature.

To measure internal damping at very low temperatures, Bordoni<sup>90</sup> selected four pure metals of cubic face-centred crystal structure (Pb., Cu., Al., Ag.,) and a large copper single crystal. The method used was an electrostatic one described by him in 1947.<sup>91</sup>

The driving force was supplied by the electrostatic pressure between the rod and a small electrode facing one of its ends. The same electrode, connected to a high frequency oscillating circuit, was employed to measure the vibration amplitude.

To avoid any appreciable change of resonance frequency and damping, due to external causes, the vibrating rod was supported at nodal planes by needle points as shown in the fig. 20 . Additional damping due to air was also avoided by keeping the vibrating rod in an evacuated container. Even at low temperature, joints were made air-tight by Wood's metal soldering. Resonant frequency and damping were first measured at fixed temperatures keeping the rod and its container



inside a Dewar flask filled with a constant temperature bath until a thermal equilibrium was reached. The apparatus for low temperature measurement is described in fig. 21. The baths employed for constant temperature are listed below:-

Baths at Constant Temperature

<u>Bath</u>	<u>Temperature<sup>o</sup> K</u>	<u>Measured by</u>
Melting ice	273	. . .
Ethyl alcohol with solid CO <sub>2</sub>	203	Pentane Thermometer
Liquid air	81	Pentane Thermometer
Liquid Helium	4.5	" "

Bordoni did a wide number of measurements and the results can be listed by the following tables.

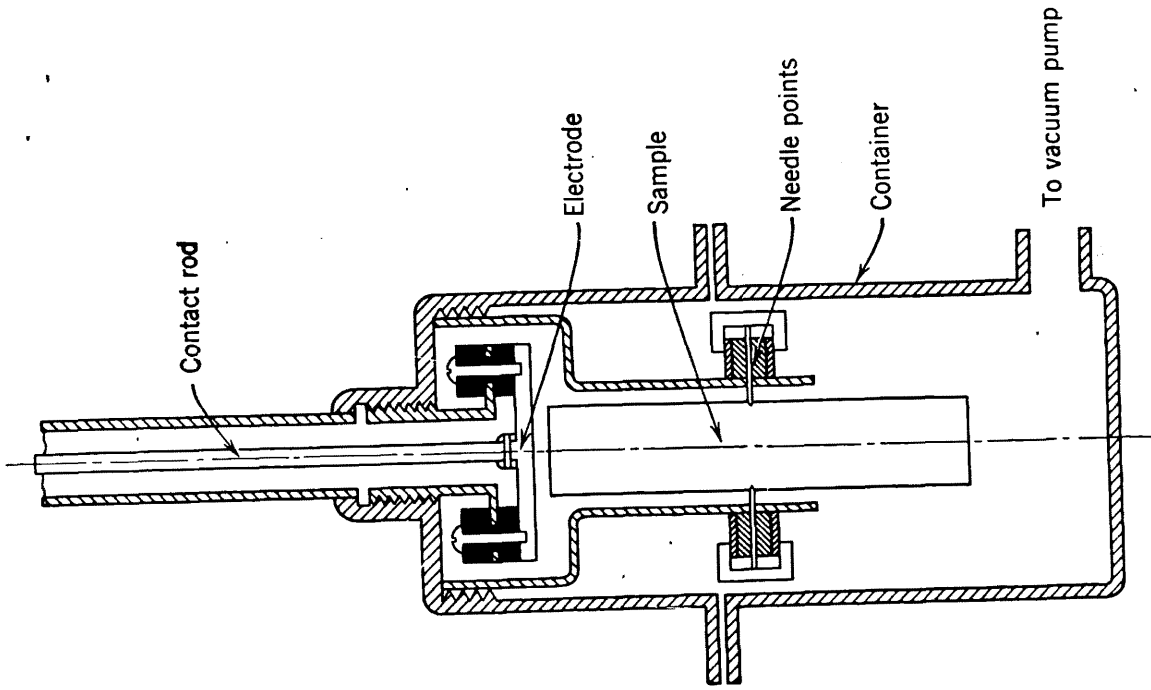


FIG. 20 ELECTROSTATIC EXCITATION OF RESONANT METALLIC BAR

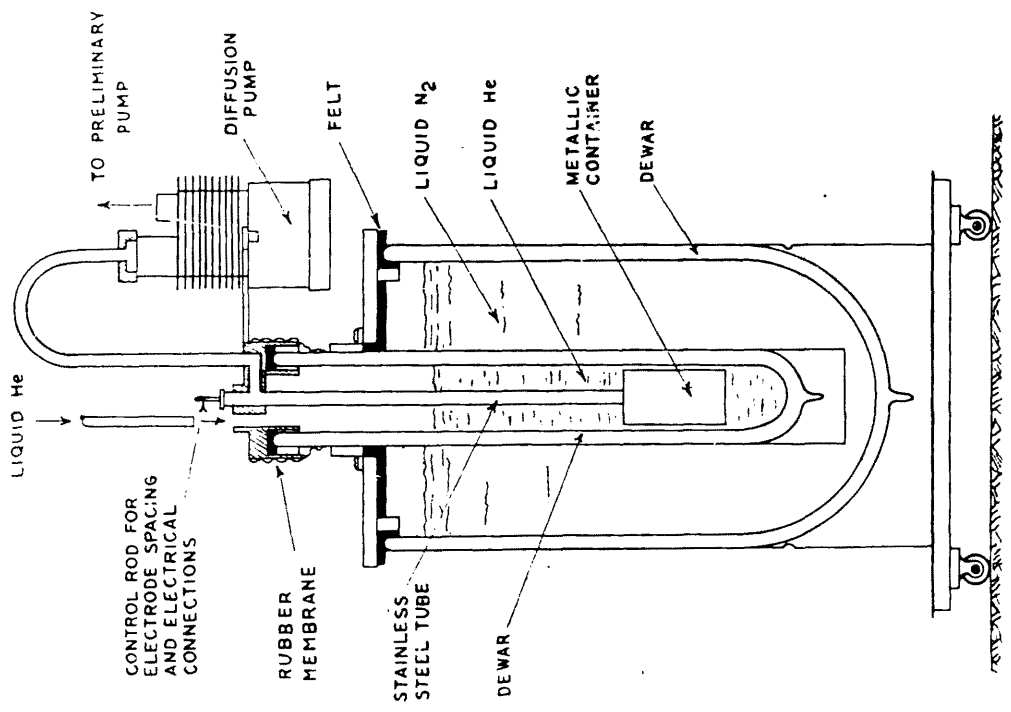


FIG. 21 LOW TEMPERATURE APPARATUS

Comparison between damping at  $T = 0$  and at  $T = 4.5^{\circ}\text{K}$ .

Material	Harmonic	$T = 0$	$T = 4.5^{\circ}\text{K}$
Pb. Commercial, unannealed	1st	$6.0 \times 10^{-5}$	$2.2 \times 10^{-5}$
Pb. Chemically pure, unannealed	1st	$5.7 \times 10^{-5}$	$1.3 \times 10^{-5}$
Pb. " "	2nd	$3.4 \times 10^{-5}$	$0.64 \times 10^{-5}$
Pb. " "	3rd	$4.7 \times 10^{-5}$	$0.80 \times 10^{-5}$
Cu. Commercial, unannealed	1st	$22.7 \times 10^{-5}$	$6.0 \times 10^{-5}$
Cu. Commercial annealed	1st	$9.6 \times 10^{-5}$	$2.4 \times 10^{-5}$
Cu. Chemically pure, unannealed	1st	$21.3 \times 10^{-5}$	$11.5 \times 10^{-5}$
Al. Commercial, annealed	1st	$4.6 \times 10^{-5}$	$1.4 \times 10^{-5}$
Al. Chemically pure, annealed	1st	$2.7 \times 10^{-5}$	$0.7 \times 10^{-5}$
Al. Chemically pure, cold worked	1st	$5.7 \times 10^{-5}$	$3.0 \times 10^{-5}$
Ag. unannealed	1st	$6.5 \times 10^{-5}$	$0.7 \times 10^{-5}$

Values of Young's modulus for annealed and unannealed materials.

<u>Material</u>	<u>Young's Modulus (dynes/cm<sup>2</sup>)</u>	
	<u>At room temp.</u>	<u>at 4.5 k.</u>
Cu, Commercial (unannealed (annealed	1.358 × 10 <sup>12</sup>	1.483 × 10 <sup>12</sup>
	1.373 ..	1.483 ..
Cu, Chemically pure unannealed	1.275 ..	1.430 at 23 k :-
	annealed	1.310 ..
Ag. (unannealed (annealed	0.804 ..	0.888 ..
	0.814 ..	0.888 ..

Temperatures of maximum damping and their ratio to Debye's temperature.

<u>Material</u>	<u><math>\theta</math> (°K)</u>	<u><math>T_d</math> (°K)</u>	<u><math>T_d/\theta</math></u>
Pb.	88	35	0.40
Cu.	315	80	0.25
Al.	398	110	0.28
Ag.	215	60	0.28

Bordoni concluded from the above measurements that the damping values of extensional vibrations in Pb, Cu, Al, and Ag, reached a maximum at about  $\frac{1}{3}$  Debye's temperature, both in crystalline samples and in a single crystal. The maximum value is always increased by cold work and reduced by annealing. This points out the existence of a new relaxation effect which may be explained as follows:-

When a solid is permanently strained, some imperfections are introduced in the crystal lattice such as, for instance, dislocations. These imperfections make it easier for some crystallographic planes to slide and therefore an anelastic strain is added to an elastic one. A certain amount of sliding occurs at room temperature owing to the thermal agitation of atoms and to the local fluctuations of energy even when the values of stress are small (as is the case with vibrations excited by electrostatic pressure).

So the value of Young's modulus computed from the velocity of extensional waves is always lower for a permanently strained material than for the same material after an annealing process has eliminated some of the imperfections of the crystal lattice.

The value of modulus at room temperature measured in this way does not depend on vibration frequency at least below 100 kilocycles. The time required by the anelastic strain to reach its full value

at room temperature must then be much shorter than  $10^{-5}$  sec. The thermal energy of atoms decreases above  $\theta$  as a linear function of  $T$ . Below  $\theta$ , the energy decreases as a higher power of temperature and goes to zero as  $T^4$ . It may therefore be expected that the time required by the anelastic strain to take place under the effect of elastic stress and thermal agitation, becomes larger when  $T$  is lowered. So the difference found at room temperature between the elastic modulus for a permanently strained material and the value measured after the material has been annealed, must decrease with  $T$  as the anelastic strain decreases. This agrees well with the results, and it is found that at  $4.5^\circ\text{K}$ , no appreciable difference exists between the values of Young's modulus when the material is permanently strained and when it is annealed. The experimental results show that at liquid helium temperature and for very low stresses, the sliding of atom planes requires a time much larger than the vibration period. For some value of  $T$  between  $4.5^\circ\text{K}$  and  $300^\circ\text{K}$ , the sliding time must then be equal to the period of vibrations and according to the relaxation theory, at this temperature damping must reach its highest value, and Bordoni observed the same maximum with all the four metals.

The ratio of maximum damping temperature to Debye's temperature is very near to  $1/3$  and this agrees very well with the statistical treatment of the problem by Bordoni<sup>92</sup> (1949) who showed that the changes in sliding time are always small when  $\tau > \theta$ , but become very large for  $\tau = \theta/3$ .

The metals used in the experiment have the same crystal structure, their resonant frequencies are of the same order, and Bordoni concluded that they must reach their highest damping for temperatures above the value.

The resonant frequencies were found to be almost linear functions of  $\tau$  above Debye temperature and near the absolute zero, the changes in frequency and damping vanish with a high power of temperature. This is also confirmed theoretically by Bordoni<sup>93</sup> (1953)

Much interest has been shown in Bordoni's results at low temperature, by Mason, Bommel, Filmer and Hutchison. This subject has been further discussed in chapter VIII.

#### Measurements in rubber and rubber like high polymers.

Rinehart<sup>46</sup> (1941) used ~~the~~<sup>a</sup> method similar to that used by Quimby<sup>77</sup> (1925) and Zacharias<sup>79</sup> (1933) <sup>for</sup> measuring the Young's modulus and specific energy loss in lucite and Karolith.

Both Lucite and Karolith are thermo-plastic and have a wide softening range and they are suitable for studying internal losses during softening of the material.

Frequencies used were around 50 Kc/sec. Both Lucite and Karolith were studied in the temperature ranges of  $-55^{\circ}\text{c}$  to  $65^{\circ}\text{c}$  and  $25^{\circ}\text{c}$  to  $110^{\circ}\text{c}$  respectively.

Rinehart tried several kinds of cement and the results seemed independent of the type of cement used. Similar behaviour was noticed by Durand (1936). The most suitable cement for work above room temperature was found to be a cellulose acetate and for low temperature measurements para-rubber dissolved in vaseline was used.

The composite bar and its holder were placed at the centre of a long Alundum-cored furnace and the temperature was measured by means of a chromel-alumel thermo-couple placed close to the specimen. At low temperature, measurements were made by using a cryostat consisting of a suitably insulated test tube into which the composite bar and holder could be placed, and the whole was immersed in a bath of low temperature mixture. The temperature close to the bar/<sup>was</sup> measured by means of a copper-constantan thermocouple. The bar was hung vertically and supported by fine threads, but the internal damping of the material was so great that no particular precaution was necessary in the form of supports used.



Two types of cooling mixture were used (1) ice and water, (2) dry ice and acetone.

The experimental results of loss measurements were found to vary with frequency for both the materials.

One of the serious difficulties in the measurement of internal frictional losses by resonance method in the dissipation of energy at the supports and in most of the investigations mentioned so far, the specimen was suspended by fine wires and threads. Even so, some of the energy will travel along the suspension. Forster and Koster (1939) used the wire supports to detect the flexural oscillations.

Gremant<sup>94</sup> (1940) extended the method to measure the internal damping of paraffin wax at room and elevated temperatures up to the softening range. Two other materials, namely glass and polystyrene, were also tested to check the efficiency of the method. In this apparatus the specimen was in the form of a hollow metal cylinder suspended by two fine wires each of which was attached to the centre of the diaphragm of an earphone. One of the earphones which acted as a generator was connected to an oscillator, whilst the electrical output of the other was used for measuring the amplitude of vibrations. The internal damping of the paraffin wax was measured by finding first the loss in the metal tube

when empty and then when filled with wax.

Using the electrostatic method as described by Bancroft and Jacobs<sup>98</sup> (1938), Parfitt<sup>95</sup> (1949) measured the internal dissipation in high polymers at frequencies in the range of 5 to 60 kilocycles. Two types of polymers were examined - one was amorphous polymethyl methacrylate (Perspex) unplasticized and plasticized with 5% dibutyl phthalate and the other was polystyrene. Parfitt's idea was to explain the fractional energy loss per cycle apart from the well defined relaxation phenomena. It was observed in the measurements that the fractional energy loss per cycle varied comparatively little with frequency. Young's modulus was also found to be constant. Perspex and polystyrene, which differ chemically in the nature of the side group of the main carbon chain, gave losses differing by a factor about six. The presence of plasticizer in perspex, however, caused little change in the loss. In polystyrene, the loss in torsional vibrations was found to be equal within experimental error to that in longitudinal vibration, a result to be expected in a material in which the compressibility is small compared with the shear compliance, so that longitudinal vibrations mainly involve shear strains. The magnitude of energy loss in perspex was of a similar order to that

obtained by Rinehart, but the loss observed by Rinehart, was increasing with frequency, a case which is not confirmed by Parfitt. Attenuations measured for Polystyrene perspex by Mason were 10 and 24 times greater than those corresponding to the loss figures at 60 kilo cycles measured by Parfitt.

Nolle<sup>96</sup> (1948) investigated the elastic properties of rubber-like materials at frequencies between .1 cycle per second to 120 kilo cycles per second and employed five different experimental methods to cover this range of frequency. At the highest frequency Nolle used a magnetostriction resonance method. A schematic diagram of the magnetostriction apparatus is shown in fig. 22 .

A small disc sample of rubber is held under compression between a resonant magnetostrictive rod and an anti-resonant rod. The length of the anti-resonant rod is half the length of the resonant rod. The anti-resonant rod is backed by a layer of spongy rubber which offers a mechanical impedance at least smaller than the characteristic impedance of the rod material. The rubber sample may be regarded as backed by an effectively infinite impedance when the anti-resonant rod presents several times its own characteristic impedance. The resonant rod is clamped at its centre in a ring of natural rubber, which has little effect upon the system because the impedance of the rod is very large at the centre. The resonant rod is magnetostrictively driven

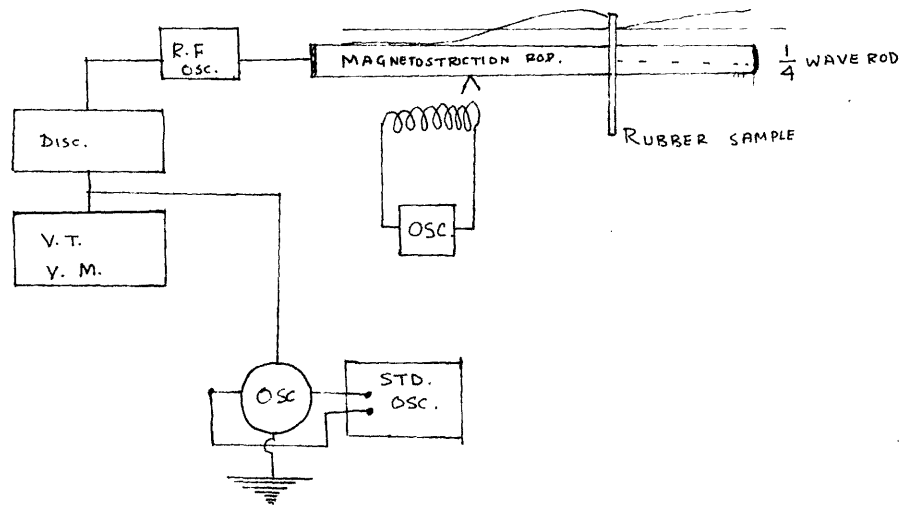


FIG. 22. MAGNETOSTRICTION RESONANCE APPARATUS.

by means of a coil surrounding the rod, to which is supplied several watts of a.c. signal. In addition, the coil carries direct current somewhat greater in magnitude than the peak a.c. flow in order to produce magnetic polarization. The relative amplitude of vibration of the rod is measured by means of an electrostatic pick-up plate which is located very near to the free end of the rod. The motion of the rod varies the capacity between this plate and ground, which results in frequency modulation of a high frequency oscillator (about 10 Megacycles). The frequency modulated oscillator signal is applied to a discriminator which supplies an output at the signal frequency. This output is amplified in a selective receiver and applied to the vertical input of a cathode ray oscilloscope.

A small change in the frequency of resonance occurs when a rubber sample is forced into contact with the end of the rod. This change of resonance frequency is proportional to the real part of the modulus of the sample, and the accompanying change in band width is proportional to the imaginary part of the modulus. The real and imaginary parts of the Young's modulus are found from the following relations.

$$E_1 = t (4 \pi^2 \rho L) \nu_c (\nu_c - \nu_0)$$

$$E_2 = t (4 \pi^2 \rho L) \nu_c (\Delta \nu - \nu_0 \Delta) / 2$$

where  $t$  = Thickness of the sample  
 $\nu_c$  = centre frequency of the loaded resonance  
 $\nu_0$  = centre frequency of the unloaded resonance  
 $\Delta\nu$  = band width of the loaded rod  
 $\Delta\nu_0$  = band width of the unloaded rod  
 $4\pi^2\rho L$  = constant for a particular rod,  $\rho$  is the density of the rod material and  $L$  is the length of the rod.

$E_1 - iE_2 = E$  = complex Young's modulus in dynes/cm<sup>2</sup>

The magnetostriction resonance method is best suited for use in a frequency range from 10 kc to somewhat more than 100 kilocycles. The method is advantageous because in principle, it is always possible by this method to obtain visco elastic measurements no matter how large the loss factor  $E_2/E_1$  .

Nolle did not claim a very high accuracy of the method which gave variations in the results of 10 to 20%. Though the method can be extended to a wide frequency and temperature range, Nolle described the method as tedious. The experimental measurements are inherently time consuming, rate of securing data is slow and the frequency is not continuously adjustable.

CHAPTER VIII  
PULSE TECHNIQUE

The recent development of short pulse technique has made available pulsed ultrasonics as a very convenient tool for investigating mechanical properties of matter.

The fundamentals of the pulsed ultrasonic system used mainly for the measurement of propagation constant ~~is~~ are given in block diagram (23) and in more detail in block diagram (24) .

The pulse generator consists essentially <sup>of</sup> a piezoelectric crystal cemented to the specimen under test and excited by a series of short pulses from an oscillator working at r. f. carrier frequency.

The acoustic pulse travels through the specimen under consideration and is then reconverted into an electric pulse by a transducer at the other end of the sonic course. There it is amplified, detected and used to trigger another pulse so that a continuous succession is generated.

The sound velocity can be calculated by counting the number of pulses generated in the specimen in an accurately measured interval of time, the average time delay experienced by a single pulse in traversing the closed path and the accurately known length of the sonic path.

Sometimes the pulse is reflected from the end surface to the transmitting crystal where the successive echoes are

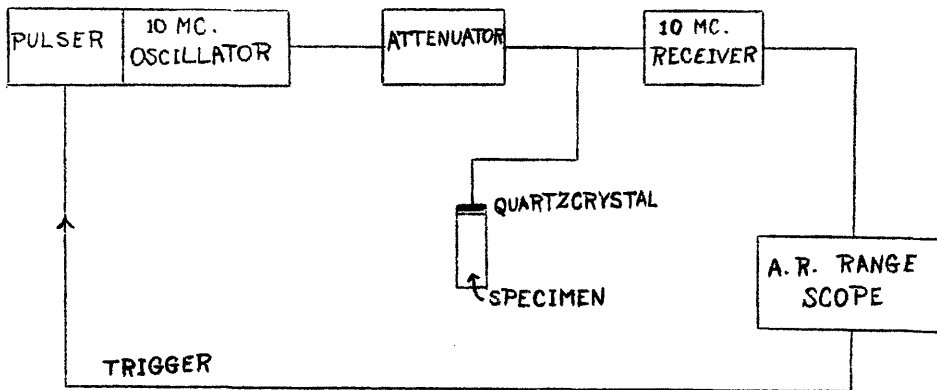


Fig. (23)

SIMPLE BLOCK DIAGRAM OF PULSE TECHNIQUE

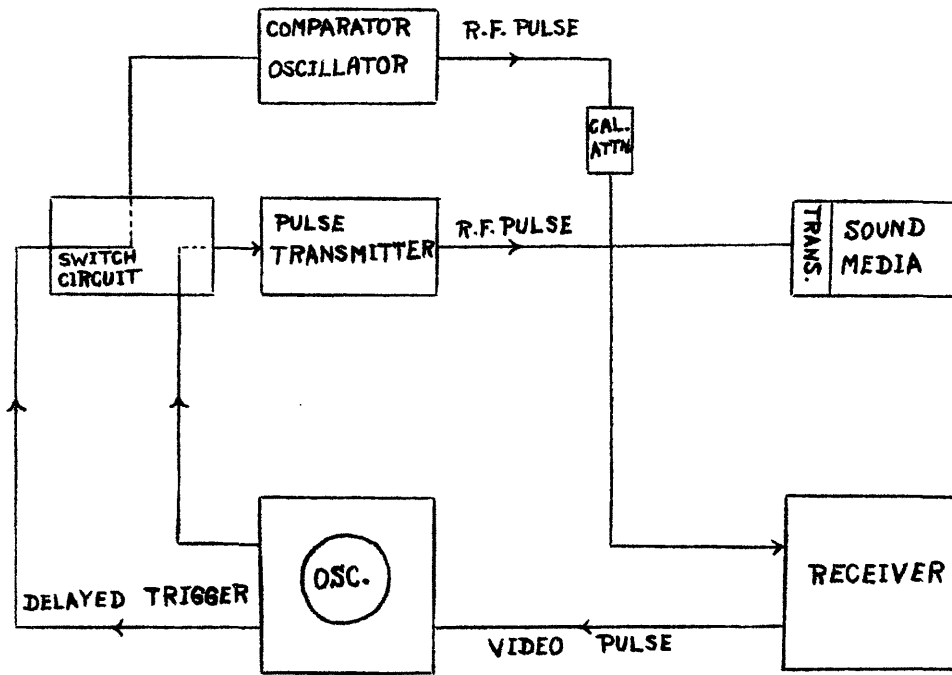


Fig. (30)

ARRANGEMENT OF MASON & MC. SKIMIN.



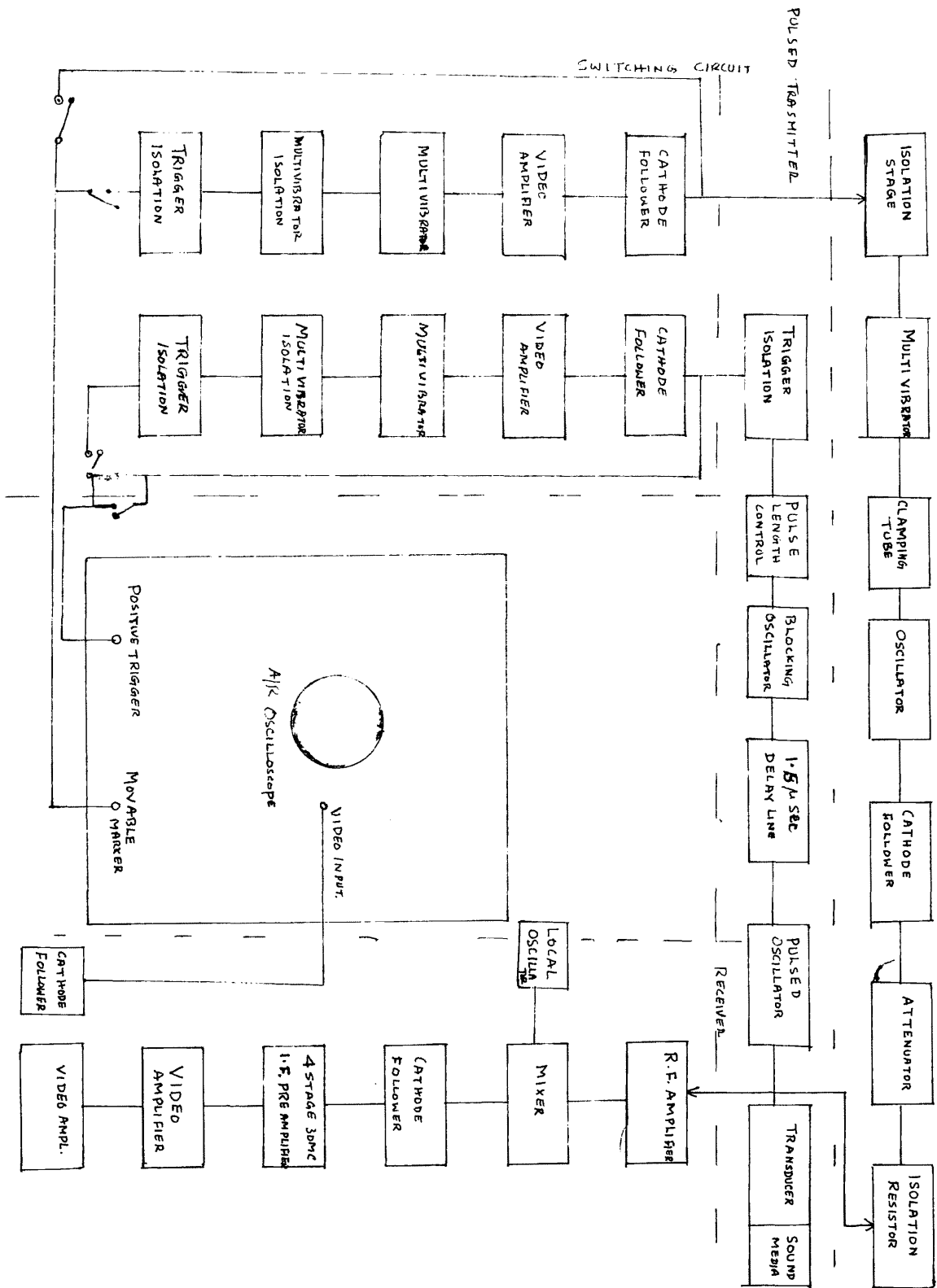


FIG. 24.

RECEIVER UNIT

converted into electric pulses, amplified and displayed on a time base sweep.

The relative amplitude of successive echoes gives a measure of the attenuation.

Advantages:

The advantages of the pulse method are that once the apparatus has been set up the measurements of velocity and attenuation are rapid and simple, and very high frequencies can be employed.

The method is capable of giving a very high degree of accuracy.

Disadvantages:

The principal difficulty of the method often lies in the interpretation of the experimental results. When the lateral dimension of the specimen is large compared with the length of the specimen and with the wavelength of the ultrasonic waves, the time of transit will correspond to either the dilational or distortional wave velocity depending on the type of pulse.

When the specimen is in the form of rods the pulses are reflected from the sides and a number of separate pulses which have travelled by different routes arrive at the detector.

The measured attenuation of the successive echoes must be interpreted with caution as there are many possible causes <sup>for</sup> ~~from~~ such attenuation other than the direct

absorption by the medium itself.

In the first place, the inhomogeneity in the specimen under test will give rise to scattering which will break up the intensity of the beam.

In the megacycle range slight impurities cause scattering. Residual thermal stresses also have the same effect. Extensive scattering can also be caused by the individual polycrystals of the specimen if the grain size is not very small compared to the wavelength of the ultrasonics.

Secondly even for homogenous specimens there will be some amount of beam spreading from diffraction effects. The spreading is ordinarily not serious because narrow angle beams are obtained at high frequency. However it is necessary for all specimens to be carefully prepared with two opposite surfaces as flat and parallel as possible. Any misalignment of surfaces will cause a distortion in the pattern of multiple echoes. As a result, the successive echoes decrease unevenly and may show an oscillatory character where some echoes are actually larger than their immediate predecessor.

In the third place, any thermal gradient in the specimen will cause refraction and consequent pulse distortion.

Finally the character of the film between

crystal and specimen is increasingly critical at shorter wavelengths. It is essential that the surfaces be clean and all particles and air bubbles should be removed so that the film should be of uniform character. It should be thin and must have low acoustic impedance, otherwise the crystal element will not have a sufficiently broad band character to maintain good pulse shape.

For work with transverse waves, it is impracticable to use a liquid or wax film. For the measurement of attenuation the effect of pulse distortion is more pronounced. To obtain precise values would require repeated measurements on the same specimens to evaluate the reproducibility and the influence of the film used and on specimens of different size and shape to eliminate the effect of geometry, beam spreading, reflection and the like.

The effect of pulse distortion on velocity measurement although much smaller than that on attenuation, is the limiting factor in the accuracy of results. For successive pulses which maintained essentially the same pulse shape, the precision of velocity measurement is as good as 0.1%.

With the appearance of pulse distortion for one reason or another, the determination of time between pulses become difficult. Results of the various investigators varied depending on the procedure and the

interpretation of the Oscillo-scope pattern and for this reason accuracy of measurements varies considerably.

Experimental methods:-

The first reliable measurements of energy loss in solids with the aid of pulse techniques <sup>were</sup> was made by Mason and McSkimin<sup>9</sup> (1947) and the energy loss in solids due to scattering was calculated on lines similar to Raleigh's formula for scattering of sound in gases caused by inhomogenities in the medium.

The method was later applied by Roth (1948) to study the scattering effect in polycrystalline metals. Huntington<sup>97</sup> (1950) and Price and Huntington<sup>98</sup> (1950) made similar experiments on single and polycrystals and studied the scattering effect and the grain size. Roderick and Truell<sup>99</sup> (1952) used the pulse method to study the ultrasonic attenuation in steel and using the water buffer method he eliminated some of the difficulties as cited before.

Nolle and Mowry<sup>100</sup> (1948) studied mechanical relaxation effects in high polymers and used pulsed ultrasonic waves in the frequency range 10-30 mcs/sec.

Ivey, Mrwca and Goth<sup>101</sup> (1949) used pulsed ultrasonic waves to investigate viscoelastic constant of rubbers in the frequency range from 40 kcs/sec to 10 Mcs/sec and the temperature range  $-60^{\circ}$  to  $+60^{\circ}$  c.

Mason (1950) measured the propagation constant of plastics at ultrasonic frequencies and a similar method was applied by him and McSkimin<sup>102</sup> (1952) to measuring the mechanical properties of polymers.

Experimental arrangement of Mason and McSkimin.

A variable frequency oscillator is the source of the carrier frequency. This is sent to a wide-band tuned amplifier. The bias on the input tube of the amplifier is controlled by the pulser. The firing of the pulser is controlled by a sinusoidal wave of frequency from several hundred cycles to 5000 cycles and this timing wave also controls the sweep circuit of the cathode ray Oscillograph. The pulser is of conventional design and puts a square top pulse of positive voltage on the two balanced input tubes of the amplifier that are connected in a push pull arrangement. The carrier frequency is inserted in the suppressor grid of one of the tubes and is not balanced out in the output. When the grid is negative, the carrier output of the tube is neutralised and a steady state output appears in the amplifier.

When the gating pulse is impressed on the input, a pulse of alternating current of controllable time duration is impressed on the sending crystal.

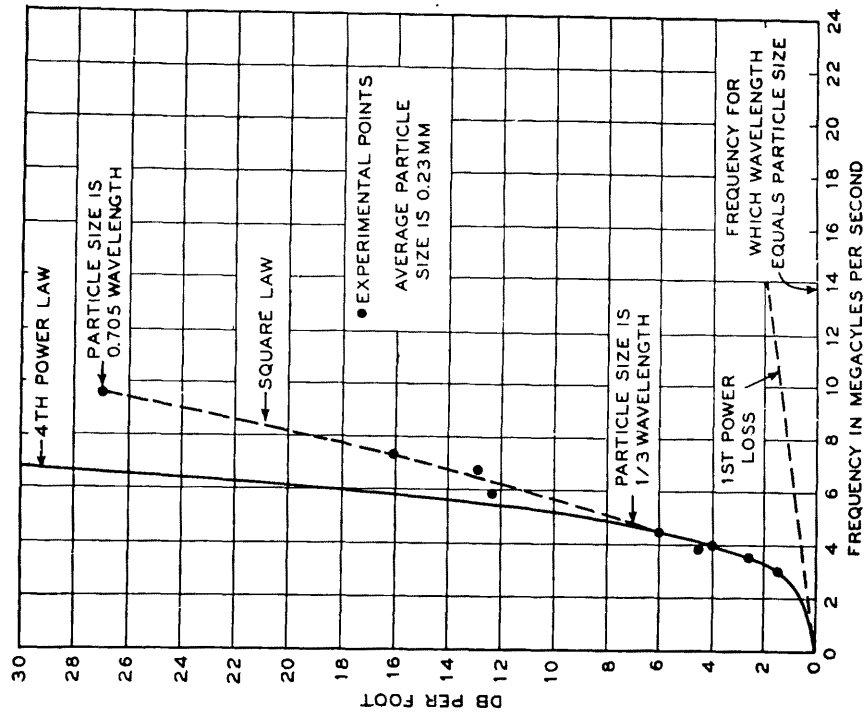


Fig. 26. Scattering losses for aluminum rod when particle size approaches the wave-length.

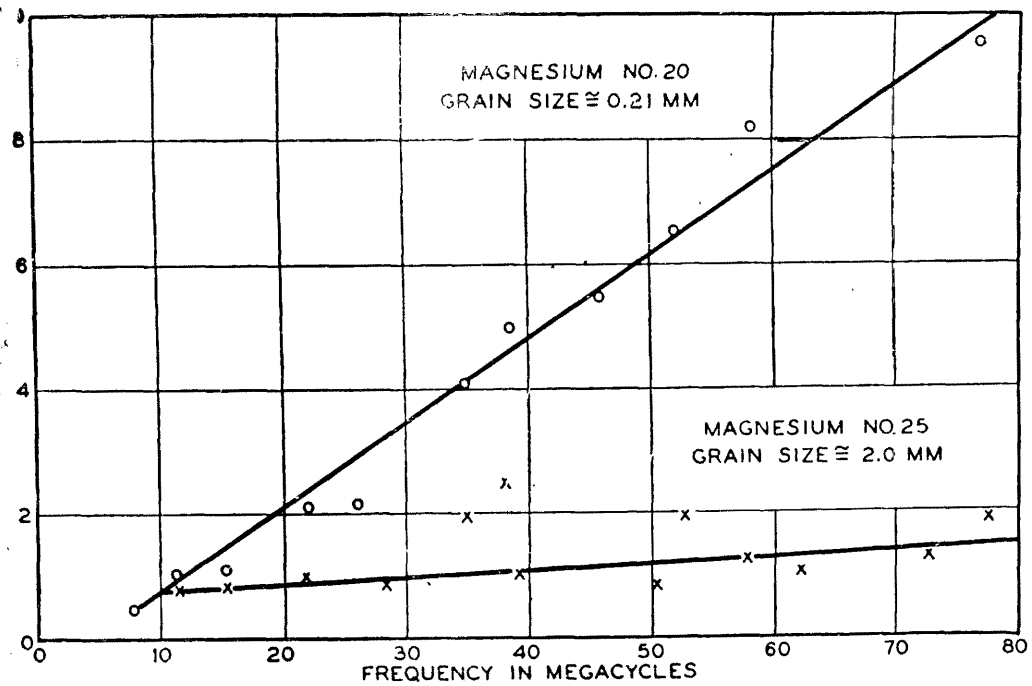


Fig. 27. Attenuation measurements of Roth for two magnesium rods for longitudinal waves.

values are considerably different.

Microphotographs of the grain size revealed that the average grain size of the rods are  $0.23 \pm 0.01$  mm and  $.130 \pm .01$  mm. This caused a larger scattering for the rod and resulted in a higher attenuation. Attenuation measurements are shown in graph (26) and the empirical formula for attenuation was given as

$$A = B_1 f + B_2 f^4 \text{ as explained before.}$$

Roth<sup>10</sup>(1948) performed the similar experiment with aluminum rods of the same grain size and found serious disagreement with that published by Mason.

Mason and McSkimin found that attenuation varies with  $D$  whereas Roth found that the attenuation varies as  $\frac{1}{D}$  and secondly Mason and McSkimin report a variation with wavelength  $1/\lambda^4$  at low frequencies (changing in one case to  $1/\lambda^2$  at higher frequencies), while Roth found a relation  $1/\lambda$  variation. The attenuation curve plotted by Roth is given in fig. 27. Huntington<sup>97</sup>(1950) repeated the same experiment and pointed out another approach to this problem which appears to be applicable over an intermediate frequency range and theoretically he predicted the attenuation varying as  $D/\lambda^2$ .

The absolute value predicted by this formula is considerably less than what is found experimentally and Huntington attributed the losses due to mode conversion.



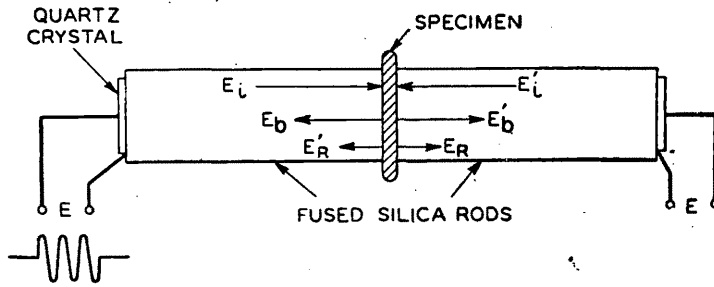


FIG 24. Symmetrical arrangement for comparing reflected and transmitted components.

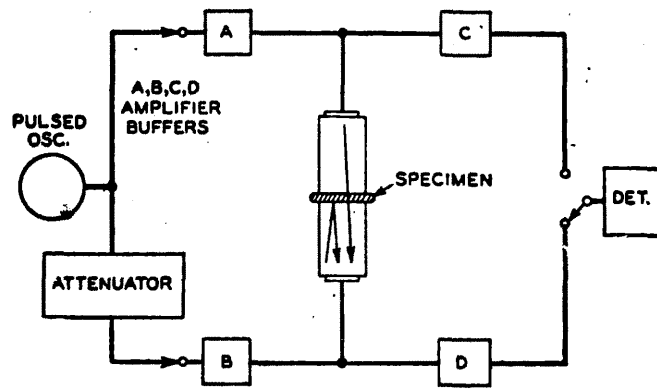


FIG. 56 Balancing circuit for error compensation.

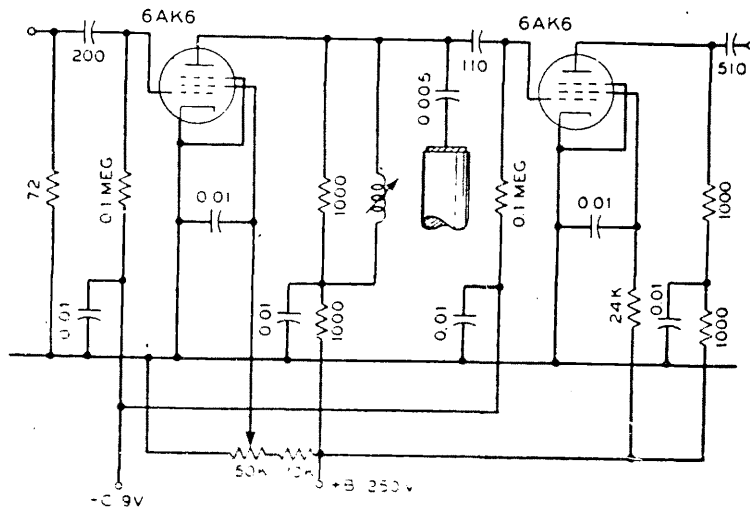


FIG 20. Buffer-amplifier circuit.

Buffer amplifier:-

The vacuum tube buffer amplifiers serve two major purposes:- (a) they allow individual adjustment of the level and phase shift through each channel and they prevent the undesirable signals of one channel from entering the other.

The electronic circuit arrangement of the Buffer amplifier is given in fig. 28.

Use of Seals.

To minimize phase shift errors Mc Skimin (1950)<sup>14</sup> used plastic seals approximately  $\lambda/4$  thick between specimen and rods. The seal must be uniform over the entire area and must be thin enough so that errors introduced by additional phase shift and loss are negligible. For moderate temperatures a liquid seal of poly d - methyl styrene was found to be satisfactory. This liquid is very viscous at room temperature. It flows quite well above 60°C, so that with pressure of approximately 25 lbs/sq.inch, film thickness of less than 0.0001" can be obtained. Further more this liquid is capable of transmitting transverse waves. At temp. above 30°C for transverse waves, a wax such as Carnaube should be used in order to provide a seal with an impedance more nearly matching the plastic.

Method for More Precise Measurement.

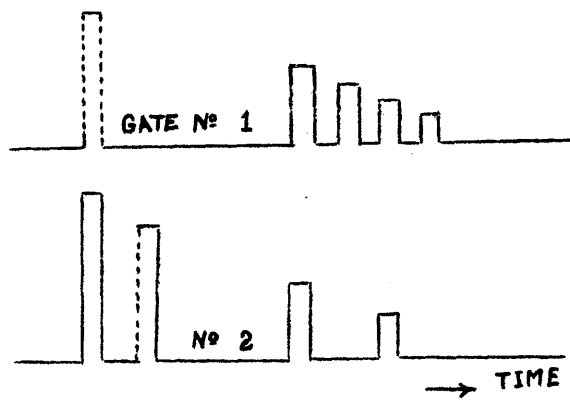
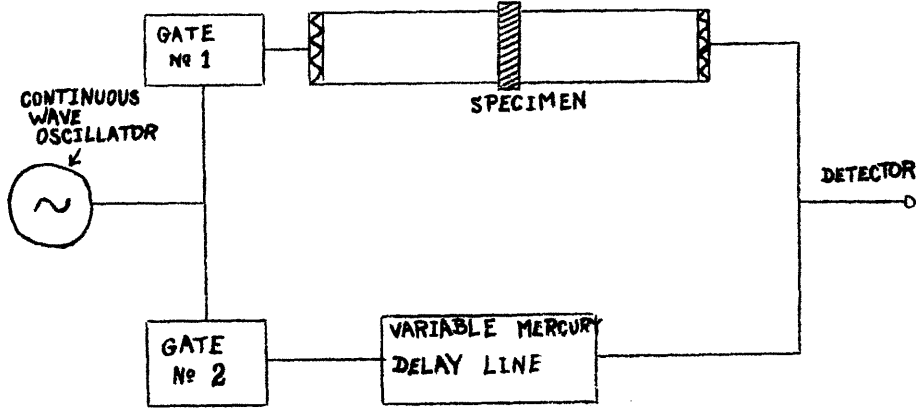


Fig. (55)

For testing small solid specimens McSkimin (1950) used a pulsed oscillator which was employed to initiate ultrasonic waves within the silica rods and specimen. The pulse width was variable from about 1 - 100  $\mu$  sec. Detection equipment consisted of a wide band (3 Mc) converter-amplifier with diode detector. The video signals were amplified and viewed on an oscilloscope.

The accuracy obtained was limited by the precision with which the "in phase" condition was indicated and by the phase shift at reflection. So for a more precise method a continuous wave oscillator gated by D.C. pulses was used instead of a pulse oscillator. One gate (fig. 55) feeds the unit including the specimen to be measured, the other a variable mercury delay line.

These gates must be capable of suppressing the carrier at least 40 db between pulses to minimise phase errors. Also the pulse position must be variable. The outputs of the two channels are fed into the detector circuit.

Roderick and Truel preferred the water buffer method to the direct mount method for measurements of attenuation in steel. The actual experimental technique is described in block diagram 25. Here the water buffer and the sample are the sound media.

A crystal calibrated time delay is used with

the oscilloscope so that 4, 10 and 25 micro-second sections of the full sweep at any time delay up to 1000micro seconds can be picked out. The delayed trigger can be initiated at any time up to 1000  $\mu$  seconds after the main trigger going to the transmitter.

Use of the Comparator Oscillator:-

The attenuation is determined by introducing an auxiliary radio frequency pulse from another pulsed transmitter called the comparator oscillator operated at the same frequency as the transmitter. The variable delay trigger which operates the comparator oscillator makes <sup>it</sup> possible to delay this pulse in relation to the radio frequency pulse from the transmitter and so place the comparator pulse near the echo to be measured. The relative amplitude of each echo ~~is~~ is determined by matching the pulse from the pulse comparator to it by inserting attenuation by means of a calibrated attenuator box and recording the attenuator readings. These readings give the relative amplitudes of the reflected pulses in decibels.

Advantage of water buffer.

The difference between the direct mounting method and the water buffer method lies in the provision of an isolation medium between the sound source and the specimen. The isolation medium makes <sup>it</sup> possible

to measure directly the reflection loss. In the direct mounting technique the reflection loss can-not be measured directly and is dependent on the technique of crystal mounting and the thickness of the resulting cement film as well as on pulse length and other factors. There is more-over no pulse distortion at the reflecting surfaces as with the direct mounting technique. The maximum measurable attenuations are as large as those that can be made by directly mounting the transducer on the specimen. The band pass of the water loaded transducer limits the minimum pulse length whereas with a solid loading transmission of very short pulses is possible but distorted.

Nolle<sup>104</sup> (1950), Nolle and Mowry<sup>100</sup> (1948), Nolle and Mifsud<sup>105</sup> (1952) have used pulsed ultrasonic for measuring dynamic mechanical properties of Rubbers and rubber like polymers.

Nolle and Mowry used a slightly modified form of the method of Pellam and Galt<sup>106</sup> (1946) and Teeter<sup>107</sup> (1946) for absorption measurement in liquid.

Fig. 31 illustrates the apparatus schemetically. Here the ultrasonic pulse travels to a reflector block spaced about 5 cm. from the crystal and returns to the crystal as an echo.

The echo gives rise to an r.f. pulse which passes from the crystal through an attenuator to a wide band r.f. amplifier. A deflection representing the echo envelope appears on the oscilloscope screen. The

relative intensity of the echo is measured by selecting an attenuator-setting switch which brings the echo pulse to a standard height on the oscilloscope screen. The echo return time can also be obtained from a direct reading dial. Intensity and range readings are obtained once for the case in which the sound path consists entirely of liquid and again for the case in which a flat sample of a rubber mounted on a gate-like frame has been swung into the sound path. The acoustic attenuation in the sample may be computed from the difference of the intensity readings.

For temperatures between 0°c and 100°c the tank is filled with water and for temperature below 0°c Ethyl alcohol was used as it has a low freezing point and <sup>is</sup> also a non solvent for high polymers. Velocity measurements in this low temp. in alcohol display an uncertainty as a result of the temperature sensitivity of the velocity of sound in alcohol. So the tank is equipped with an electric stirring device to reduce temperature gradients.

The introduction of the polymeric substance into the sound path increases the echo return time in seconds by an amount  $\Delta t$  which is given by

$$\Delta t = 2 \left( \frac{d}{c_s} - \frac{d}{c_{liq}} \right)$$

where  $d$  is the thickness in cm. of the sample

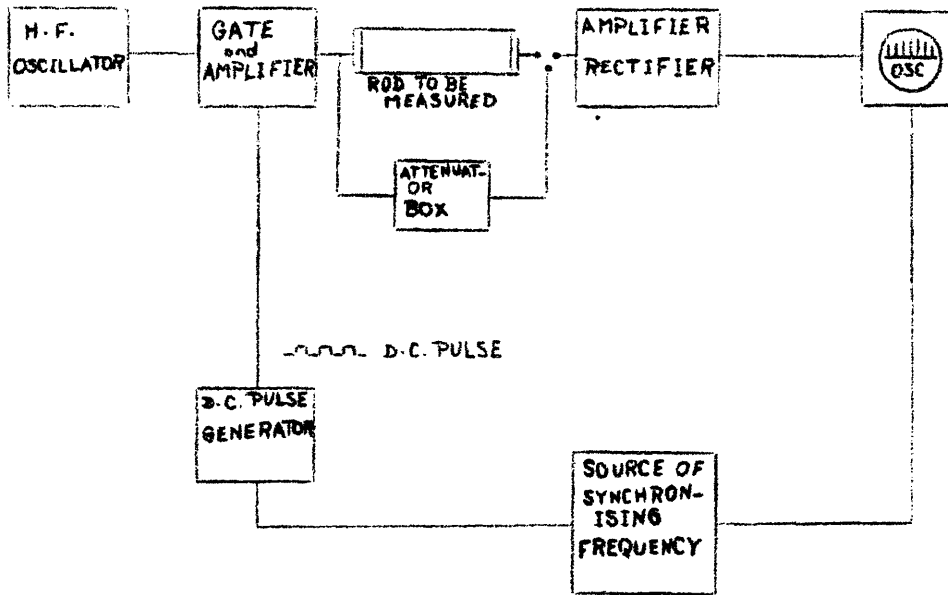


Fig. (25) ARRANGEMENT OF MASON AND Mc SKIMIN.

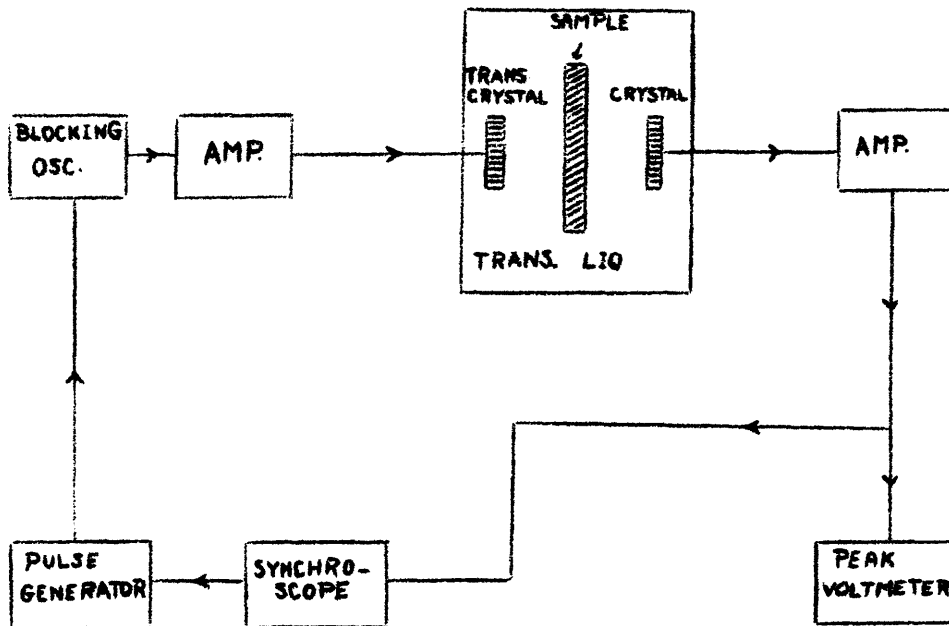


Fig. (31)  
BLOCK DIAGRAM OF THE CIRCUIT USED BY  
DONALD MROWCA and GOTH.



$C_L$  = bulk wave velocity in the sample

$C_{liq.}$  = velocity of sound in liquid in cms/sec.

Ivey, Mrwca and Goth<sup>101</sup> (1949) used also liquid medium as a buffer. The apparatus is shown schemetically in fig. 31

The method is simple and accurate. Here a pulsed compressional wave is generated and received in a liquid by a pair of crystal transducers. When a sample (rubber) is inserted in the path of the beam, the bulk wave velocity and attenuation can be calculated by observing the time shift and amplitude change of the received signal.

The velocity in the sample is obtained from the relationship

$$C = d C_{liq.} / d \pm C_{liq.} \Delta t$$

where  $d$  = sample thickness (measured by a dial micrometer at each temperature)

$C_{liq.}$  = velocity in liquid.

$\pm \Delta t$  = time shift observed on insertion of the sample.

The transmitting liquid used had negligible attenuation compared to that of rubber, so that the sample attenuation was obtained directly assuming no reflection at the liquid-sample interfaces. The assumption is valid if liquids of approximately <sup>the</sup> same acoustic impedance as rubber are used.

The measurements were made in the temperature range  
- 60°c to + 60°c.

Above 0°c, water was used as a transmitting liquid because of its negligible attenuation and desirable acoustic impedance.

Below 0°c, an ethylene - glycol - water mixture was used which had negligible attenuation down to about - 30°c. Below this temperature a small correction had to be made. The velocity in this mixture is higher than that in water which is taken as an advantage, because the velocity in rubber is higher at lower temperatures. Thus the mismatch at the interface is minimized and can be neglected.

Another advantage is that the error in velocity measurements is a minimum when  $C = C_{L_1}$ , since errors in  $d$  and  $\Delta t$  are then eliminated.

Measurements were made at 44 Kc, 1 Mc, 3 Mc and 10 Mc.

At each frequency complete velocity - temperature and attenuation-temperature curves were obtained. Velocity measurements were accurate within 2% at high frequencies and 5% at low frequencies. Attenuation measurements were within an accuracy of 10%.

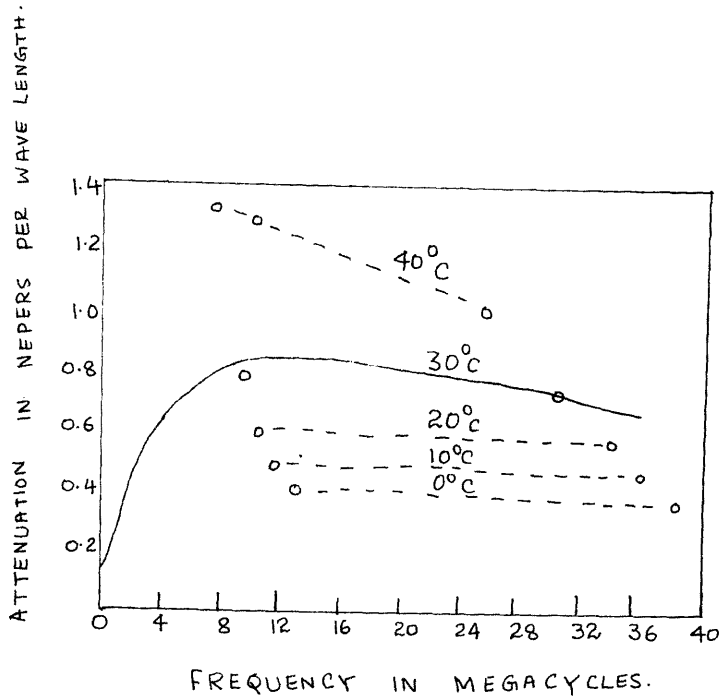


FIG. 34. Attenuation per wavelength for Shear waves in Polyethylene.

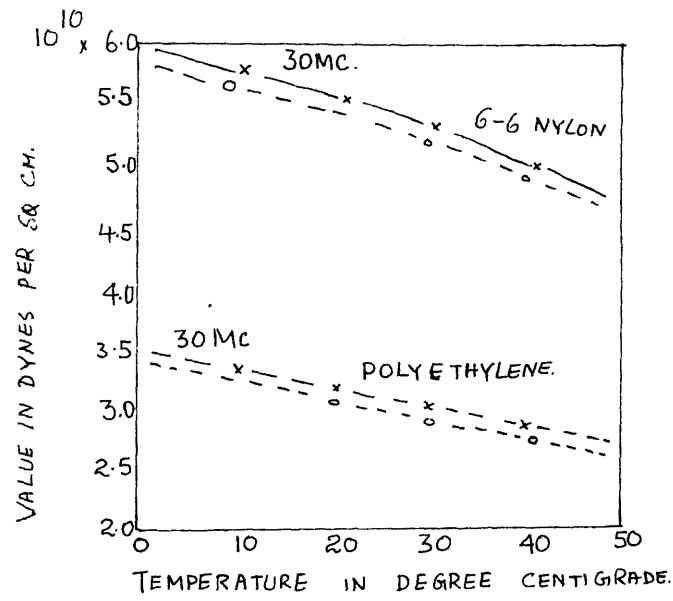


FIG. 35. VALUE OF  $\lambda$  (LAME ELASTIC CONSTANT) FOR POLYETHYLENE AND NYLON 6-6 PLOTTED AS A FUNCTION OF FREQ. AND TEMP.

Analysis of Experimental Results on Polymers.Polyethylene, Nylon 6-6 and Polystyrene.

Mason and McSkimin (1951, 1952) measured the longitudinal and shear wave velocities on the above materials. Fig. 32 Shows the longitudinal velocity of polyethylene plotted as a function of frequency and temperature. The velocity rises with frequency and a dispersion is indicated. This is confirmed by attenuation per wavelength curve for two different frequencies (25 Mc and 8 Mc) plotted as a function of temperature.

Fig. 34 shows attenuation per wavelength for shear waves.

Comparing the longitudinal and shear wave measurements, the Lamé elastic constants can be calculated and this is plotted in fig. 35 for both polyethylene and Nylon 6-6 as a function of temperature for two frequencies.

The dispersion of  $\lambda$  (Lamé elastic constant) for polyethylene is small but is more prominent in Nylon 6-6. This correlates with the larger compressional viscosity component present for Nylon 6-6. According to rearrangement theory of compressional viscosity due to Debye (1939), compressional viscosity can enter when some part of the chain can arrange from one stable state to another stable state as a function

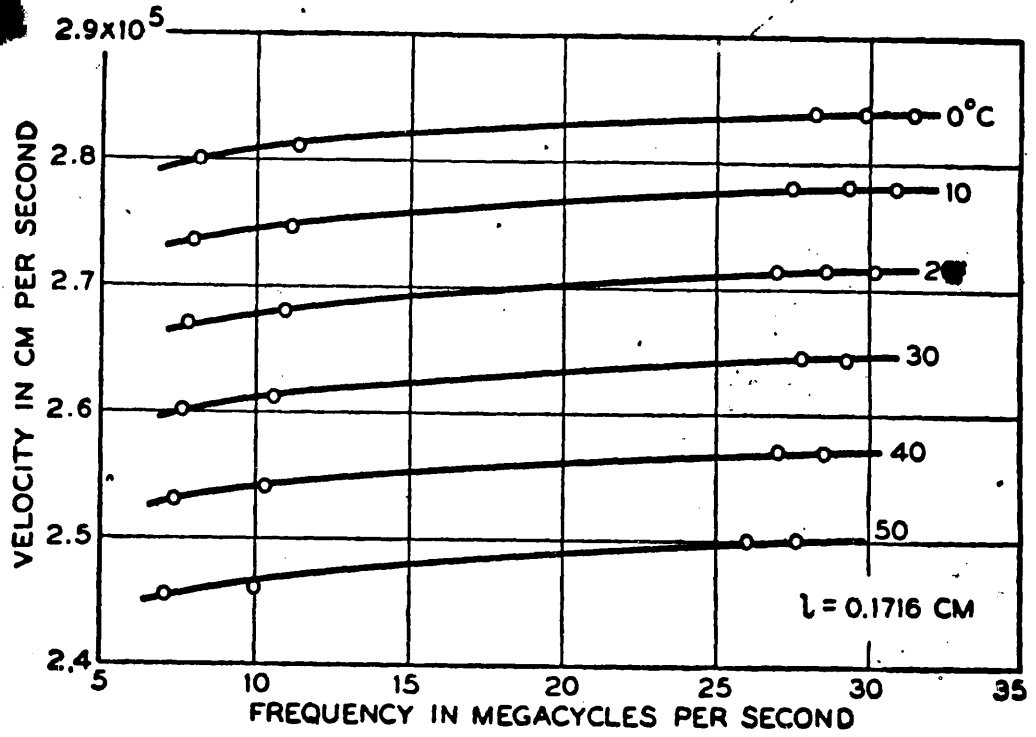


FIG. 57 Velocity of longitudinal waves in Nylon.

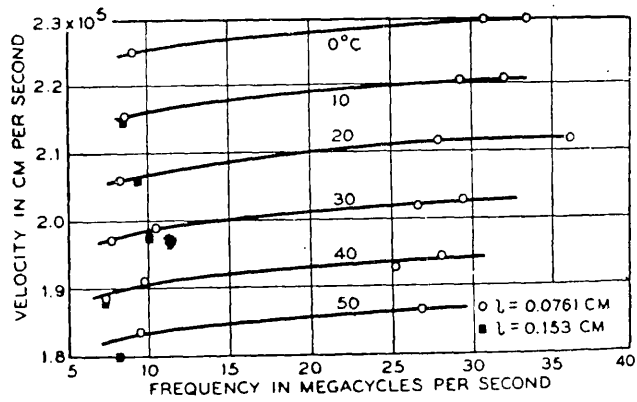


FIG. 32 Velocity of longitudinal waves in polyethylene.

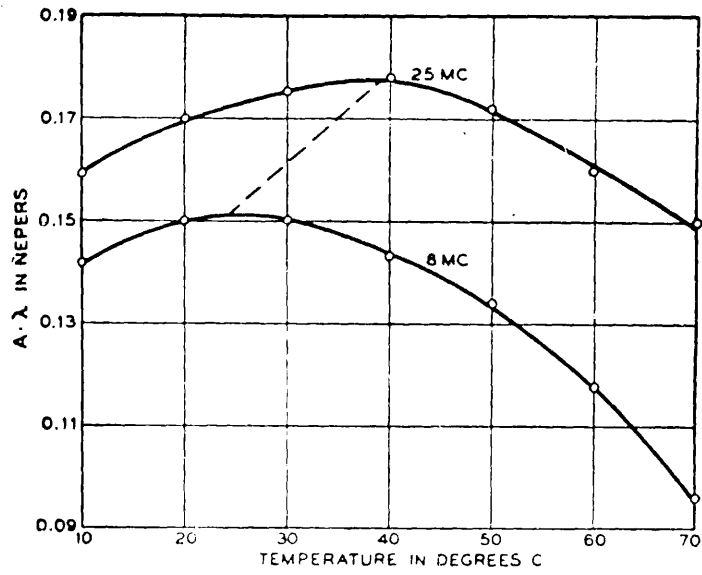


Fig. 35 Attenuation in nepers per wavelength for longitudinal waves in polyethylene.

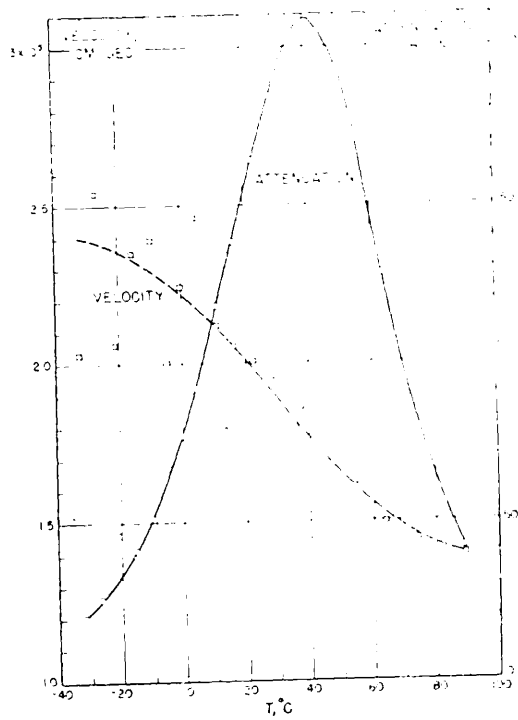


Fig. 36 Buna-N (Hycar OR-15) gum vulcanizate B-100. Bulk-wave velocity and attenuation at 10 mc.

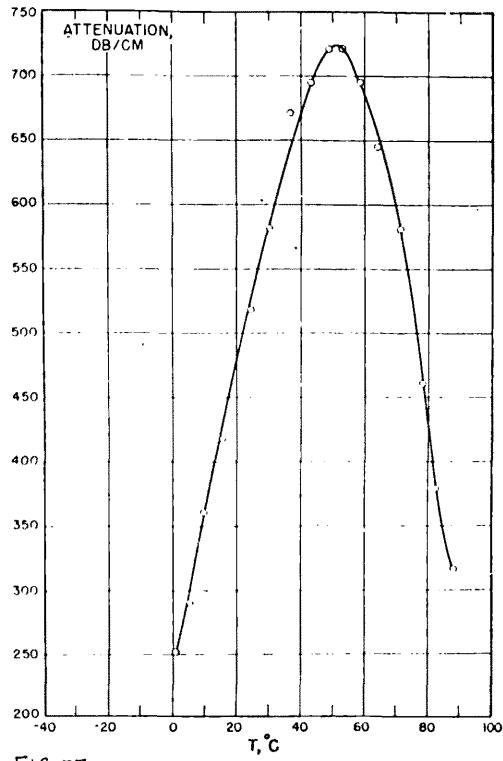


FIG. 37  
Buna-N (Hycar OR-15) gum vulcanizate B-100.  
Bulk-wave attenuation at 30 mc.

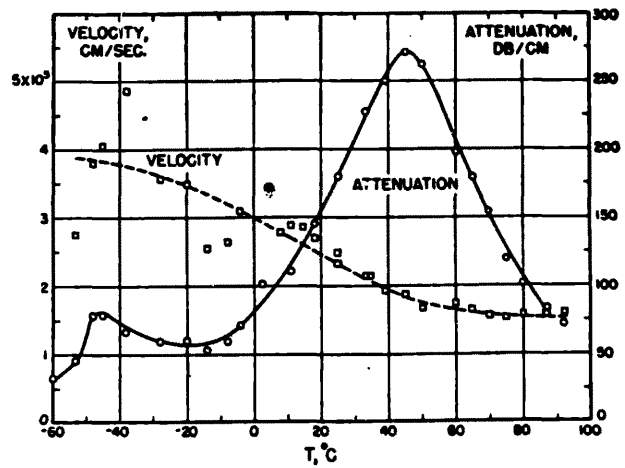


FIG. 38 Buna-N (Hycar OR-15) carbon-loaded vulcanizate B-5. Bulk-wave velocity and attenuation at 10 mc.

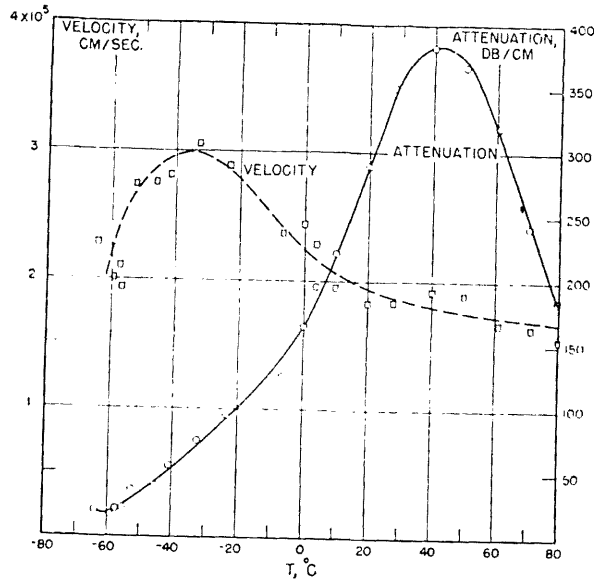
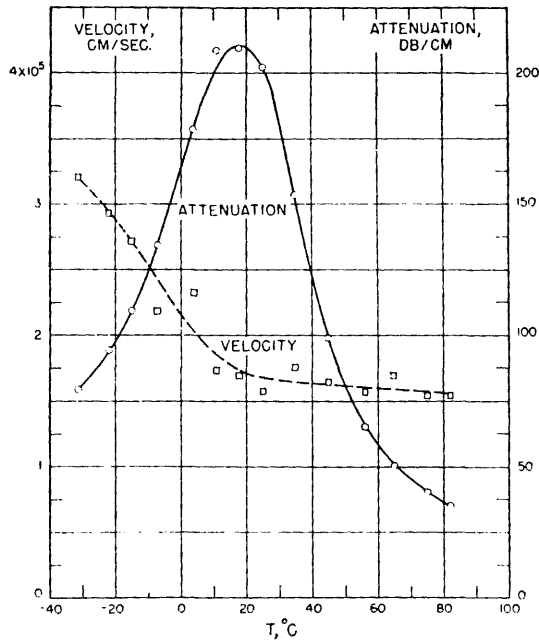


FIG. 39 Butyl gum vulcanizate U-50. Bulk-wave velocity and attenuation at 10 mc.



Perbunan gum vulcanizate P-1-A. Bulk-wave velocity and attenuation at 10 mc.

FIG. 40



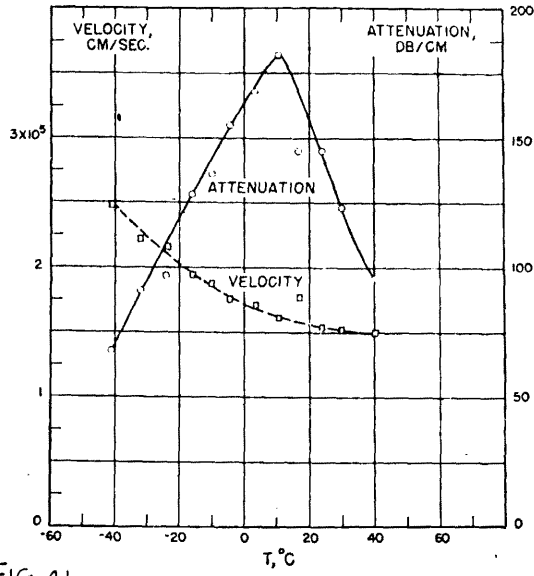


FIG. 41.  
 b. GR-S gum vulcanizate S-100. Bulk-wave velocity and attenuation at 10 mc.

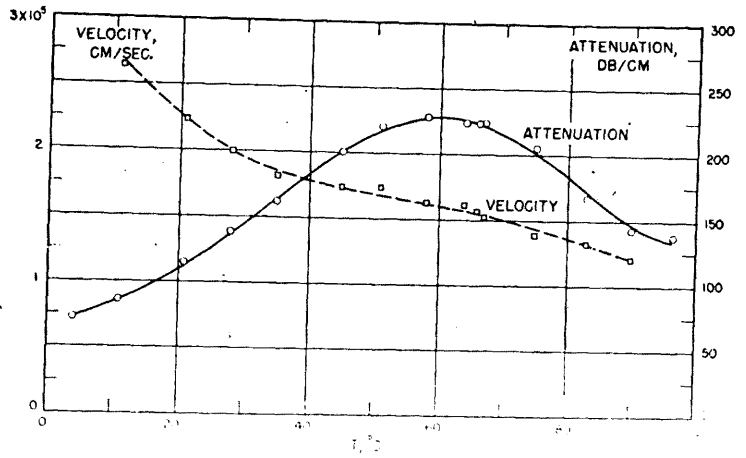


FIG. 42.

of pressure. This rearrangement occurs across a potential barrier and hence requires a finite amount of time to occur. This lag in the rearrangement results in a compressional viscosity. As the frequency is increased, a frequency is found for which the motion can no longer occur in the time of a single cycle and  $\lambda$  constant increases. It appears from these measurements that the dipole binding present in Nylon 6-6 allows a greater structural rearrangement under pressure than can occur for polyethylene which has only linear chains.

Synthetic and natural rubbers:-

Ivey, Mrwca and Goth, Nolle and Mowrey, Nolle and Mifsud (1952) measured the velocity and attenuation on a wide number of rubber samples.

Figs. 36 to 42 and the table no. 7 give the result obtained by Nolle.

TABLE NO. 710 Mc. BULK WAVE ATTENUATION DATA.

<u>MATERIAL</u>	<u>Temperature of attenuation peak.</u> °C
B-100 (Hycar OR-15 gum vulcanizate)	40
B-5 (Hycar OR-15, carbon loaded vulcanizate)	45
U-50 (Butyl gum vulcanizate)	42
S-100 (GR-S, gum vulcanizate)	10
GN-50 (GN neoprene vulcanizate)	10
P-1-A (Perbunan gum Vulcanizate)	18
Natural rubber latex film (Vulcanized)	18
Vynylite No. 1040 (plasticized)	below 0
Vynylite No. 1310 (hard)	61
Polystyrene	above 90
Teflon	-10
	34.

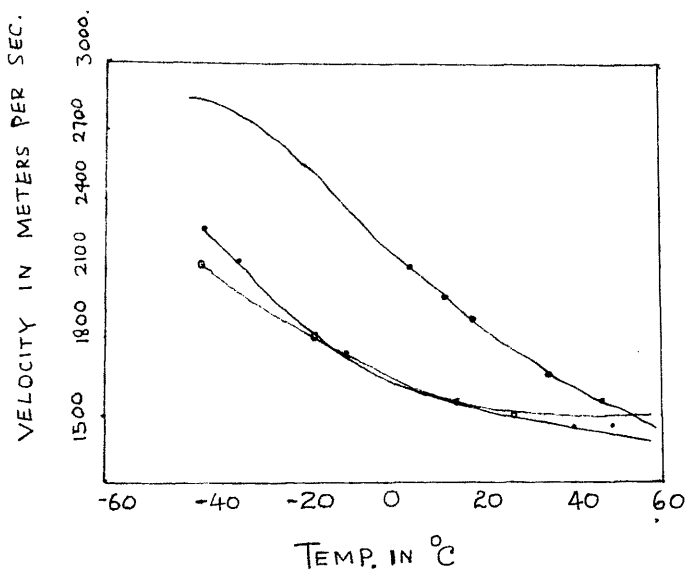


FIG. 43 BULK WAVE VELOCITY VERSUS TEMPERATURE AT 1 MC/SEC. FOR HEVEA, GR-S, AND BUTYL RUBBERS.

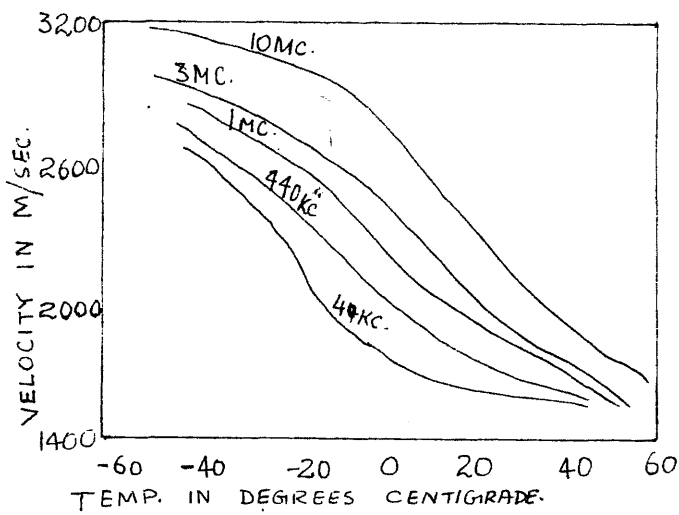


FIG. 44

VELOCITY VERSUS TEMPERATURE FOR BUTYL AT ALL FREQUENCIES.

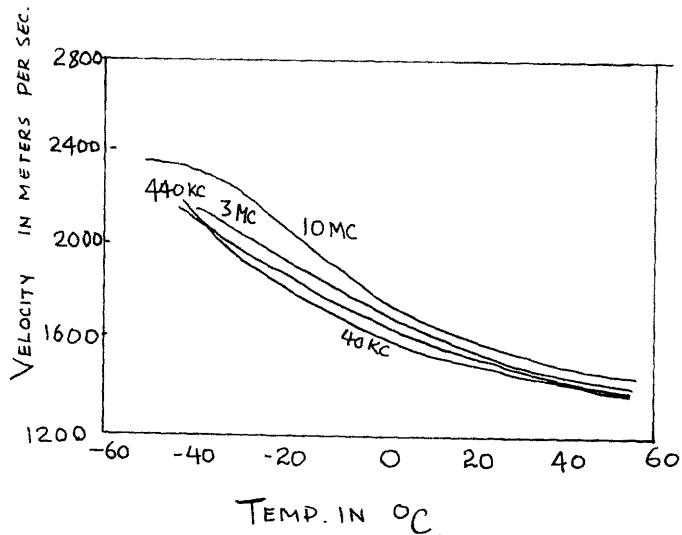


FIG. 45 VELOCITY VERSUS TEMPERATURE FOR GRS AT ALL FREQUENCIES.

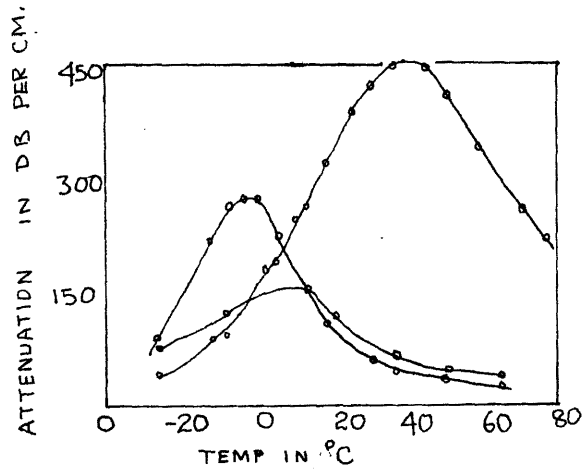


FIG. 46. BULK WAVE ATTENUATION VERSUS TEMPERATURE AT 10MC/SEC FOR HEVEA, GRS AND BUTYL RUBBERS.

Fig. 43 shows the dependence of velocity on temperatures for three types of rubber at a frequency of 1 Mc. The velocity increases with temperature and in butyl gum, the change is most prominent.

The fig. 44 shows the velocity temperature curves for butyl at 10 mc, 3 Mc, 1 Mc, 440 Kc, 40 Kc. Here also an increase in velocity with frequency is observed.

For GR-S rubber the velocity-temperature curve fig. 45 shows the dependence of attenuation on temperature for three types of rubber at 10 Mc. In this temperature region all these curves show a peak. Similar behaviour has been observed by Nolle and Mowry for synthetic rubbers and by Mason for other polymers. These curves have relatively the same form at all frequencies, but as the frequency is decreased, the curves decrease in amplitude and shift to lower temperatures.

(fig.46)

From the attenuation measurements, it is apparent that the decreasing the temperature has the same effect on attenuation as increasing the frequency, i.e. a given change in attenuation can be produced by either an increase in frequency or a decrease in temperature.

Measurements at low temperature and the relation to dislocation theory.

The attenuation and velocities of sound in a number of polycrystalline metals was first measured by Bordoni<sup>90</sup> (1954, vide chapter v<sup>11</sup>) at frequencies in the range of 10 - 50 Kcs. per second and in the temperature range 4° to 300° K. Bordoni observed that the velocities in lead, copper, aluminium and silver increased as the temperature decreased. The attenuation falls exponentially with temperature from 300° K to 200° K and then rises to a maximum at a temperature characteristic of the metal. Below the peak temperature the attenuation again decreases with temperature approaching the value zero. Bordoni pointed out the existence of a new relaxation effect due to the displacement of structural imperfections in the crystal lattice.

Much interest has been shown by Mason<sup>108</sup> (1955) and Hutchison and Filmer<sup>109</sup> (1956) in the results of measurements of Bordoni.

Hutchison and Filmer measured attenuation of 5 Mc/s sound in aluminum at a temperature as low as 4° K. Mason used the values obtained by Bommel<sup>110</sup> (1954) who using the pulse technique measured the velocity and attenuation for a single crystal lead to a temperature down to 1.5 k and in the frequency range of 9-27 Mc/s.

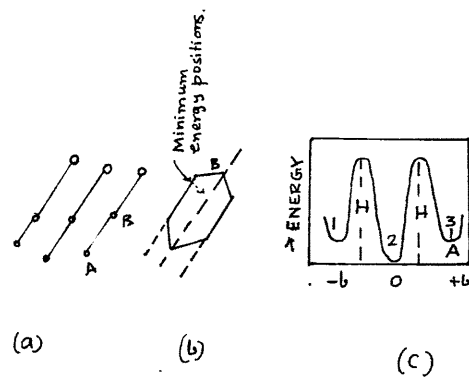


FIG. 47 Model for dislocation relaxations

- (a) Dislocations pinned by impurity atoms
- (b) Displacement form for a dislocation displaced by one atomic spacing  $b$ .
- (c) Potential well model for dislocation displacement.



To prove conclusively that there is a relaxation, Mason theoretically evaluated the relaxation term from Bommel's results on lead, and showed that attenuation peaks may be due to the displacement of a dislocation from one atomic line to an adjacent one against the limiting shear stress in the metals used by Bordoni.

Hutchison and Filmer also found the attenuation maximum at  $155^{\circ}\text{K}$  for polycrystalline aluminium and this attenuation maximum observed by Bordoni was explained by Mason to be due to dislocation relaxation process. Dislocations are supposed pinned down at irregular intervals by impurity atoms giving loops of average length (see model fig. 47 )

Thermal agitation causes the loops to be displaced to adjacent minimum energy positions against the limiting shear stress and the force to stretch dislocations. Mason calculated that the energy changes associated with those two restrictions:-

$$H = \sigma b^2 l / \pi$$

$$A = 2 b^3 \left[ \sigma \mu / 2\pi \right]^{\frac{1}{2}} \text{ ergs.}$$

where

- $b$  = atomic spacing along the glide plane
- $l$  = average loop length
- $\mu$  = shear elastic constant
- $\sigma$  = limiting shear stress

The decrement  $\Delta$  resulting from relaxation is given by the reaction rate theory as

$$\Delta = \frac{2\pi e^{-A/RT}}{1 + 2e^{-A/RT}} \left[ \frac{N_0 (1-p) b^4 l^2 \mu}{KT} \right] \left[ \frac{\omega/\omega_0}{1 + (\omega/\omega_0)^2} \right]$$

where

$$\omega_0 = C e^{-(H-A)RT}$$

$N_0$  = total number of loops per c.c.

$l$  = average dislocation loop length

$p$  = fraction of the total loop covered by one kink or bent portion of the dislocation connecting the two minimum energy positions

$b$  = distance between adjacent atoms along the glide plane

$K$  = Boltzmann's Const.

$T$  = absolute temperature.

A single sized loop would then result in an attenuation versus temperature curve showing maximum at a specific temperature.

Mason computed from Bordoni's and Bommel's results the activation energy  $(H - A)$  for lead and then deduced the value of  $\sigma/\mu$  for lead, aluminium, silver and copper.

At higher temperatures, the dislocations become freed from the impurity atoms and the attenuation rises exponentially.

The results of attenuation measurements on aluminium by Hutchison and Filmer is given in figs. 48 and 49 .

These graphs also tend to confirm the suggestion ~~that~~

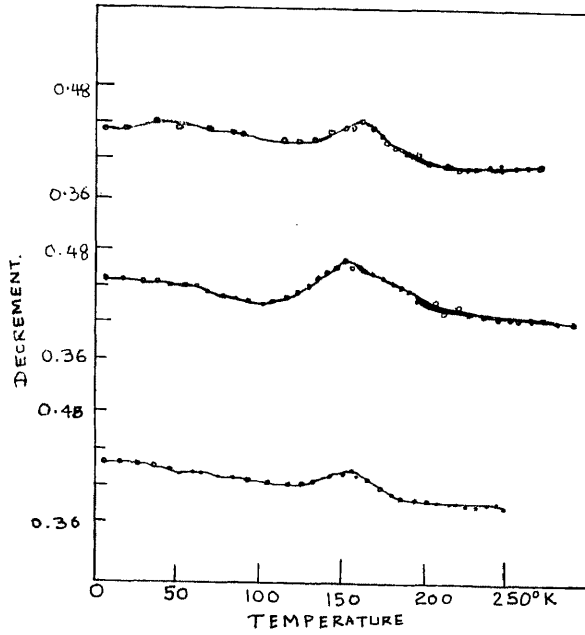


FIG.48. Attenuation of sound in aluminum  
 A. Annealed 10hr at 520°C  
 B. Cold worked 1.4%  
 C. Annealed 6hr at 180°C.

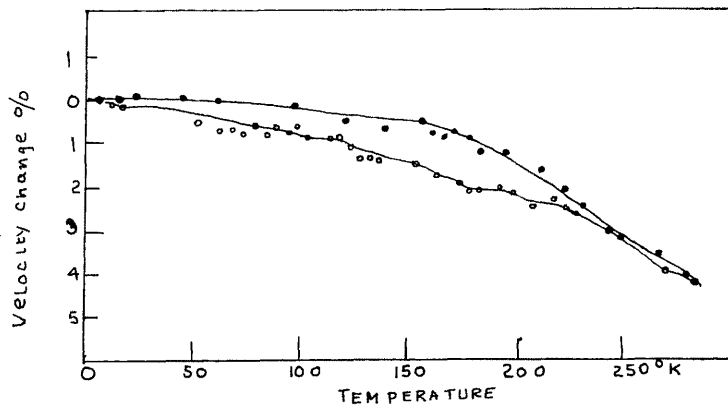


FIG.49. Temperature dependence of the velocity of sound in aluminum.  
 ● Annealed 10hr at 520°C.  
 ○ Cold worked 1.4%

that around 155°K dislocation movement plays an important part in the strains caused by high frequency stresses.

Hutchison and Filmer also deduced an activation energy from their results, compared them with those of Mason and found the values reasonably in agreement.

CHAPTER IXSolid Delay Lines.Introduction:

Ultrasonic ~~attenuation~~<sup>velocity</sup> studies in solids lead to an important practical application of certain solids as delay lines in Radar systems and in storing information devices. Hence these delay lines are briefly discussed.

These delay lines consisted of a wide band piezo-electric transducer usually a quartz crystal sending out a train of amplitude modulated sound waves into an appropriate medium at the end of which was another transducer and equipment to receive the sound energy and convert it back to an electrical signal whose modulation was identical with the input.

Very long delays can be obtained by this method, in comparison with purely electrical devices, because of the greatly decreased velocity of sound as compared to the velocity of electromagnetic propagation.

Again, the velocity of sound in liquids is about a third of that in solids. Hence a good deal of research has been done in liquid delay lines but, promising results have been obtained with multiply-reflected beams in solids.

Early History:

To trace the background history of these delay lines, it should be pointed out that the first liquid

delay line was the Shockley delay unit for the production of a variable calibrated trigger. Quartz crystals were employed for transducers. The transmitting medium was a mixture of water and ethylene glycol held at a constant temperature of 55°c. The unit was developed and engineered by the Bell Telephone Laboratories in 1942.

A second ultrasonic device, using mercury for the transmission medium, was investigated at the Pennsylvania University in 1943 and towards the end of 1943, M.I.T. Radiation Laboratory Staff started to investigate the possibilities of using mercury delay lines for Radar systems. The original research was carried out by G.D. Forbes and H. Shapiro.

Mercury delay lines built according to their design gave very faithful pulse reproduction at the required delay items of the order of 500 to 1000 micro second.

Forbes and Shapiro investigated other possibilities such as solid rods, narrow tubes, wires etc and following all these successful experimental systems, several different radar systems were developed which incorporated ultrasonic delay lines as an essential component.

### Design Considerations.

In delay line design, three parameters, namely, length of the delay, band width requirements and overall attenuation allowable, determine the choice of material, carrier frequency and crystal size. A fourth requirement at times is the reduction of secondary signals to a definite minimum. The mechanical construction should also be rugged as they are generally used in extreme conditions.

### Factors Influencing Delay Time.

The velocities of longitudinal and shear wave propagation are given as

$$C_l = \left( \frac{\lambda + 2\mu}{\rho} \right)^{\frac{1}{2}}$$

$$C_t = \left( \frac{\mu}{\rho} \right)^{\frac{1}{2}}$$

The delay time  $D$  of a line can be expressed as

$$\begin{aligned} D &= \frac{L}{C_t} \\ &= L \left( \rho/\mu \right)^{\frac{1}{2}} \end{aligned}$$

where  $L$  is the physical length of the delay line.

$L$ ,  $\mu$  and  $\rho$  are temperature dependent.

It can be shown that for any change in temperature  
(Voznak and Mebs 1955) <sup>111</sup>

$$\frac{1}{D} \left( \frac{dD}{dt} \right) + \frac{1}{2L} \left( \frac{dL}{dt} \right) + \frac{1}{2\mu} \left( \frac{d\mu}{dt} \right) = 0$$

Hence in order to maintain negligible variation of delay line length with change in temperature, the temperature coefficient of expansion  $\frac{1}{L} \frac{dL}{dt}$  must be about equal and opposite to the temperature coefficient of shear modulus  $\frac{1}{\mu} \frac{d\mu}{dt}$  .

For most metals, the temperature coefficient of modulus is negative and of greater magnitude than the positive expansion coefficient.

Thus the material for the delay line should have a zero or small negative temperature coefficient of the shear modulus.

The total attenuation of a signal transmitted through an ultrasonic delay line is determined by

- (a) electro-acoustic conversion efficiency of the quartz crystal transducers at the sending and receiving ends of the delay line, including the acoustic coupling devices employed, such as pressure clamps and cements, and by
- (b) internal attenuation of the propagated wave within delay media as discussed in chapter III .

#### Equivalent Circuit.

The equivalent electrical circuit for delay lines using quartz crystals has been discussed



by W.P. Mason and H.J. McSkimin (1947) and their results were repeated as a basis for considering the use of Barium Titanate ceramic ( $\text{BaTiO}_3$ ) transducers by J. May (1954). The simple equivalent circuit of an ultrasonic delay line when driven at the resonant frequency of the quartz crystal is given by Voznak and Mebs (1955) as represented in the figure below.

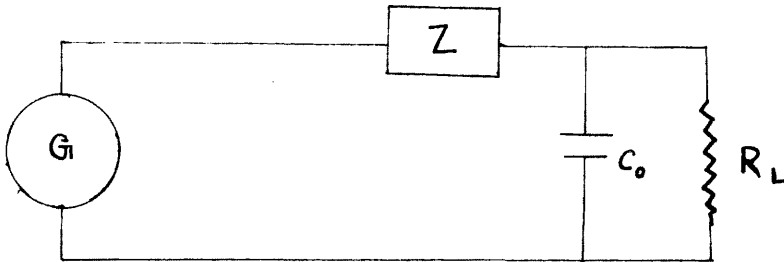


FIG. 50

where  $Z$  is the equivalent generator impedance  
 $C_0$  is the delay line output capacity  
 $R_L$  is the load.

The impedance  $Z$  may be expressed as

$Z = K(\rho c)$  where 'K' is a constant which depends on the characteristic of the quartz crystal transducer, i.e. its dimensions and electric and piezo electric properties and  $(\rho c)$  is the specific acoustic impedance of the delay medium,  $\rho$  is the density and  $c$  the velocity of the ultrasonic propagation in the medium.

$C_0$  is usually resonated at the crystal frequency by means of an inductor. The value of  $R_L$  is selected to be as high as possible consistent with obtaining the desired electrical band width of the load circuit.

The value of  $Z$  is usually large, particularly when a wide band width is required. The band width of the delay line is governed by the relative acoustic impedance of the quartz crystal transducer and the delay medium. It is also influenced by the transducer mounting devices as shown by Mason and McSkimin (1947). The frequency response of the delay line has a maximum at the resonant frequency of the quartz crystal and falls off at the low frequencies. So in order to obtain undistorted transmission of pulses, it is necessary to send the pulses through the line on a carrier whose frequency is near to that of the crystals. This allows exceedingly faithful transmission. Solid lines are particularly suited for purposes where relatively short delays are wanted, but delays longer than 300 micro second can be obtained by multiple reflection paths.

Waves in solids with Poissons ratio  $\sigma \leq .26$  have two angles of incidence (Arenberg<sup>113</sup> 1948) at which total conversion from the transverse to the compressional mode is obtained.

Fused quartz, the most promising material, has a

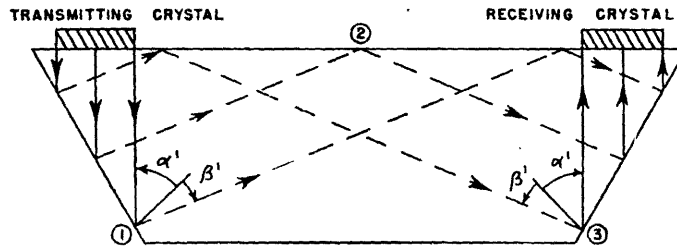


FIG. 51. Simple delay line involving transformation of mode of propagation.

1. Transformation from compressional to transverse mode.
2. Reflection beyond critical angle in transverse mode.
3. Transformation from transverse to compressional mode.

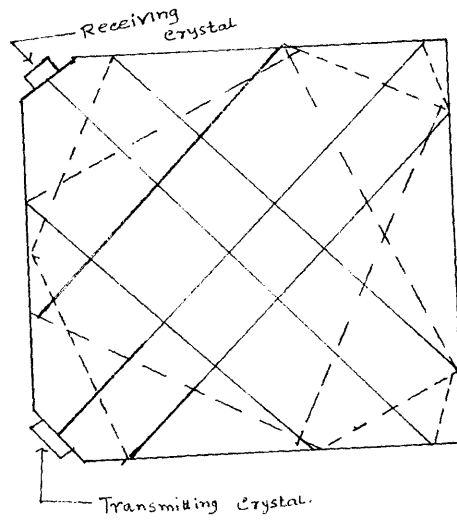


FIG. 52. DELAY PATHS WHEN  $n = 5$

Poisson's ratio of about .162, for which the conversion angles are 46.70 and 27.45. Its intrinsic attenuation is very low and it can also be procured commercially very pure and relatively strain free.

Hence fused quartz is used in the design of two dimensional paths as illustrated in the figure.51.

Following the path traced in fig. 52 where the compression mode is represented by a full line and the transverse propagation as a dotted line, it is seen that the beam starts initially from the 45° facet in the compressional mode as excited by an X-cut quartz crystal, crosses the block and upon striking the quartz-air interface is reflected in the transverse mode. Because of the different velocities of the two modes, the angle of reflection differs from the angle of incidence. On the next reflection, the beam strikes outside the critical angle for exciting the compressional mode and it is totally reflected.

At the third reflection a situation arises that is identical with the first reflection except for the reversal in time. Consequently the beam is transformed from transverse to compressional vibration. This cycle is repeated every three reflections and eventually the beam in the compressional mode strikes the receiving crystal at normal incidence. There is then a family of such paths distinguished by the value of

of  $n$  where  $3n$  gives the number of reflections. The ratio of block length to block width determines which path is used. The figure 52 shows the case when  $n = 5$ , and this type has given the most successful results. The delay of such a block is over 400 microseconds.

As with two dimensional patterns, if the transverse waves can be initiated directly by properly cut crystals, reflections in three dimensions form a very efficient use of available space and weight.

#### Other Materials.

Single crystals when annealed have very low attenuation and the small specimens of lithium fluoride, sodium chloride, and potassium bromide which were tested showed a promise of rivalling fused quartz. Isotropic media, such as single component glasses of high purity may also have attenuation, and German workers using glass as delay lines, have claimed better results both as regards absorption and temperature coefficient of sound.

#### Variable Solid Delay Lines.

By cutting the solid in three pieces, so that the middle wedge-shaped piece can move perpendicular to the sound beam, the length of the path can be shifted by the upward motion of the top piece. As a liquid film

180

must be used to maintain acoustic contact between solid surfaces, losses due to mismatch in this thin film can be minimised by cutting the wedge angle at  $45^\circ$  and using the transverse mode.

ACKNOWLEDGMENT.

I wish to express my indebtedness to Dr. W.H. George, Head of the Department of Physics, Chelsea Polytechnic, for his encouragement and continuous guidance in the preparation of this dissertation.

I also wish to express my thanks to Dr. R.W.B. Stephens, Reader in Acoustics, Imperial College of Science and Technology, for his two years extensive lectures on Acoustics.

Thanks are also due to my brothers, Mr. Binoy K. Som, B.Sc., and Mr. Bijan K. Som, B.A., B.Com., A.C.A., for their continuous encouragement and financial help.

List of symbols used.

$C$	=	velocity of sound.
$D$	=	diffusion coefficient.
$E$	=	Young's modulus.
$E_s$	=	adiabatic Young's modulus.
$E_T$	=	Isothermal Young's modulus.
$M$	=	mass of an atom.
$N$	=	number of atoms in a gram atom.
$Q$	=	internal friction.
$T$	=	absolute temperature.
$C_p$	=	specific heat at constant pressure.
$C_v$	=	specific heat at constant volume.
$d$	=	thickness.
$f$	=	frequency of sound.
$f$	=	relaxation frequency.
$h$	=	Planck's constant.
$k$	=	Boltzmann's constant.
$l$	=	length.
$r$	=	radius.
$\alpha$	=	pressure attenuation coefficient.
$\rho$	=	density.
$\mu$	=	refractive index.
$\lambda$	=	Lame Constant.
$\sigma$	=	Poisson's ratio.
$\lambda$	=	wavelength of sound.



List of symbols used.

- $\tau$  = relaxation time.
- $\Delta$  = decrement resulting from relaxation.

LIST OF TABLES.

1. Elastic constants of alkali halides.
2. Elastic constants of sodium chlorate and sodium bromate.
3. Elastic constants of cubic crystals.
4. Velocity and attenuation values in some polymers.
5. Velocity of ultrasonic waves in some rocks.
6. Values of Young's modulus of rock salt.
7. 10 Mc. Bulk wave attenuation data in some high polymers.

List of Diagrams.

1. Magnetostriction oscillator.
2. Pierce's oscillator.
3. Modified Pierce circuit.
4. Pierce Muller circuit.
5. Cady's oscillator.
6. Cutting of a quartz from a crystal.
7. Crystal structure of barium titanate.
8. Domain alignment by polarization in barium titanate.
9. Simple crystal holder for work in solids.
10. Button Helder.
11. Holders for angular propagation.
12. Composite oscillator (Zacharias).
13. Electrical circuit arrangement (Zacharias).
14. The Cady circuit.
15. The electrical connection to the quartz cylinder.
16. Triple oscillator.
17. Air Core solenoid driver and detector (Randal, Rose  
and Zener).
18. Arrangement of apparatus for producing longitudinal  
oscillations of rods by electrostatic traction.
19. Electrical circuit for the above arrangement.
20. Electrostatic excitation of resonant metallic bar.
21. Low temperature apparatus.
22. Magnetostriction Resonance Apparatus.
23. Simple block diagram of pulse technique.

List of Diagrams.

24. Complete block diagram of ultrasonic pulse equipment.
25. Arrangement of Mason and Mc.Skimin.
26. Measured attenuation versus frequency.
27. Attenuation measurement of Roth for two magnesium rods for longitudinal waves.
28. Buffer amplifier circuit.
29. Symmetrical arrangement for comparing reflected and transmitted components.
30. Circuit arrangement of Mason and Mc.Skimin.
31. Block diagram of the circuit used by Doland, Mrowca and Goth.
32. Velocity of longitudinal waves in polyethylene.
33. Attenuation per wavelength for longitudinal waves in polyethylene plotted as a function of temperature and frequency.
34. Attenuation per wave length for shear waves in polyethylene.
35. Value of  $\lambda$  (Lame elastic constant) for polyethylene and Nylon 6-6 plotted as a function of frequency and temperature.
36. Buna-N (Hycar OR-15) gum vulcanizate B-100 bulk wave velocity and attenuation at 10 Mc.
37. Buna-N (Hycar OR-15) gum vulcanizate B-100 bulk wave attenuation at 30 Mc.
38. Buna-N (Hycar OR-15) Carbon loaded Vulcanizate B-5 bulk wave velocity and attenuation at 10 Mc.
39. Butyl gum vulcanizate U-50 bulk wave velocity and attenuation at 10 Mc.
40. Perbunan gum vulcanizate P-1 A. bulk wave velocity and attenuation at 10 Mc.

List of Diagrams.

41. GR-S gum vulcanizate S-100. bulk wave velocity and attenuation at 10 Mc.
42. Vinylite No. 1940 (plasticized) bulk wave velocity and attenuation at 10 Mc.
43. Bulk wave velocity versus temperature at 1 Mc/sec. for Hevea, GR-S and butyl rubbers.
44. Velocity versus temperature for butyl at all frequencies.
45. Velocity versus temperature for GR-S at all frequencies.
46. Bulk wave attenuation versus temperature at 10 Mc/sec for Hevea, GR-S, and butyl rubbers.
47. Model for dislocation relaxations.
48. Attenuation of sound in aluminium.
49. Temperature dependence of sound in aluminium.
50. Equivalent electrical circuit for delay lines using quartz.
51. Two dimensional paths.
52. Delay path when  $n = 5$ .
53. Experimental arrangement of Schaffer and Bergmann.
54. Typical diffraction images.
55. Continuous wave oscillator gated by d.c. pulses.
56. Balancing circuit for error compensation.
57. Velocity of longitudinal waves in Nylon.
58. Curves showing relation between temperature and time. Solid line for heat transmission, dashed line for sound transmission at ultrasonic frequencies.

REFERENCES

1. R.W. Boyle and D.O. Sproule (1929) "Oscillations in ultrasonic generators and velocity of longitudinal vibrations in solids at high frequencies". Nature 123. 13.
2. Lord Raleigh "Theory of sound". Vol. I and II. 1929
3. R.W. Boyle and D.O. Sproule (1931) "Velocity of longitudinal vibrations in solid rods (Ultrasonic method) with special reference to the elasticity of ice". Canad. J. Res. 5. 601
4. E. Giebe and A. Scheibe (1931) "Über die Seriengesetze der elastischen Eigenfrequenzen Von Quarzstäben". Ann. Phys. Lpz.(v) 9. 93
5. K. Rohrich (1932) "Ausbreitungsgeschwindigkeit ultraakustischer schwingungen in Zylindrischen Stäben". Z. Phys. 73. 813.
6. H. Schoeneck (1934) "Experimentelle Untersuchungen der Schwingungen Zylindrischer Einzelkristalle bei hohen elastischen Frequenzen." Z. Phys. 92. 390.
7. R. Ruedy (1935) "Anomalous dispersion of sound in solid cylindrical rods". Can. J. Res. A. 13. 10.
8. E. Giebe and E. Blechschmidt (1933) "Experimentelle und theoretische Untersuchungen über Dehnungseigenschwingungen Von Stäben und Röhren". Ann. Phys. Lpz.(V) 18. 417.
9. W.P. Mason and H.J. McSkimin (1949) "Attenuation and Scattering of high frequency sound waves in metals and glasses". J.A.S.A. 19. 466.

10. W. Roth (1948) "Scattering of ultrasonic radiation in polycrystalline metals".  
J. Appl. Phys. 19. 901
11. R.W. Boyle and J.F. Lehmann (1926) "The relation between the thickness of a partition in a medium and its reflection of sound waves by the ultrasonic method".  
Phys. Rev.(II) 27. 518.
12. R.W. Boyle and W.F. Rawlinson (1928) "Theoretical notes on the passage of sound through contiguous media".  
Trans.Roy.Soc.Canada (III) 22. 55.
13. W.T. Richards (1932) "A method for the determination of the velocity of sound in solids".  
Science. 76. 36.
14. L. Brioullin (1922) "Diffusion de la lumière et des rayons X par un corps transparent homogène; influence de l'agitation thermique".  
Ann. de Phys. 17. 88.
15. P. Debye and F.W. Sears (1932) "Scattering of light by supersonic waves".  
Nat. Acad. Sc. Proc. 18. 409.
16. R. Lucas and P. Biquard (1932) "Propriétés optiques des milieux solides et liquides soumis aux vibrations élastiques ultrasonores."  
J. Phys. radium. 3. 464.
17. C.V. Raman and N.S. Nath (1935,1936) "The diffraction of light by high frequency sound waves".  
Part I - V.  
Proc. Ind. Acad. Sc. (A) 2. 406.413; 3. 75.119.495.
18. H. Mueller (1937) "The intensity and polarization of the light diffracted by supersonic waves in solids".  
Phys. Rev. 52. 223.
19. N.S. Nath and H. Mueller (1938) "Diffraction of light by supersonic waves in solids".  
Nature. 141. 37.

20. A.E.H. Love (1920) "A treatise on the mathematical theory of elasticity." Cambridge University Press 1920.
21. I.S. Sokolnikoff (1956) "Mathematical theory of elasticity". Mc. Graw Hill. (1956)
22. C. Kittel (1947) "Ultrasonic research and properties of matter". Report on Progress in Physics. Phys. Soc.(London) XI. 205.
23. C. Zener (1937) "Internal friction in solids". Phys. Rev. 52. 230.
24. C. Zener (1938) "Internal friction in solids". Phys. Rev. 53. 90.
25. C. Zener (1948) "Elasticity and Anelasticity of metals". Chicago University Press 1948.
26. Ting-Sui Ke (1947) "Experimental evidence of the viscous behaviour of grain boundaries in metals". Phys. Rev. 71. 533.
27. R.L. Wegel and H. Walther (1935) "Internal dissipation in solids". Physics. 6. 141.
28. T.A. Read (1940) "The internal friction of single metal crystals". Phys. Rev. 58. 351.
29. L. Landau and G. Rumer (1937) "Über schallabsorption in festen Körpern". Phys.Zeit. Sowjetunion.11.18.
30. A. Akhieser (1939) "On the absorption of sound in solids". J. Phys. U.S.S.R. 1.227.
31. L. Gurevich (1945) "On the absorption of high frequency sound in metals". J. Phys. 9. 383.(U.S.S.R.)



32. H. Kolsky (1953) "Stress waves in solids". Clarendon Press. Oxford.
33. W.P. Mason (1950) "Piezo electric crystals and their application to ultrasonics". D. Van Nostrand Co.N.Y.
34. W.P. Mason (1949) "Sound transmission in solids at ultrasonic frequencies". Bell. Lab.Record. 27. 421.
35. C. Zucker (1955) "Elastic constants of aluminium". J.A.S.A. 27. 318.
36. G.W. Pierce (1928) "Magnetostriction Oscillators". Proc.Ame.Acad.Boston. 63. 1.
37. G.W. Pierce (1929) "Magnetostriction Oscillators". Proc. I.R.E. (N.Y.) 17. 42.
38. J.H. Vincent (1929) "Experiments on magnetostrictive oscillators at radio frequencies". Proc. Phys. Soc. 41. 476.
39. J.H. Vincent (1931) "Experiments on magnetostrictive oscillators at radio frequencies". Proc. Phys. Soc. 43. 157.
40. G.W. Pierce and Atherton Noyes (1938) "An improved magnetostriction Oscillator". J.A.S.A. 9. 185.
41. L. Bergmann (1949) "Der Ultraschall". 5th Edition, S. Hirzel Verlag. Zurich.
42. J. Gruetmacher (1935) "Piezoelektrische Kristall mit Ultraschall Konvergenz". Z. Phys. 96. 342.
43. L.W. Lablaw (1945) "Curved quartz crystals as supersonic generators". J.A.S.A. 17. 19.
44. P. Vigoureux (1950) "Ultrasonics". Chapman and Hall (London)

45. R. Bechmann (1934) "Messung der schallgeschwindigkeit in anisotropen Medien, Insbesondere in quarz mittels piezoelectrischer Erregung". Z. Phys. 91. 670.
46. J.S. Rinehart (1941) "Temperature dependence of Young's modulus and internal friction of lucite and Karolith". J. Appl. Phys. 12. 811.
47. M.A. Durand (1936) "Temperature variation of the elastic moduli of NaCl, KCl, and MgO". Phys. Rev. 50. 449.
48. C. Bachem, E. Hiedemann and H.R. Asbach (1934) "New methods for the direct visualisation of ultrasonic waves and for the measurement of ultrasonic velocity". Nature. London. 133. 176.
49. Cl. Schaffer and L. Bergmann (1934) "Über neue Beugungserscheinungen an schwingenden Kristallen". Naturwiss. 22. 685.
50. R. Bar and A. Walti (1934) "Über die Bestimmung der Poissonschen Elastizitätskonstanten mit Hilfe von Ultraschallwellen". Helv. phys. Acta. 7. 658.
51. W. Bez-Bardili (1935) "Über ein Ultraschall - Total reflektometer Zur Messung von Schallgeschwindigkeiten sowie der elastischen Konstanten fester Körper". Z. Phys. 96. 761.
52. S. Bhagabantam and J. Bhimsenacher (1944) "Elastic constants of Crystals". Proc. Ind. Acad. Sc. (A). 20. 298.

53. W.G. Schneider and  
Ch. J. Burton (1948) "Determination of elastic constants of solids by ultrasonic methods".  
J. Appl. Phys. 20. 48.
54. G.W. Willard (1951) "Improved method for measuring ultrasonic velocity".  
J.A.S.A. 23. 83.
55. E. Fues and  
H. Ludloff (1935) "Weitere Untersuchungen über die Beugungserscheinungen an schwingenden Kristallen."  
Theoretischer Teil,  
Sitz-Ber.  
Berliner Akad. 248.
56. Cl. Schaffer and  
L. Bergmann (1935) "Weitere Untersuchungen über die Beugungserscheinungen an schwingenden Kristallen".  
Sitz-Ber. Berliner Akad. 222.
57. Cl. Schaffer,  
L. Bergmann and  
H.J. Goehlich (1937) "Die Bestimmung der elastischen Konstanten optischer Glasser mittels der Lichtbeugung an Ultraschallwellen."  
Glastechn. Ber. 15. 447.
58. W.T. Szymanowski  
(1944) "Rapid determination of elastic constants of glass and other transparent substances".  
J. Appl. Phys. 15. 627.
59. E. Hiedemann and  
K.H. Hoesch (1935) "Eine neue Methode zur Messung der elastischen Konstanten von durchsichtigen isotropen Festkörpern".  
Naturwiss. 23. 577.
60. R. Bar and  
E. Meyer (1933) "Über einige Versuche zur Beugung des Lichtes an Ultraschallwellen".  
Helv. Phys. Acta. 6. 242.
61. S. Bhagabantam and  
B. Rao (1946) "Determination of elastic constants of isotropic media, a new method".  
Proc. Ind. Acad. Sc. A.  
23. 254.
62. S. Bhagabantam and  
J. Bhimsenachar (1946) "Elastic constants of diamond".  
Proc. Roy. Soc. (London) 187. 381.

63. S. Phagabantam and J. Bhimsenachar (1946) "Elastic constants of Zircon". J.A.S.A. 27. 922.
64. S.R.V.G. Rao (1948) "Elastic constants of ammonium alum". Current Sc. 17. 50.
65. S.R.V.G. Rao (1949) "Elastic constants of sodium chlorate and sodium bromate". Current Sc. 18. 204.
66. S.R.V.G. Rao (1948) "A modified method for determination of elastic constants of crystals". Proc. Ind. Acad.Sc. (A) 28. 475.
67. S. Balkrishna (1955) "Transmission of Ultrasonics through rocks". Proc. Ind. Acad. Sc. 41A. 12.
68. B. Ramchandra Rao and P. Venugopal Rao (1955) "Determination of shear wave velocities in isotropic solids by a modified wedge method". Acustica. 5. 217.
69. M. Krishnamurthi and S. Balkrishna (1953) "Measurement of Ultrasonic velocities in some Indian rocks". Proc. Ind. Acad. Sc. A.38. 495.
70. F.H. Sanders (1939) "Transmission of sound through plates at oblique incidence". Phys.Rev. 55. 1127.
71. K. Vedam (1950) "Elastic and photoelastic constants of fused quartz and some optical glasses". Proc. Ind.Acad.Sc. 31. 450.
72. Ramchandra Rao (1950) "A new method for determining elastic constants". Current Sc. 19. 148.
73. G.M. Sreekandath "New method for measuring ultrasonic velocity in solids". J.A.S.A. 28. 312.

74. L. Bergmann and E. Fues. (1936) "Bestimmung elasto-optischer Konstanten aus Beugungsversuchen". Naturwiss. 24. 492.
75. H. Mueller (1938) "Determination of elasto-optical constants with supersonic waves". Z. Kristallographie (A). 99. 122.
76. K.S. Iyengar (1955) "Diffraction of light in solids by ultrasonic waves". Proc. Ind. Acad. Sc. 41A. 25.
77. S.L. Quimby (1925) "On the experimental determination of the viscosity of vibrating solids". Phys.Rev.(2) 25. 558.
78. S.L. Quimby (1932) "Some new experimental methods in ferromagnetism". Phys. Rev. 39. 345.
79. J. Zacharias (1933) "Temperature dependence of Young's modulus for nickel". Phys. Rev. 44. 116.
80. W.T. Cooke (1936) "Variation of the internal friction and elastic constants with magnetization in iron". Phys. Rev. 50. 1158.
81. W.F. Brown (1936) "Variation of the internal friction and elastic constants with magnetization in iron". Phys. Rev. 50. 1165.
82. T.A. Read (1938) "The internal friction of metallic crystals". Phys. Rev. 54. 389.
83. F. Forster and W. Korster (1937) Zeits.f. Metallkunde. 30. 345.
84. L. Balamuth (1934) "Elastic moduli and temperature variation of the principal Young's modulus of rock salt. Phys. Rev. 45. 715.

85. W. Voigt (1910) "Lehrbuch der Kristallphysik"  
Berlin: Teubner.
86. L. Hunter and S. Siegel (1942) "Variation with temperature of the principle elastic moduli of NaCl near the melting point".  
Phys. Rev. 61. 84.
87. R.H. Randall, F.C. Rose and C. Zener (1939) "Intercrystalline thermal currents as a source of internal friction".  
Phys. Rev. 56. 343.
88. Dennison Bancroft and Robert B. Jacobs (1938) "An electrostatic method of measuring elastic constants".  
Rev. Sc. Inst. 9. 279.
89. M. John Ide (1935) "Some dynamic methods for determination of Young's modulus of Al., Pb., Ni., Ag., steel and glass".  
Rev. Sc. Inst. 6. 296.
90. P.G. Bordoni (1954) "Elastic and anelastic behaviour of some metals at low temperature".  
J.A.S.A. 26. 495.
91. P.G. Bordoni (1947) "Metodo elettroacustico per ricerche sperimentali sulla elasticita".  
Nuovo Cimento. 4. 177.
92. P.G. Bordoni (1949) *Ricerca Sci* 19. 951
93. P.G. Bordoni (1953) "Dipendenza della autofrequenze di un solido dalla temperatura e dal volume, secondo la meccanica statistica".  
Nuovo cimento. 10. 268.
94. Andrew Gemant (1940) "The measurement of solid friction of plastics".  
J. Appl. Phys. 11. 647.
95. G.G. Parfitt (1949) "Energy dissipation in solids at sonic and ultrasonic frequencies".  
Nature 164. 489.

96. A.W. Nolle (1948) "Methods of measuring dynamic mechanical properties of rubber like materials". J. Appl. Phys. 19. 753.
97. H.B. Huntington (1950) "On ultrasonic scattering by polycrystals". J.A.S.A. 22. 362.
98. W.J. Price and H.B. Huntington (1950) "Acoustical properties of anisotropic materials". J.A.S.A. 22. 32.
99. R.L. Roderick and R. Truell (1952) "The measurement of ultrasonic attenuation in solids by the pulse technique and some results in steel". J. Appl. Phys. 23. 267.
100. A.W. Nolle and S.C. Mowry (1948) "Measurement of ultrasonic bulk wave in high polymers". J.A.S.A. 20. 432.
101. Doland G. Ivey, A. Mrwca and E. Goth (1949) "Propagation of ultrasonic bulk waves in high polymers". J. Appl. Phys. 20. 486.
102. W.P. Mason and H.J. Mc.Skimin (1952) "Mechanical properties of polymers at ultrasonic frequencies". Bell.Syst. Tech.J. 31. 122.
103. H.J. Mc. Skimin (1951) "Methods for determining the propagation constants of plastics at ultrasonic frequencies". J.A.S.A. 23. 429.
104. A.W. Nolle (1950) "Ultrasonic study of rubber at low temperatures". J.A.S.A. 22. 86.
105. A.W. Nolle and J.F. Mifsud (1952) "Use of a differential phase delay method for study of ultrasonic wave propagation in swollen rubber like materials". J.A.S.A. 24. 118. (Abstract)
106. J.R. Pellam and J.K. Galt (1946) "Ultrasonic absorption and velocity measurements in liquids by means of pulse technique". Bull.American.Phys.Soc. 21. 21.

107. Ch. E. Teeter  
(1946) "Absorption of supersonic waves in liquids".  
J.A.S.A. 18. 488.
108. W.P. Mason (1955) "Relaxations in the attenuation of single crystal lead at low temperatures and their relation to dislocation theory".  
J.A.S.A. 27. 643.
109. T.S. Hutchison and A.J. Filmer (1956) "Attenuation of 5 Mc. sound in Aluminium at low temperatures".  
Canad. J. Physics. 34. 159.
110. H.E. Bommel (1954) "Ultrasonic attenuation in super conducting lead".  
Phys. Rev. 96. 220.
111. Edwin Voznak and R.W. Mebs (1955) "A temperature invariant solid ultrasonic delay line".  
I.R.E. Transactions on Ultrasonic Engineering, N.Y. 1955.
112. J. May (1954) "Characteristic of ultrasonic delay lines using a quartz and barium titanate ceramic transducers".  
J.A.S.A. 26. 347.
113. D.L. Arenberg (1948) "Ultrasonic solid delay lines."  
J.A.S.A. 20. 1.
114. H. J. Mc. Skimin. (1950) "Ultrasonic measurement technique applicable to small solid specimens"  
J.A. s.A. 22. 413
115. F. C. Rose (1936) "Variation of adiabatic elastic moduli of rock salt with temperature between 80°K and 270°K"  
Phys. Rev. 49, 50.